1992

Instrumental and theoretical development of capillary electrophoresis and its application to biological systems

Thomas Tsang Lee
Iowa State University

6

93

02007

Order Number 9302007

Instrumental and theoretical development of capillary electrophoresis and its application to biological systems

Lee, Thomas Tsang, Ph.D.

Iowa State University, 1992

U·M·I
300 N. Zeeb Rd.
Ann Arbor, MI 48106

Instrumental and theoretical development of capillary electrophoresis and its application to biological systems

by

Thomas Tsang Lee

A Dissertation Submitted to the

Graduate Faculty in Partial Fulfillment of the

Requirements for the Degree of

DOCTOR OF PHILOSOPHY

Department: Chemistry
Major: Analytical Chemistry

Approved:

Signature was redacted for privacy.

In Charge of Major Work

Signature was redacted for privacy.

For the Major Department

Signature was redacted for privacy.

For the Graduate College

Iowa State University
Ames, Iowa

1992

TABLE OF CONTENTS

GENERAL INTRODUCTION

Format of the Dissertation

This dissertation is arranged in a format in which the research publications of the author are presented as separate sections within the dissertation. The style of captions, figures and text are as required for the journals of submission. A general introduction presents the background concepts and literature necessary for a thoughtful appreciation of the work presented. A general summary presents final comments on the work presented and a listing of the literature cited within the general introduction concludes the dissertation.

Union of Biology and Chemistry

Since the beginning of the industrial revolution, the exponential growth of science and technology has radically transformed every aspect of society. Mass production was made possible by the replacement of manual labor with machinery, a joint product of physics and engineering. The proliferation of the chemical industry was largely a consequence of the cooperation between chemists, geologists and engineers. The emergence of the nuclear industry saw the assembly of a still more diverse team of experts skilled in physics, chemistry, geology and engineering. In fact, as the growth rate of science and technology continues to increase, the demand and need for multi-disciplinary work teams are likely to grow in the future. The burgeoning industry of biotechnology is no exception.

However, there is much more to inter-disciplinary cooperation than merely the pooling together of expertise in different areas. Frequently, the intentional application of one's specialized know-how could facilitate fundamental breakthroughs

in a separate discipline. An example of this is the impact that nuclear magnetic resonance (NMR) and absorption spectroscopy, mass spectrometry as well as gas and liquid chromatography (the realms of physical and analytical chemistry) had on the development of organic and inorganic chemistry in the 1960's. The first half of this century witnessed the union of physics and chemistry which, again, provided an illustration of the immense significance of cross-disciplinary visions. By now, it is quite obvious that the marriage of chemistry and biology is about to be consummated. For the past decade, molecular biology has been knocking on the door of chemistry and the ensuing conversation has been convivial. This is exemplified by the emergence of a new journal entitled *Journal of Bioconjugate Chemistry* which represents the response of mostly organic chemists to the invitation from molecular biologists. Although an exact analogy cannot be drawn in the case of analytical chemistry, an urgent demand for the transfer of knowledge and cooperation exists. It is in this context where the development of precise and quantitative chemical methods for biological applications becomes valuable.

Historically, many advances in the biological sciences were method driven. Recent examples of these include polymerase chain reaction (PCR) and DNA sequencing technology, multi-dimensional NMR as well as X-ray diffraction techniques. As Nobel laureate Arthur Kornberg had remarked, "Molecular biology appears to have broken into the back of cellular chemistry, but for the lack of chemical tools and training, it is still fumbling to unlock the major vaults" (1). Another driving force behind the push for developing chemical methods for biological applications results from the rapid growth of the now multibillion-dollar industry of biotechnology which is certain to transform health care, agriculture or, for better or worse, the ecosystem. The appearance of recombinant DNA-derived

products and the largely unknown effects of their presence on the environment and human health call for analytical methods with higher sensitivity and specificity than those afforded by the more traditional techniques. To these ends, the potential that capillary electrophoresis (CE) holds in the rapid identification and quantitation of DNA, proteins, viruses, bacteria and many other potentially harmful (and/or useful) biological agents could directly influence the acceptance of recombinant DNA products by society at large and facilitate fundamental breakthroughs in biological research.

Historical Background

From the early observation by F.F. Reuss in 1809 (2) that clay particles migrate under an electric field to the present, separation techniques based on the differential mobilities of constituents in a mixture have evolved into an indispensable tool in the laboratory. Although much pioneering work on the utilization of electrophoresis for the separation and identification of charged species can be attributed to Picton and Linder (3), Hardy (4) and Ellis (5), the moving boundary experiments of Tiselius in 1937 (6) signalled the beginning of practical implementation and acceptance of electrophoresis as a viable method in conjunction with various chromatographic techniques in the field of separation science. The incorporation of Schlieren optics for the refractometric detection of the solution boundaries in the U-tube of Tiselius' apparatus made possible the accurate measurement of the mobilities of analytes. However, a serious drawback of the technique is that only the fastest- and slowest-moving components can be separated from the mixture in any given run, as the differences in the densities of the remaining analyte zones result in convective mixing in the free solution medium. Consequently,

numerous approaches to perform electrophoresis in anti-convective media were executed in realizing "zone separation."

The first successful demonstration of zone electrophoresis was that of Consden *et al.* (7) with their ingenious use of a silica gel as the medium. Subsequently, zone electrophoresis had been performed on soaked paper and fabrics (8,9). Equally common materials used as anti-convective media included powders and granulated gels (10-12). The introduction of polyacrylamide (13) in the late 1950's revolutionized electrophoresis in the separation of biomolecules for analytes can be fractionated in accordance to size through the mechanism of sieving. Enhanced resolution is attained through a pore size gradient along a cylindrical tube in the technique of disc electrophoresis where, in addition to analyte stacking, advantage is taken of the use of multiphasic buffers (14,15). Since then the concept of pore size gradient had been extended to the slab gel format to widen the size distribution of analytes amenable to separation in a single run (16).

Although still widely practiced today, zone electrophoresis in the slab gel format suffers from the necessity to employ low field strengths due to the poor heat-dissipating capability of the separation medium. Since a large cross-sectional temperature gradient results in a wide distribution of analyte mobilities, zone electric field strengths or even gel pore sizes, conventional electrophoretic methods fail to qualify as high-resolution techniques. Besides, the skill of gel-casting is as much of an art as the interpretation of band shapes and locations on electropherograms. The labor-intensive nature and poor quantitative capability of the technique are also undesirable. Hence, electrophoresis in the slab gel format remains inefficient and semi-quantitative at best. Nonetheless, the emergence of disc electrophoresis in 1964 (14,15), where separation is performed in a narrow cylindrical tube with good heat-

dissipating capability, permits the use of higher field strengths and foreshadows the transformation of electrophoresis into a modern, automated method.

Various attempts, notably those of Hjerten (17) and Kolin (18), had failed to demonstrate zone electrophoresis in free solution as an effective separation technique. Excessive heating of the separation medium remains the stumbling block to the maintenance of zone integrity. It was not until 1974 when Virtanen (19) succeeded in obtaining reasonably good efficiencies in free zone electrophoresis with 200- to 500-μm inner diameter (i.d.) glass tubes. Five years later, Mikkers *et al.* (20) decreased the plate height to less than 10 μm with 200-μm i.d. Teflon tubes. In 1981, harnessing the latest in capillary manufacturing technology, Jorgenson and Lukacs (21) demonstrated plate heights of only a few μm and adapted many of the automated features of the then more mature microcolumn high-performance liquid chromatography (μHPLC) to the method, thereby laying down the foundation of the earliest versions of CE.

By turns deliberate and surrendipitous, the ensuing development of CE can adequately be described as explosive. This is evidenced by a total of 5 references on the technique before 1982 relative to the 743 between 1982 and 1991 (22,23). The timely capability of CE in the determination of biomolecules complements the equally fast-paced developments in the fields of biotechnology and biomedical science. The seminal works of Jorgenson and Lukacs (21,24,25) characterized the most rudimentary operating parameters of the technique. Some of these include the sub-100-μm i.d. of the capillary tubing, high voltage (20-30 kV) operation and on-column ultraviolet-visible (UV-VIS) absorbance detection scheme. In addition, they expounded the virtues afforded by the flat flow-profile of electroosmotic pumping, rendering molecular diffusion the sole source of band dispersion in capillary zone

electrophoresis (CZE) with efficient heat dissipation. In 1985, isoelectric focusing and molecular sieving were shown to be feasible in gel-filled capillaries by Hjerten (26). Since then significant progress had been made in improving the efficiency of capillary gel electrophoresis (CGE) in size-based separations of proteins and DNA fragments (27). The utility of CE was extended to neutral species by Terabe *et al.* in 1984 (28) through the incorporation of a surfactant present at above its critical micelle concentration in the running buffer, thereby spawning the technique of micellar electrokinetic chromatography (MEKC), an important diversion from the traditional concept of electrokinetic chromatography originally demonstrated by Pretorius and co-workers (29).

Modes of Operation

Despite its instrumental simplicity, CE has emerged as one of the most versatile analytical techniques. If versatility is the hallmark of wide applicability, CE stands to become one of the most popular analytical tools. A major part of this can be attributed to the highly diverse modes of operation at the disposal of the analyst. Besides, the switching from one mode to another does not go beyond the simple act of changing the buffer and/or capillary tubing. Nonetheless, if appropriately performed, such ostensibly trivial efforts could bring about dramatic effects in terms of selectivity and speed of analysis. Given the rapid progress in CE, only brief descriptions of the basic principles of operation and highlights of application for each mode will be presented below.

Capillary zone electrophoresis (CZE)

Charged species migrate at different velocities in an electric field, thereby effecting separation in CZE. Ordinarily, the part of the capillary directly exposed to solution is charged through surface ionization and gives rise to a diffuse electrical double layer in the solution adjacent to the wall. When a potential difference is applied between the two ends of the capillary, the movements of the mobile ions in the double layer create a drag on the neighboring solvent molecules, resulting in electroosmotic flow. A remarkable feature of electroosmotic flow is its flat profile which is unlike that of pressure-driven flow where the profile is parabolic. In other words, bulk flow in CZE does not contribute to band dispersion. Since other causes of band dispersion in typical pressure-driven chromatographic systems such as resistance to mass transfer and channel irregularities are also absent, CZE is able to deliver a few million theoretical plates in less than ten minutes on a routine basis.

Because most interesting analytes are weak electrolytes, selectivity in CZE is usually manipulated by changing the pH of the buffer. In addition, one could enhance resolution through the modification of the capillary wall in attempting to alter the charge on the capillary wall, thereby changing the electroosmotic flow rate which has a direct bearing on resolution. The use of pH-determining buffer components which form complexes with the analytes of interest (e.g., borate-sugars) has also been utilized to control selectivity (30). Provided that the overall dielectric constant of the buffer is reasonably high, polar organic solvents can be used in conjunction with aqueous solutions to achieve unique selectivity. Although not widely practiced, gradient schemes including pH, organic solvent content, flow and temperature have been shown to offer advantages in either selectivity, resolution or speed in certain situations.

Whether the task at hand is the determination of protein structures by tryptic digestion, speciation of ions in ground water or analysis of drugs and their metabolites in physiological fluids, CZE presents itself as a complementary technique to HPLC and, as a consequence of its superior speed and efficiency, proves to be the method of choice for numerous applications. For instance, the simultaneous quantitation of the chemical contents of single cells, long considered the basic building blocks of life, is made possible by the small sample size requirement (pL) and high efficiency of the technique (31,32).

Electrokinetic chromatography (EKC) with carriers

While the concept of controlling the migration velocities of analytes in electrophoresis with mobile carriers in the separation medium is not new, its ramifications have never been more pervasive than in CE. Although cyclodextrans, polyelectrolytes, microemulsions and inorganic fine particles have served as carriers, their appearance in the field of CE is too recent and their applications too limited to deserve discussion here. In fact, complexation agents and micelle-forming surfactants remain the two most popular forms of carriers in EKC today.

In CZE, the migration velocity of an analyte is determined by its electrophoretic mobility in free solution. In the presence of a complexation agent (e.g., EDTA), however, the electrophoretic mobility of the same analyte depends on not only its electrophoretic mobility in free solution, but also that of the complex, the complexation constant and the concentration of the complexation agent. The analyst is, therefore, presented with ample opportunities by way of control over the above factors in the fine-tuning of particular EKC separations. If complexation constants and electrophoretic mobility values are available, one could optimize separations by

simulation, dramatically shortening method development time. The landmark application of complexation EKC involves the resolution of 14 pairs of dansyl amino acid enantiomers with Cu(II) and L-histidine as the complexation agents (33).

Identical in category but entirely different in mechanism is MEKC where the aqueous buffer contains a micelle-forming agent (e.g., SDS) present at concentrations above its critical micelle concentration (CMC). The hydrophobic microenvironment of the micelle provides temporary refuge for those analytes possessing attributes similar to that of the interior of the micelle. Naturally, this partitioning behavior is more pronounced for analytes having more hydrophobic character than otherwise. As indicated by the large aggregation number of the typical micelle (e.g 32 for SDS), the micelle is normally the slowest-moving species in the system for typical directions of electroosmotic flow. Hence, the degree of affinity of the analyte for the micelle offers, in addition to the electrophoretic mobility, extra selectivity in the separation. Since neutral species partition into micelles, they can be resolved with MEKC, a feat unrealizable with CZE alone. A unique feature of MEKC is that all analytes must migrate past the detector before the appearance of the peak corresponding to the micelle. This renders MEKC ideal for the rapid screening of unknown mixtures as the migration times of all the components must be less than that of the micelles.

However, the generality of EKC does not come without a price. What one gains in extra selectivity is often offset by the ensuing loss of efficiency. Among the factors contributing to this are carrier mobility differences, the slow kinetics of inter-species conversion and increased buffer ionic strength. Rather than the few million in CZE, typical EKC separations offer only several hundred thousand theoretical plates. While the performance of EKC dims in the lights of CZE, it still qualifies as a phenomenal improvement over the few thousand plates offered by conventional

HPLC, as illustrated in the resolution of normal and deuterated dansylated methylamines (34).

Electrokinetic chromatography (EKC) without carriers

Ever since its conception in the 1960's, major strides have continually been made toward the attainment of the ultimate in HPLC in terms of speed and efficiency. Problems associated with channel irregularities and resistance to mass transfer have adequately been addressed through the use of open tubular columns with small inner diameters and thin stationary phases. This renders the parabolic profile of pressure-driven flow the stumbling block to further improvement in efficiency. However, the use of electroosmosis in place of pressure overcomes the hurdle of flow-induced band dispersion and brings HPLC in the form of EKC to new levels of performance.

Much like MEKC, separation in electrically driven HPLC is effected by both partitioning and electrophoretic migration. Thus, two entirely distinct mechanisms are responsible for analyte resolution. However, the distinctive feature of electrically driven HPLC over MEKC lies in the much higher efficiency of the former where inhomogeneity in carrier mobility is nonexistent. Whereas the early efforts of the academic community in the 1980's failed to persuade the practitioners of conventional HPLC to embrace microbore or microcolumn HPLC, with its unique selectivity and high efficiency, the 1990's could witness the wide acceptance of miniaturized HPLC in the form of EKC.

Capillary gel electrophoresis (CGE)

Electrophoresis in slab gels is commonplace in biology and biochemistry. Its special ability in effecting size-based separations through sieving provides a powerful means of analyzing complex biological matrices and isolating valuable biomolecules. Moreover, the method allows the estimation of the molecular weights of large biopolymers. Despite all its virtues, however, slab gel electrophoresis is labor-intensive, time-consuming, inefficient and semi-quantitative at best.

Performing electrophoresis in gel-filled capillaries promises to advance gel electrophoresis into a modern, automated and quantitative technique capable of high-speed and highly efficient separations. Once again, the possibility of employing large voltage gradients across small-diameter capillaries accounts for much of the gain in speed and efficiency while the sophisticated injection and detection devices render the technique labor-saving and quantitative. Although CGE is suitable for the determination of a wide array of analytes, none of its applications is more critical than the resolution of DNA fragments. The recent demonstration of a sequencing rate of 1000 bases/h makes CGE a promising alternative to conventional methods for DNA sequencing (35). Further development of CGE through the incorporation of novel features such as non-traditional media and pulsed voltage sequences could increase the speed of DNA sequencing by several orders of magnitude. Consequently, given the explosive pace at which advances in CGE are being made, it is entirely conceivable that the technique could vastly alter the rate at which genetic information at the molecular level is being deciphered, thereby accelerating the revolution in molecular biology whose ramifications are already sweeping through society today.

Isotachophoresis (ITP)

ITP is to displacement chromatography as CZE is to elution chromatography. In ITP, the analytes are sandwiched between a leading and a trailing electrolyte. Provided that the leading and trailing electrolytes are, respectively, the fastest and slowest migrating species in the capillary tubing, all analytes are forced to migrate at a single velocity at steady state. Because the current density along the entire length of the capillary tubing is uniform, distinct analytes from adjacent zones migrate in accordance to mobility between the leading and trailing electrolytes. Although efficient separations are not possible, ITP can serve as a sample preconcentration technique for other modes of CE when detection sensitivity is a concern. Beside, the compatibility of ITP with large quantities of analytes renders it the mode of choice in CE for preparative applications.

Isoelectric Focusing (IEF)

IEF is by no means an unfamiliar method, especially to biologists and biochemists. The advantages accompanying the ability to utilize high field strengths and the characteristic of efficient heat-dissipation of small-diameter capillaries permit the resolution of analytes with small pI differences when IEF is performed in the CE format. Since analytes are resolved on the basis of pI, IEF offers unique selectivity amongst the various modes of CE.

Injection

In order for CE to qualify as a quantitative technique, reliable and reproducible means of introducing analytes into the capillary tubing are necessary. By far, the most widely practiced injection methods are electrokinetic (EK) and

hydrodynamic (HD) injection.

In HD injection, analyte introduction is typically achieved by immersing the injection end of the capillary tubing in the sample solution which is then raised to a level above that of the other buffer. The pressure differential thus resulted induces flow of the sample solution into the capillary tubing. Provided that no significant differences in the viscosities, densities and temperatures between the running buffer and sample solution exist, HD injection can adequately be described Poiseuille's Law. Noteworthy is that HD injection is a constant-volume injection method and, hence, no sampling biases based on analyte mobilities and sample solution conductivities are expected. Nevertheless, the instrumental requirements of HD injection are often cumbersome, as a precise means of controlling pressure is necessary.

On the other hand, EK injection equipment is relatively simple. The injection end of the capillary tubing is immersed in the sample solution. Rather than generating a pressure difference, a voltage difference is applied across the tubing such that the ensuing electroosmotic flow carries the sample solution into the capillary tubing, giving rise to analyte injection. However, since charged analytes migrate according to their electrophoretic mobilities, some analytes are preferentially injected and, hence, over-represented in the electropherogram. For analytes which are weak electrolytes, the amounts introduced are also a function of the pH of the sample solution, for mobility is sensitive to pH. Furthermore, the electric field experienced by the analytes in the injection zone depends on the conductivity of the sample solution. This also results in another source of sampling biases.

Detection

Despite the vehement efforts of proponents of microbore or microcolumn HPLC in the early 1980's, the technique never fulfilled the promise of supplanting conventional HPLC. Notwithstanding the numerous innovative approaches undertaken, inadequate detection sensitivity remains a major impediment to the wide acceptance of μHPLC. While most analysts can always abandon μHPLC in favor of conventional HPLC and, thereby, sacrifice some degree of separation efficiency in exchange for better detection sensitivity, the orthogonal selectivity and unparalleled efficiency afforded by CE are irreplaceable. Unfortunately, the nL detector volume of CE together with the necessity of employing the on-column format render the detector technology originally developed for μHPLC unsuitable for CE. Given the vast attention that detection in CE has received, only a general survey of the more common schemes will be outlined here.

Absorbance

As most analytes absorb at least moderately in some parts of the electromagnetic spectrum, absorption has become the most widely practiced detection scheme in HPLC. Even though the same is valid in CE at present, the performance of absorbance detectors in CE in terms of concentration sensitivity is a far cry from that in HPLC and proves to be inadequate in many applications. This can be attributed to the short pathlength provided by the small diameter (10-75 μm) of the capillary tubing. Even with the use of ball lenses, the focusing of light form a divergent source into the small volume of space confined by the imperfectly shaped cylindrical detection region of the capillary tubing remains difficult and, hence, limits the linearity of the detector. The μM-detection limits for most unlabeled but

interesting analytes such as proteins, nucleotides, pharmaceuticals, etc. render CE impractical in many situations. On the other hand, the attachment of desirable chromophores to analytes may result in undesirable effects including the formation of multiple peaks, loss of efficiency and degradation of precision due to increased sample handling. In some instances, the lack of appropriate functional groups on the analyte, interaction between the labeled species with the capillary wall and interference from concomitants in the derivatization process also impede the strategy of labeling.

Fluorescence

In light of the inadequate sensitivity of absorbance detection, it is not surprising that fluorescence detection in CE has attracted much attention. A major reason for this is that the sensitivity of fluorometry does not depend on pathlength. As a consequence, as long as one can couple light into the nL-detector volume while avoiding scattering, fluorometric detection is compatible with CE. Although the first fluorescence detector for CE utilizes a conventional light source, the difficulty inherent in focusing a large amount of light from a divergent source into the small detection region in an on-column manner while minimizing scattering renders the resulting sensitivity not much better than absorbance detection. However, it is possible to focus a large amount of light from a laser to a beam waist of just a few μm. Thus, laser-induced fluorescence (LIF) is able to satisfy the criteria of high photon flux and low scattering for high sensitivity.

At present, four LIF detection schemes of significance have been demonstrated. The simplest and most convenient to implement involves the direct focusing of the laser beam into the interior of the capillary tubing whereby the

fluorescence is collected by a photomultiplier tube at an angle perpendicular to the direction of the beam (36). Even though the beam is tightly focused, scattering from the fused silica of the tubing still limits detectability. A more elaborate setup consists of axially illuminating the buffer solution from the detection end, thereby reducing the amount of scatter. The low level of fluorescence is then registered on a charge-coupled device detector (37). However, photobleaching of the analytes precludes the use of high laser powers. The attachment of a sheath flow cuvette to the end of the capillary tubing represents the state-of-the-art in LIF detector technology for CE today (38). Because of the excellent optical quality of the cuvette together with the well-defined location of the eluent stream confined by the sheath flow, high power levels are not compromised by increased scattering. Detection limits at the pM and ymole (yoctomole or 10^{-21} mole) levels can routinely be attained for labeled analytes. More recently, the adaptation of a confocal fluorescence microscope as a CE detector offers sensitivity levels comparable to those with the sheath flow cuvette design (39). Besides, the confocal arrangement confers sturdiness and ease of alignment on the detector so that the important task of multiplexing can more readily be implemented.

Nonetheless, LIF is not a universal solution to the problems associated with detection in CE. In nature, analytes which absorb vastly out-number those which fluoresce appreciably. Thus, the applicability of LIF detection to CE requires the tagging of analytes with fluorescent derivatization agents. However, labeling complicates sample preparation and may not be suitable for some analytes or sample matrices. Besides, the high cost and bulkiness of most lasers are a deterrent to practical implementation. Nevertheless, advances in diode laser technology and derivatization methodologies may render LIF the detection scheme of choice in CE

in the future.

Electrochemistry

In μHPLC, the selectivity and high sensitivity of electrochemical detection are well-known. However, the direct transfer of microelectrode-based amperometric detection schemes to CE is not so straightforward. This is largely a consequence of the high applied potentials necessary for effecting separations in CE. The presence of the electrode in a high-field region adversely perturbs the transport process of the analyte. Fortunately, through the introduction of a small crack in the wall just prior to the end of the capillary tubing, the electric field responsible for separation can be terminated prematurely so that the electrochemical reactions occur in an essentially field-free region. With this design, the detection of electroactive analytes at sensitivity levels within two orders of magnitude to those with LIF has been demonstrated (40). With respect to selectivity, as with fluorescence, amperometric detection in CE is useful only if the analytes concerned are electroactive. Besides, exposure of the electrode to high-molecular weight species (e.g., proteins, etc.) frequently leads to electrode-fouling. Therefore, although electrochemical detection is a welcome addition to the battery of detection methodologies, it by no means solves the problems of detection in CE for most applications.

Mass spectrometry

The success enjoyed by gas chromatography/mass spectrometry(GC/MS) as a sensitive separation/identification technique for volatile organics cannot be overstated. On this note, the potential that CE/MS holds in the determination of nonvolatile and thermally labile species is equally immense. Notwithstanding the

failure of LC/MS in gaining popularity in the modern analytical laboratory, the small dimensions of CE promise to alleviate some of the problems associated with the maintenance of low pressure during the introduction of the eluent to the vacuum chambers of the mass spectrometer. As with LC/MS, sample introduction by means of electrospray atmospheric pressure ionization and analysis with a quadrupole mass spectrometer offer the best performance (41). Albeit structural information can be obtained, so far the achievable sensitivity is unsatisfactory for most applications, especially for the more interesting high-molecular weight analytes. The poor reliability of the technique is also a deterrent to wide acceptance. Nevertheless, the continued development of more efficient sample introduction methods and innovative approaches such as the use of ion-trap MS promise to enhance the performance of CE/MS in routine analyses in the future.

PAPER I.

FACILITATING DATA TRANSFER AND IMPROVING PRECISION IN CAPILLARY ZONE ELECTROPHORESIS WITH MIGRATION INDICES

INTRODUCTION

The tremendous potential that capillary zone electrophoresis (CZE) holds in modern separation science is well known (1-3). The unparalleled efficiency and speed of CZE in the resolution of nonvolatile and thermally labile species have led to its ever increasing popularity. This is reflected in the availability of commercial instruments from several companies on the market. With the rapid development in the field of biotechnology, it is certain that CZE will play an even larger role in the analytical arena in the future.

Much like gas chromatography (GC) in the 1960s and high-performance liquid chromatography (HPLC) in the 1970s, the current version of CZE is plagued with several problems which preclude its routine and wide-spread use. Most notably, problems associated with poor migration time and quantitative precision, analyte-wall interaction, unreliable coating manufacturing procedures, inaccurate temperature control and low detector sensitivity remain to be solved. While many fine efforts have been expended in the areas of coating and detection technologies, the aspects of migration time precision and reproducibility have received relatively little attention. In fact, as the application of CZE expands in scope and complexity, more stringent requirements will likely be placed upon the accuracy and precision with which analytes can be specified in an electropherogram. The reliable transfer of results between laboratories is vital for quality control/quality assurance purposes, whether for satisfying government protocols or ensuring product quality. Furthermore, the ability to relate results obtained under different separation conditions would prove to save both time and effort in method development. In this context,

research directed toward addressing these issues is paramount to the general acceptance of CZE as a mainstream analytical technique.

In the present work, the mechanisms and problems underlying the behavior of migration times are discussed. Two migration indices are then introduced to circumvent some of these shortcomings. Finally, experiments are carried out to compare the performances of these parameters in typical analytical runs.

THEORY

Problems with electrophoretic mobility and migration time

Separation in CZE is achieved via the distinct migration velocities of analytes under the influence of an electric field. An analyte is typically identified by its migration time (t_m) in an electropherogram. A more general parameter that specifies an analyte is the electrophoretic mobility (μ_{ep}). When contributions from relaxation are neglected, μ_{ep} can be expressed as (4):

$$\mu_{ep} = \frac{2\varepsilon\xi_a}{3\eta} f(\kappa a) \tag{1}$$

where ε is the dielectric constant of the solvent, ξ_a the zeta potential of the analyte, η the viscosity coefficient, κ the reciprocal of the analyte double layer thickness, a the "radius" of the analyte and $f(\kappa a)$ is a function dependent upon the shape and κa of the analyte in the buffer. The electrophoretic migration velocity (v_{ep}) of an analyte is as follows:

$$v_{ep} = \mu_{ep} E \tag{2}$$

where E ($\approx V/L$) is the local electric field, V the applied potential and L the length of the capillary. The approximation is valid if E is constant throughout the capillary. This will be the case when the analyte is present at much lower concentrations compared to the buffer components. We will also neglect band distortions due to differences in electrophoretic mobility between the analyte and the buffer ions, which will affect our ability to determine v. In all practical situations, the velocity of electroosmotic flow (v_{eo}) in a cylindrical capillary is given by (5):

$$v_{eo} = \frac{\varepsilon\xi_c}{\eta} E \tag{3}$$

where ξ_c is the zeta potential of the inner wall of the capillary and the proportionality constant relating v_{eo} to E is known as the electroosmotic flow coefficient (μ_{eo}). Strictly speaking, the η's in Eq. (1) and (3) are different (analyte-solution vs. wall-solution). For most applications however, these can be treated as being identical. Combination of equations (1), (2) and (3) yields the following expression for v_m, the net migration velocity of an analyte:

$$v_m = \frac{\varepsilon E}{\eta}[\xi_c + \frac{2\xi_a}{3}f(\kappa a)] \tag{4}$$

It follows that the analyte migration time is:

$$t_m = \frac{\eta L}{\varepsilon E[\xi_c + \frac{2\xi_a}{3}f(\kappa a)]} \tag{5}$$

As shown in equation (5), t_m is dependent upon E, L, ξ_c and $\xi_a f(\kappa a)$. While E and L can freely be chosen by the practitioner, ξ_c and $\xi_a f(\kappa a)$ are essentially determined by the nature of the running buffer, i.e. pH, electrolyte type, electrolyte concentration, solvent and, in the case of $\xi_a f(\kappa a)$, the analyte itself. Although it is possible to control ξ_c (without affecting $\xi_a f(\kappa a)$) by means of an external electric field (6) or addition of a surfactant to the running buffer (7) to optimize a given separation, they do not represent general approaches. The method of choice for this seems to be modification of the inner surface of the capillary through chemical derivatization. However, good precision and reproducibility as well as successful inter-capillary comparison hinge critically upon the reliable manufacture of capillary coatings with adequate chemical and temporal stability. Derivatization sometimes also leads to retention of the analytes, further complicating the interpretation of migration times. While it is too early to declare this insuperable, no rigorously proven method for this

exists today. As a result, the search for alternative solutions to deal with variations in ξ_c remains urgent.

Numerous workers have found that v_m (or $1/t_m$), as a function of E (or V), deviates positively at high values of E, an effect attributed to increase in the temperature of the running buffer as a consequence of Joule heating (8-14). More specifically, this stems from the large temperature coefficient of the η of water which decreases by roughly 2%/°C between 20 and 40°C (15). On the other hand, the changes in ξ_c, ξ_a and ε as a function of T are negligibly small (11,12,16,17). The sensitive dependence of v_m and, hence, t_m through η upon temperature is a drawback to the use of t_m in specifying an analyte in an electropherogram because precise control of the temperature is essential to obtaining adequate precision of t_m. Although some commercial CZE instruments are equipped with temperature control through air- or liquid-cooling of the capillary, accurate T control of the capillary and assurance of temperature uniformity along the capillary is difficult, if not impossible, to attain for two reasons. First, the two ends of the capillary in contact with the buffer solutions and the region through the detector are not subjected to temperature control in all existing instruments. Even if the buffer solutions and the air in the oven are maintained at the same temperature, differences in their heat capacities, and, thus, heat-dissipating capabilities persist. Secondly, Joule heating of the buffer solution during a run, an inevitable result of passage of electrical current through the capillary, almost always gives rise to significant temperature elevations in the capillary. In fact, a temperature increase of approximately 45°C from the ambient temperature at the start of a run to the steady state temperature during the run under typical operating conditions (with natural air convection) has been reported (11). Examination of equation (1) reveals that even the traditionally popular μ_{ep}

(used in specifying an analyte in electrophoresis and isotachophoresis) is afflicted with the same malady through its association with η in that the operating temperature needs to be specified. To this end, the generality of μ_{ep} cannot be exploited in relating the results obtained with different CZE instruments as the temperature at which separation occurs can neither be precisely controlled nor accurately measured. The same is observed even with forced-air and liquid cooling (13). However, this by no means undercuts the necessity to control the temperature of the separation condition so as to avoid analyte denaturation or degradation, drastic pH changes of the medium and buffer evaporation. To the extent that accurate temperature control during separation is not always possible, it becomes necessary to explore other means of specifying an analyte in an electropherogram.

Relative migration

As defined below, the relative migration (t_m/t_r) affords a solution to the problem of capillary temperature changes. Inspection of equation (5) leads to the following expression for t_r, the migration time of a reference standard:

$$t_r = \frac{\eta L}{\varepsilon E[\xi_c + \frac{2\xi_r}{3} f(\kappa a)]} \qquad (6)$$

where ξ_r is the zeta potential of the reference standard. Combination of equations (5) and (6) gives t_m/t_r:

$$\frac{t_m}{t_r} = \frac{\xi_c + \frac{2\xi_r}{3} f(\kappa a)}{\xi_c + \frac{2\xi_a}{3} f(\kappa a)} \qquad (7)$$

Expression (7) is valid under the condition where the average temperatures during the periods from the start of a run to t_r and t_m are identical. This condition is satisfied if t_r and t_m are large compared to the time required for thermal equilibrium to be established soon after the commencement of a run and if no significant drift in the capillary temperature occurs during separation. Examination of equation (7) reveals no term that is temperature-dependent, given the fact that ξ_c, ξ_r, ξ_a and $f(\kappa a)$ are all relatively temperature-insensitive (11,12,16,17). Thus, t_m/t_r is immune to the adverse effects associated with capillary heating. Nevertheless, a reference standard is mandatory for the utility of t_m/t_r. This is problematic, particularly in the analysis of complex mixtures where selecting a well-behaved reference standard (except for neutral species) with an appropriate migration time in the electropherogram can be arduous. Besides, difficulty arises from samples containing analytes with widely different migration times, which leaves t_m/t_r vulnerable to thermal drift. t_m/t_r is also incompatible with step or gradient potential runs. Furthermore, successful inter-capillary data comparisons require that the ξ_c's are identical and a common reference standard is agreed upon by the practitioners. All the restrictions discussed above drastically limit the practical use of t_m/t_r in routine analyses.

Migration index

Plots of v_m (or $1/t_m$) against I, the current, consist of straight lines even at the high values of I typical in ordinary CZE applications with or without cooling (8-13). In fact, the relationship between E and I has been used as a test of T control (11,18).

To account for this, Hjertén (16) and Tsuda (19) had derived the following expression to relate v_m and i, the current density:

$$v_m = \frac{ei}{k\eta}[\xi_c + \frac{2\xi_a}{3}f(\kappa a)] \tag{8}$$

where k is the specific conductance of the running buffer. The slope of the plot of v_m against i contains η and k, both exhibiting rather sensitive temperature dependencies. But η and k change in such a way that $k\eta$ remains constant for small variations in temperature (20). In fact, the product of the limiting molar conductivity of an electrolyte ($\Lambda°$) and the viscosity coefficient of the solvent ($\eta°$) is known as the Walden product whereas the assertion that $\Lambda°\eta°$ is independent of temperature is termed the Walden rule (21,22). The condition of the Walden product as well as the validity of the Walden rule have profound influences on the index and will be discussed later.

The easily measured I can be used to monitor v_m and, therefore, correct for any effect that temperature has on v_m. This is accomplished by integrating i/L against time which results in a migration index (MI) as defined below:

$$MI = \int_0^{t_m} \frac{i}{L} dt \tag{9}$$

It can be shown that MI can be expressed as follows (see Appendix):

$$MI = \frac{k\eta}{e[\xi_c + \frac{2\xi_a}{3}f(\kappa a)]} \tag{10}$$

MI is a function of ξ_c and ξ_a. This renders MI useful in specifying analytes separated in a given buffer using capillaries with identical ξ_c's. MI is, in fact, the slope of

the plot of i against v_m which, as discussed earlier, is insensitive to temperature. As a result, *MI* should show superior performances compared to t_m in terms of precision, reproducibility and inter-laboratory data transferability. In addition, *MI* is independent of the potential (or electric field) utilized in the separation. This suggests that *MI* can be used to relate the results obtained in runs carried out using different constant or gradient potentials. Moreover, *MI* is neither a function of the length nor inner diameter (i.d.) of the capillary. Consequently, data transfer between capillaries of distinct dimensions is straightforward.

Adjusted migration index

Application of t_m and *MI* is restricted to runs performed in capillaries with identical ξ_c's, as revealed in equations (5) and (10) respectively. To ensure that different capillaries possess the same ξ_c's, meticulous control of the coating manufacturing procedures, good temporal stability of the coatings and reproducible equilibration conditions are vital. Such is difficult to accomplish and, in most instances, untenable in light of the intrinsic differences that exist even amongst capillaries manufactured by the same company from batch to batch. To exacerbate matters further, undesirable adsorption of sample constituents could alter ξ_c, resulting in a changed μ_{eo}.

To allow specification of analytes without the constraints imposed by temperature- and ξ_c-related considerations, an adjusted migration index (*AMI*) is proposed. Suppose $(MI)_{eo}$ denotes the *MI* of an unretained, neutral marker. Then *AMI* is defined as follows:

$$AMI = \frac{(MI)_{eo} \cdot MI}{(MI)_{eo} - MI} \tag{11}$$

Substitution of equation (10) into equation (11) gives:

$$AMI = \frac{3k\eta}{2\varepsilon\xi_d f(\kappa a)} \tag{12}$$

It can be seen that *AMI* is dependent upon ξ_a in a given running buffer, but not ξ_c or temperature. Thus, *AMI* has the capability of being used to specify analytes determined not only in capillaries of different dimensions using distinct applied potentials, but also those with different surface compositions (and, hence, ξ_c's). This relaxes the stringent requirements placed upon the capillary coating manufacturing processes while facilitating the practical transfer of *AMI* data between laboratories.

A problem arising from the use of MI and AMI in the transfer of data between capillaries with different i.d.'s is that the i.d.'s of the capillaries concerned have to be known with an accuracy of within 0.5%. This aspect of capillary manufacturing technology presents a problem to the performance of AMI. In addition, application of AMI in data transfer requires that the concentrations of the buffers used be controlled to the same degree of accuracy. However, the latter problem can be solved with adequate attention to detail.

MATERIALS AND METHODS

Detection

The laser-induced fluorescence detector employed in this study has been described elsewhere (7). Briefly, a laser beam (350 nm) is focused on-column into the detection region located at about 15 cm from the exit end of the capillary. A microscope objective is used to collect and direct the fluorescence onto a photomultiplier tube. Scattered light is excluded from passage onto the photomultiplier tube by cut-off and spatial filters.

Capillary electrophoresis

The CZE setup has also been described (23). All the capillaries used in this study (Polymicro Technologies, Phoenix, AZ) were treated with a 50/50 (v/v) methanol/water mixture followed by 0.1 *M* NaOH (aq), each for 30 min. Then they were equilibrated with the running buffer for at least 12 hours before use. The dimensions of the capillaries and other pertinent information specific to each study are given in "Results and Discussion". All injections were by electromigration at 30 kV for 1 s. All the chemicals used in preparing the running buffers are reagent grade and the water is conductivity grade. The analytes in the sample buffer are (1) coumarin 2(7-hydroxy-*4*-methylcoumarin), (2) coumarin 343(*SYN: 1,2,4,5,3H,6H,10H*-tetrahydrobenzopyrano(*9,9a,1-gh*)-quinolizin-*10*-one-9-carboxylic acid) and (3) disodium fluorescein (Eastman Kodak, Rochester, NY) each present at 1 x 10^{-6} *M* and is dissolved in the running buffer.

Data acquisition

A DT2827 A/D converter (Data Translation, Marlboro, MA) was configured in the 2-channel collection mode to simultaneously acquire signals from 2 multimeters (Keithley, Cleveland, OH) with the data stored in an IBM PC/AT microcomputer (Boca Raton, FL). The model 160B multimeter was used to monitor the current from the photomultiplier tube to record the electropherograms whereas the model 197 multimeter records the electrophoretic current. 3000 data points were collected from each channel while ensuring that at least 1500 points were acquired before the appearance of the fastest-migrating analyte peak.

Data processing

After the completion of each run, the data was processed with a BASIC program capable of first identifying the migration time of each analyte by the location of the maximum height of its peak and then calculating *MI* through numerically integrating the current with time. Depending on the study, the program also evaluated the *AMI*, t_m/t_r, μ_{ep}, Et_m and Et_m/L of each analyte.

RESULTS AND DISCUSSION

Precision of migration data

The importance of precision of migration data to a separation technique needs no further elaboration. It is, therefore, of interest to compare the performances of t_m, t_m/t_r and *MI* in this regard. As depicted in Table 1, the precision of each of the parameters, as indicated by the RSDs, is impressive. However, the precision of *MI* and t_m/t_r is clearly superior to that of t_m. This lends support to the contention that thermal effects figure prominently in the variations of t_m in the present set of experimental conditions, which is quite typical for a homemade system with natural air convection cooling. As mentioned before, both t_m/t_r and *MI* are rather temperature-insensitive, in contrast to t_m. The RSDs for *MI* are four times smaller than those for t_m/t_r. An explanation for this might be the vulnerability of t_m/t_r to thermal drift on the time-scale of the t_m's of the analytes. In the case of *MI*, since *I* is measured throughout the run time, the v_m of the analyte is known at any instant and, as a result, any changes in v_m due to thermal effects are corrected for in the evaluation of *MI*. This accounts for the slightly better precision of *MI* than t_m/t_r.

Relating results obtained in constant potential runs

In CZE method development, other than varying the pH, buffer type and ionic strength, the most common parameter to manipulate is the *E* employed. Whereas separation efficiency at low *E*'s is limited by molecular diffusional spreading of the analyte zone, high *E*'s cause thermal band broadening (1). A compromise between these two extremes needs to be struck to minimize the separation time while allowing adequate resolution of the components of interest. Besides, it is

Table 1: Comparison of Precision of t_m, t_m/t_r and *MI*

	$t1^a$	$t2^a$	$t3^a$	$t2/t1$	$t3/t1$	$MI1^b$	$MI2^b$	$MI3^b$
mean	2.63	3.56	4.11	1.36	1.57	1.38	1.87	2.16
RSD (%)	0.7	0.7	0.7	0.2	0.2	0.05	0.05	0.05

[a]in *min*; [b]in *C cm*$^{-3}$

Condition: V=30.0 *kV*; L=65.0 *cm*; i.d.=50 μm; Buffer: 10 *mM* sodium phosphate; pH 6.62; T: capillary cooled by ambient air (22 °*C*)

Procedure: Successive injections were made between 1-2 *min* after the completion of each previous run.

Notation: *tj* and *MIj* denote the t_m and *MI* of analyte *j* respectively while the degrees of freedom (n-1) were 10.

advantageous to be able to make use of CZE data obtained using a different E in the literature or in the same laboratory at an earlier time. Hence, it would prove to save both time and effort if the parameter which specifies an analyte in the electropherogram is independent of the applied E.

An obvious candidate for this is μ_{ep}. However, due to the fact that different amounts of power are generated in the capillary at different E's, the average temperature of the buffer solution within the capillary differs from one E to another. As shown in ref. (18) and (24), the temperature rise within the capillary is roughly proportional to E^2. This results in large changes in μ_{ep} through its dependence upon η (equation (1)), which renders the assignment of previously identified analytes to peaks obtained using a different E a separate effort. With analyte (1) indicating ν_{eo}, it can be seen in Table 2 that the magnitude of μ_{ep} increases as E increases and the changes in the μ_{ep}'s of analytes (2) and (3) obtained at 154 vs. 462 *V/cm* exceed

11%. Even though attempts have been made in minimizing temperature elevation in the capillary through air- (18,25-27) and liquid-cooling (13,27) in typical running conditions, significant decreases in η persist at high E's. It has been demonstrated that a Peltier thermoelectric device can effectively control capillary temperature (18), but it is not conveniently accessible. Therefore, it is not fruitful to utilize μ_{ep} to relate results from runs performed at different E's. By the same token, multiplying t_m by E does not rid the resulting parameter of its dependence upon η, and thus, T, as revealed in Table 2 and equation (5).

t_m/t_r, MI, μ_{ep}, t_m and Et_m at various E's are compared in Table 2. As expected on the basis of equation (5), the t_m's vary widely as a function of E. The μ_{ep}'s and Et_m's exhibit the same behavior except that the variations are somewhat smaller than those for the t_m's. This can be explained by the fact that the dependence of μ_{ep} and Et_m on E is, unlike t_m, not explicit but manifests itself through η. On the other hand, both t_m/t_r and MI remain quite constant as E is changed. Thus, it can be concluded that t_m/t_r and MI are virtually independent of the E used in the separation. Hence, t_m/t_r and MI can conveniently be utilized in the comparison of data obtained in separations carried out with distinct E's.

Relating results obtained in gradient potential runs

Although disparate in principles of operation, GC, HPLC and CZE all share a common attribute, namely: the capability of rapidly resolving a mixture of analytes with widely different physical properties through the temporal adjustment of a parameter in the separation condition. In GC and HPLC, the most popular choices are temperature and eluent programming to allow adequate resolution of analytes

Table 2: Comparison of Parameters in Constant- and Programmed-Potential Runs

	$E(Vcm^{-1})$			
	154	307	462	3.5min 307→462
$t1^a$	8.40	4 31	2.48	3.94
$t2^a$	11.41	5 85	3.36	4.80
$t3^a$	13.08	6 73	3.88	5.30
$Et1^b$	1.29	1.31	2.01	1.29[c]
$Et2^b$	1.75	1.80	2.07	1.68[c]
$Et3^b$	2.01	2.07	1.79	1.91[c]
$\mu 2^d$	-10.2	-10.4	-11.4	-9.3[e]
$\mu 3^d$	-13.8	-14.0	-15.8	-12.9[e]
$t2/t1$	1.36	1.36	1.36	1.22
$t3/t1$	1.56	1.56	1.57	1.35
$MI1^f$	1.38	1.38	1.37	1.38
$MI2^f$	1.88	1.87	1.85	1.87
$MI3^f$	2.15	2.15	2.14	2.15

[a]in *min*; [b]in 10^{-3} *V min* cm^{-1}; [c]calculated from $t_s(307\ Vcm^{-1}) + (t_m\text{-}t_s)(462\ Vcm^{-1})$ where t_s=3.50 *min*; [d]in $cm^3kV^{-1}min^{-1}$; [e]calculated from $L\{1/[t_s(307\ Vcm^{-1})+(tj\text{-}t_s)(462\ Vcm^{-1})] - 1/[t_s(307\ Vcm^{-1})+(t1\text{-}t_s)(462\ Vcm^{-1})]\}$; [f]in $C\ cm^{-3}$

Condition: as in Table 1 except for the *V* used

Procedure: The value of each parameter was computed from the mean of the data from two separate but consecutive runs with the second injection made within 2 *min* of the completion of the first run.

possessing, respectively, a wide range of volatilities and hydrophobicities in a reasonably short period of time. The demand for this in CZE is no less rigorous, since samples might consist of analytes with opposite polarities and very different electrophoretic mobilities. Depending on the application, one way of shortening the separation time of analytes having a wide range of p*K* values is the employment of a dynamic pH gradient (28,29). An equally promising approach involves the use of a potential gradient (14).

The upper limit of the *E* utilized in a constant-potential separation is determined by the pair of analytes that are most difficult to resolve. Hence, the potential can be stepped up immediately subsequent to the elution of the two components corresponding to the potential-limiting pair of analytes. The potential to step up to is, in turn, decided by the next pair of analytes that are hardest to resolve but yet to emerge. Likewise, the potential can be manipulated in a similar fashion to minimize the separation time while optimizing the resolutions of all the remaining components. Of course, care must be taken not to exceed the critical point where thermal convection becomes intolerable.

In the implementation of such a strategy, one is faced with the task of assigning each analyte to a different migration time or relative migration once a new potential-program is attempted. This renders the process both cumbersome and time-consuming. However, the use of *MI* bypasses such difficulties since the v_m's of all the analytes are monitored continuously through *I* throughout the run time. Thus, any change in v_m due to the application of a changing potential is corrected for in *MI*. The behaviors of t_m, t_m/t_r and *MI* at constant and gradient potentials are documented in Table 2 where the last column depicts the results obtained in a programmed-potential run with an abrupt increase in *V* from 20.0 to 30.0 *kV* at 3.50

min into the separation. As expected, t_m varies widely in the constant- and programmed-potential runs whereas t_m/t_r remains unchanged at different constant potentials, but decreased in the programmed-potential run. The behavior of t_m/t_r can be attributed to the fact that equation (7) is derived on the assumption that E is invariant with time. This is valid for constant-potential runs, but not programmed-potential runs. Simply correcting t_m, t_m/t_r and μ_{ep} with the temporal function of E still fails to relate the t_m's, t_m/t_r's and μ_{ep}'s in constant- and programmed-potential runs as the change in the temperature-dependent η at different E's is left unaccounted for as shown in Table 2. *MI*, however, is not only unaltered in the programmed-potential run, but its value is the same as in the corresponding constant-potential runs. Consequently *MI* can be used to relate the results obtained in different constant- and gradient-potential runs.

Relating results obtained in capillaries of different lengths

In GC and HPLC, it is possible to relate the results obtained in columns of different lengths by simple geometric corrections provided that the capacity factors of the analytes can be reproduced from column to column. Extension of the previous statement to CZE is valid if $(\mu_{eo}+\mu_{ep})$ can be made constant from capillary to capillary. In practice, the transfer of data between capillaries of different lengths in CZE is, however, not so straightforward. This is largely a consequence of the inevitable temperature differences of the buffer solutions during separation because of the distinct extents of Joule heating and varied heat-dissipating capabilities of the capillaries with different lengths when a constant V is employed. The resulting temperature differences render $(\mu_{eo}+\mu_{ep})$ different in capillaries with different lengths through η (equations (1) and (3)). As shown in ref. (18) and (24), the

temperature rise of the buffer solution within the capillary from the start of a run to the steady state is roughly proportional to $1/L^2$. Hence, even if the effects of the distinct E's together with the L's are taken into account, the transfer of results between capillaries with different lengths remain untenable in the case where the capillary is cooled by natural air convection. A substantiation of this is revealed in Table 3 where the Et_m/L's obtained in capillaries with three different lengths for all the analytes vary as the capillary length changes. While one could make the argument of performing separations in capillaries of different lengths with identical E's, such an approach is cumbersome in practice and inaccurate in light of the approximate nature of the proportionality of T increase and $(E/L)^2$. Nonetheless, the transfer of results between capillaries of different lengths remains useful not only in inter-capillary data comparison, but would also save time in method development. Recall that in equation (5), t_m is directly proportional to L and E is inversely proportional to L for constant V operation. Provided that secondary thermal effects are not serious, one could always shorten the analysis time by using a shorter capillary.

As mentioned earlier, t_m/t_r and MI are insensitive to effects associated with T changes. Thus, the differences in the T's of the buffer solution in capillaries with different lengths during separation would not affect either parameter. Indeed, the results shown in Table 3 are in agreement with expectation in that both the t_m/t_r's and MI's of the three analytes did not display any significant change in the three capillary lengths studied. Consequently, both t_m/t_r and MI can be used to relate the results obtained in capillaries of different lengths. Moreover, the fact that the MI's stayed constant from one length to another gives an indication of the high degree of uniformity of ξ_c throughout the length of the capillary. Since non-uniform ξ_c values within the capillary result in viscous flow and, therefore, loss of efficiency (30), the

Table 3: Comparison of t_m, t_mE/L, t_m/t_r and *MI* Obtained in Capillaries of Different Lengths

	L(cm)		
	55.0	65.0	75.0
t1[a]	1.71	2.69	3.88
t2[a]	2.35	3.68	5.36
t3[a]	2.72	4.25	6.19
Et1/L[b]	2.33	2.48	2.59
Et2/L[b]	3.20	3.40	3.93
Et3/L[b]	3.71	3.93	4.13
t2/t1	1.37	1.37	1.38
t3/t1	1.59	1.58	1.60
MI1[c]	1.31	1.32	1.32
MI2[c]	1.80	1.80	1.81
MI3[c]	2.08	2.08	2.08

[a]in *min*; [b]in $10^2 kV\ min\ cm^{-2}$; [c]in $C\ cm^{-3}$

Condition: as in Table 1 except pH 6.75
Procedure: as in Table 2

constancy of t_m/t_r and *MI* as a function of L can be utilized as a means of determining whether non-uniformity in the ξ_c of the capillary (which could be a consequence of intrinsic differences in the physical properties of the wall materials or severe solute adsorption) exists.

Relating results obtained in capillaries with different ξ_c's

The wide variety of coating materials from different commercial sources only add to the difficulty in the transfer of CZE data obtained in different capillaries. Even if the capillaries in use possess coatings comprising the same materials nominally, it is unlikely that the requirement of identical ξ_c's can be fulfilled with the most time-consuming and involved capillary pre-treatment procedures. The utility of *AMI* rids the analyst of such concerns as *AMI* is not only unaffected by T, but it is also independent of the ξ_c of the capillary. However, since resolution is dependent upon μ_{eo} (1) and, hence, ξ_c, care must be exercised to ensure that adequate resolution is preserved in separations performed in capillaries with different ξ_c's. A major area of CZE involves suppressing v_{eo} by making ξ_c negligible. In that case, MI would be adequate for inter-capillary data transfer.

A comparison of t_m, t_m/t_r, *MI* and *AMI* obtained in two capillaries with different ξ_c's is shown in Table 4. Since the capillaries are of identical dimensions and the same E is used in the separations, the difference in the ξ_c's is reflected in the distinct t_m's of all the analytes in the two capillaries. As expected on the basis of equations (7) and (10) respectively, both the t_m/t_r's and *MI*'s changed from one capillary to another. Of all the parameters outlined, only *AMI* remained relatively unaltered. In fact, the *AMI*'s for each analyte differed from each other by less than 1% between the two capillaries. This demonstrates the feasibility of utilizing *AMI* in

Table 4: Comparison of t_m, t_m/t_r, *MI* and *AMI* Obtained in Capillaries with Different ξ_c's

	Capillary A	Capillary B
t1[a]	3.46	3.13
t2[a]	4.90	4.28
t3[a]	5.76	4.93
t2/t1	1.41	1.66
t3/t1	1.37	1.58
MI1[b]	1.41	1.30
MI2[b]	1.99	1.78
MI3[b]	2.34	2.05
AMI2[b]	-4.85	-4.81
AMI3[b]	-3.57	-3.55

[a]in *min*; [b]in *C cm*$^{-3}$

Condition: as in Table 3 with L=75.0 *cm*
Procedure: Capillary A: as in Table 2
Capillary B: Capillary A was flushed with 0.1 *M* NaOH(*aq*) for 6 *hrs* followed by equilibration with the running buffer for 12 *hrs* and the subsequent procedure was identical to that for Capillary A.

relating the results obtained in capillaries with different ξ_c's. Accordingly, no theoretical barrier obstructs the use of *AMI* in the transfer of data obtained in capillaries composed of different materials (e.g., Teflon, Pyrex, etc.).

Relating results obtained in capillaries with different inner diameters

Disputes over the optimal capillary i.d. in CZE analyses are many-faceted and depend upon the relative degree of separation efficiency and detection sensitivity demanded by the task at hand. Use of a large i.d. capillary (e.g., 200 μm) maximizes the concentration detection sensitivity with the popular UV absorption detector while sacrificing some useful separation efficiency through severe thermal band broadening. On the other hand, concentration detection sensitivity becomes a matter of concern despite a gain in separation efficiency when a small i.d. capillary (e.g., 5 μm) is utilized. In fact, due to the mutual exclusiveness of detection sensitivity and separation efficiency, any efforts in pushing toward a standardized capillary i.d. are bound to be unsuccessful. Therefore the advantages realized over the ability of relating the results obtained in capillaries with different i.d.'s remain attractive. In a previous section, it has been demonstrated that one could use *MI* as a parameter in relating the results obtained in capillaries of different lengths. This is possible because of the *T*-insensitive nature of *MI*. However, *MI* is not only a function of ξ_a, but also ξ_c. While it is possible to study the behavior of *MI* with the assurance of constancy in ξ_c by simply cutting off parts of the same capillary, the same is not applicable to i.d. studies in that no readily accessible means exists that would ensure that the ξ_c's of capillaries with different i.d.'s are identical. One method which permits the determination of ξ_c in a manner free of constraints imposed by *T* effects involves the measurement of the streaming potential (31), but it necessitates the construction of

Table 5: Comparison of t_m, t_m/t_r, *MI* and *AMI* Obtained in Capillaries with Different i.d.'s

	i.d. (μm)	
	20	50
$t1^a$	3.47	3.36
$t2^a$	4.67	4.68
$t3^a$	5.33	5.43
t2/t1	1.35	1.39
t3/t1	1.53	1.62
$MI1^b$	1.26	1.40
$MI2^b$	1.70	1.95
$MI3^b$	1.93	2.26
$AMI2^b$	-4.86	-4.96
$AMI3^b$	-3.60	-3.66

^{a}in *min*; ^{b}in $C\ cm^{-3}$

Condition: as in Table 4 except V=25.0 kV and pH 6.66
Procedure: as in Table 2

specialized instruments and is, therefore, not conveniently accessible. As a result, no deliberate effort was made here to guarantee that the capillaries possess identical ξ_c's.

In the present study, even with meticulous attention devoted to ensuring that the capillaries studied were pretreated identically, the resulting ξ_c's still differed somewhat, as unveiled in the values of *MII* in Table 5. For the same reason, the *MI*'s of each of the remaining analytes differed from one capillary to another. Surprisingly, t_m displayed smaller changes from one i.d. to another in Table 5, an observation contrary to many previous studies carried out in our laboratory (data not shown). As a matter of fact, t_m is usually observed to increase by as much as 30% from a 50-μm i.d. capillary to a 20-μm one because of the poor heat-dissipating capability of the former and is assumed to be unsuitable as a parameter for the transfer of data between capillaries with different i.d.'s. In the present study, the effect of the smaller η of the buffer solution in the 50-μm i.d. capillary compared to that in the 20-μm one is accidentally offset by the smaller ξ_c of the former compared to that in the latter, thereby concealing the sensitive dependence of t_m upon T. The coincidental nature of the invariant t_m's from one i.d. to another is further supported by the clear trend of a positive rate of increase of the t_m's in the 50- over the 20-μm capillary from analytes (1) to (3). As revealed in equation (5), had η remained constant from one i.d. to another, no such increase should have been observed. Another manifestation of the smaller ξ_c in the 50-μm i.d. capillary compared to that in the 20-μm one can be found in the greater t_m/t_r in the 50-μm compared to 20-μm capillary for each analyte (equation (7)). The use of t_m/t_r in relating the results obtained in capillaries with different i.d.'s is, as discussed earlier, unsatisfactory due to its dependence upon ξ_c, which leaves *AMI* the only feasible alternative.

Despite its insensitivity to T and ξ_c, the accuracy of *AMI* in the transfer of data between capillaries with different i.d.'s is limited by the accuracy with which the i.d.'s of the capillary can be determined. Recall that i is computed from I and A, the cross-sectional area of the inner space of the capillary. Since an error of ±4% in the i.d. of an average-sized capillary (50 μm) is not uncommon (32), the small difference between the *AMI*'s from one i.d. to another in the present study (<2%) seems reasonable. Further improvement in the accuracy with which *AMI* can be used to relate results obtained in capillaries with different i.d.'s awaits a corresponding improvement in the capillary manufacturing technology.

Walden product, Walden rule and migration indices

The insensitivity of $k\eta$ to T is the basis upon which *MI* is devised. Any deviation from this would directly translate into an error in *MI*. The data in Table 2 indicates a very small decrease in the *MI*'s as E (and, thus, T) increases. This is observed to be a consistent trend even with buffers of other concentrations and pH's (data not shown). An explanation for this can be found in the context in which the Walden rule is applied to the index.

A consequence of Stokes' relation (33), the Walden rule is strictly valid only if the assumptions made in the former are fulfilled experimentally. First, $\Lambda°$ and $\eta°$ are *limiting* terms which imply that they are the Λ and η extrapolated to infinite dilution and it is $\Lambda°\eta°$, but not $\Lambda\eta$, that is independent of T. Since the increases in the Λ's of most electrolytes as T increases are less than those of the corresponding $\Lambda°$'s, $\Lambda\eta$ decreases slightly as T increases (34,35). Secondly, in the derivation of the Walden rule, it is assumed that any change in $\Lambda°$ is caused by a change in the macroscopic $\eta°$. For an ion whose dimensions are much greater than those of the solvent molecule,

this is an accurate description. However, for the small buffer ions typical in CZE, this can at best be approximate since the microscopic η° "experienced" by the migrating ion may not necessarily be identical to the macroscopic η°. This has been used to explain the decrease in $\Lambda^\circ\eta^\circ$ (about 25%) as T increases (from 0-100°C) (36,37). Thirdly, the hydrodynamics inherent in Stokes' relation applies strictly to spherical ions only. In nature, truly spherical ions are the exception rather than the norm. This also contributes to the behavior of the $\Lambda^\circ\eta^\circ$'s of non-spherical ions as a function of T (36,37).

Together, the assumptions discussed above manifest themselves in the small negative T-coefficients of the $\Lambda^\circ\eta^\circ$'s for most electrolytes (34,35). Since the T of the buffer solution in the capillary increases as the E is increased, the decrease in *MI* at high E's can be explained by the direct dependence of *MI* upon $k\eta$, as depicted in equation (10).

Future work

It can be recognized from Eq. (8) and the results presented here that a constant current mode (without using *MI* or *AMI*) is superior to a constant potential mode of operation for CZE in terms of precision in migration times. However, constant current operation still does not allow comparison of results from capillaries with different lengths, internal diameters (current density), or ξ_c's, and cannot benefit from gradient potential schemes for speeding up late eluting peaks. Constant current operation was not attempted in this work because a valid comparison cannot be made unless i is stabilized to better than 0.05%, according to Table I.

In the present study, the utility of *MI* and *AMI* has been demonstrated using a 10 *mM* sodium phosphate buffer at close to neutral pH. However, it is known that

the T dependence of $k\eta$ is abnormally perturbed by the unique transport mechanisms of H^+ and OH^- (36,37). Hence, it is necessary to explore the behavior of *MI* and *AMI* in highly acidic and basic buffer solutions. Besides, both the analyte concentration and buffer concentration dependences of *MI* and *AMI* (away from infinite dilution) are unclear. Since equations (10) and (12) are derived on the assumption that non-linear effects such as orientational effects and the "relaxation effect" (38) do not affect the analyte transport process, generalization of *MI* and *AMI* calls for further studies with other interesting analytes. Finally, the use of *AMI* in the archiving of migration data for a large number of analytes seems feasible.

APPENDICES

Derivation of expression for *MI*

From equation (8):

$$\frac{dx}{dt} = \frac{\varepsilon i}{k\eta}\left[\xi_c + \frac{2\xi_a}{3}f(\kappa a)\right] \tag{13}$$

where x denotes the axial distance of the capillary beginning at the injection end and t, the time. Since the slope of the plot of dx/dt against i is constant, rearranging and integrating equation (13) from the start of a run ($t = 0$; $x = 0$) to its finish ($t = t_m$; $x = L$) give:

$$\int_0^{t_m} i\,dt = \frac{k\eta}{\varepsilon\left[\xi_c + \frac{2\xi_a}{3}f(\kappa a)\right]} \int_0^{L} dx \tag{14}$$

Hence,

$$\int_0^{t_m} \frac{i}{L}\,dt = \frac{k\eta}{\varepsilon\left[\xi_c + \frac{2\xi_a}{3}f(\kappa a)\right]} \tag{15}$$

Derivation of expression for *MI* when detector is not at end of capillary

When the detector is not at the end of the capillary, equation (10) yields :

$$(MI)_d = \frac{(l/L)k\eta}{\varepsilon\left[\xi_c + \frac{2\xi_a}{3}f(\kappa a)\right]} \tag{21}$$

where $(MI)_d$ is the *MI* of an analyte obtained in a capillary with its detection region

located at a distance of l from the injection end. It follows that:

$$MI = \left(\frac{L}{l}\right)(MI)_d \tag{22}$$

REFERENCES

1. Jorgenson, J.; Lukacs, K. D. Science 1983, 222, 266-272.
2. Ewing, A. G.; Wallingford, R. A.; Olefirowicz, T. M. Anal. Chem. 1989, 61, 292A-294A, 296A, 298A, 300A-303A.
3. Kuhr, W. G. Anal. Chem. 1990, 62, 403R-414R.
4. Overbeek, J. Th. G.; Wiersema, P. H. In Electrophoresis. Theory, Methods and Applications, Vol. 2; Bier, M., ed.; Academic Press, New York, 1967, p. 9.
5. Rice, C. L.; Whitehead, R. J. Phys. Chem. 1965, 69(11), 4017-4024.
6. Lee, C. S.; Blanchard, W. C.; Wu, C.-T. Anal. Chem. 1990, 62, 1550-1552.
7. Pfeffer, W. D.; Yeung, E. S. Anal. Chem. 1990, 62, 2178-2182.
8. Jorgenson, J. W.; Lukacs, K. D. Anal. Chem. 1981, 53, 1298-1302.
9. Tsuda, T.; Nomura, K.: Nakagawa, G. J. Chromatogr. 1982, 248, 241.
10. Tsuda, T.; Nomura, K.; Nakagawa, G. J. Chromatogr. 1983, 264, 385.
11. Terabe, S.; Otsuka, K.; Ando, T. Anal. Chem. 1985, 57, 834-841.
12. Terabe, S.; Otsuka, K.; Ando, T. Anal. Chem. 1989, 61, 251-260.
13. Issaq, H. J.; Atamna, I. Z.; Metral, C. J.; Muschik, G. M. J. Liq. Chromatogr. 1990, 13(7), 1247-1259.
14. McCormick, R. M. Anal. Chem. 1988, 60, 2322-2328.
15. Atkins, P. W. Physical Chemistry, 3rd ed.; W. H. Freeman and Co., New York, 1986, p. 595.
16. Hjertén, S. Chromatogr. Rev. 1967, 9, 178.
17. Overbeek, J. Th. G.; Bijsterbosch, B. H. In Electrokinetic Separation Methods; Righetti, P. G.; Van Oss, C. J.; Vanderhoff, J. W., ed.; Elsevier/North-Holland Biomedical Press; Amsterdam, 1979; p. 30.

18. Nelson, R. J.; Paulus, A.; Cohen, A. S.; Guttman, A.; Karger, B. L. J. Chromatogr. 1989, 480, 111-127.

19. Tsuda, T. J. Liq. Chromatogr. 1989, 12(3), 2501-2514.

20. Robinson, R. A.; Stokes, R. H. Electrolyte Solutions, 2nd edn.; Butterworth, London, 1968, p. 130.

21. Walden, P.; Ulich, H.; Busch, G. Z. Phys. Chem. 1926, 123, 429.

22. Walden, P.; Birr, E. J. Z. Phys. Chem. 1931, 153A, 1.

23. Kuhr, W. G.; Yeung, E. S. Anal. Chem. 1988, 60, 2642-2644.

24. Lukacs, K. D.; Jorgenson, J. W. J. High Resolut. Chromatogr. Chromatogr. Commun. 1985, 8, 407-11.

25. Rasmussen, H. T.; McNair, H. M. J. Chromatogr. 1990, 516, 223-31.

26. Foret, F.; Deml, M.; Boček, P. J. Chromatogr. 1988, 452, 601-613.

27. Gobie, W. A.; Ivory, C. F. J. Chromatogr. 1990, 516, 191-210.

28. Boček, P.; Deml, M.; Pospíchal, J.; Sudor, J. J. Chromatogr. 1989, 470, 309.

29. Šustáček, V.; Foret, F.; Boček, P. J. Chromatogr. 1989, 480, 271-276.

30. Knox, J. H.; McCormack, K. A. J. Liq. Chromatogr. 1989, 12(13), 2435-2470.

31. Van De Goor, A.; Wanders, B.; Everaerts, F. J. Chromatogr. 1989, 470, 95-104.

32. From Data Sheet supplied by Polymicro Technologies for their "Flexible Fused Silica Capillary Tubing" (Polymicro Technologies Inc., Phoenix, AZ).

33. Stokes, G. G. Trans. Camb. Phil. Soc. 1845, 8, 287.

34. Wyman, J. Phys. Rev. 1930, 35, 623-634.

35. Erdey-Grūz, T. Transport Phenomena in Aqueous Solutions; Halsted Press: New York, 1974; p. 300.

36. Padova, J. In Water and Aqueous Solutions. Structure, Thermodynamics and Transport Processes; Horne, R. A., Ed.; Wiley-Interscience: New York, 1972; pp. 159, 638.

37. Erdy-Grūz, T. Transport Phenomena in Aqueous Solutions; Halsted Press: New York, 1974; pp. 266-273.

38. Grossman, P. D.; Soane, D. S. Anal. Chem. 1990, 62, 1592-1596.

PAPER II.

COMPENSATING FOR INSTRUMENTAL AND SAMPLING BIASES ACCOMPANYING ELECTROKINETIC INJECTION IN CAPILLARY ZONE ELECTROPHORESIS

INTRODUCTION

Despite the high efficiency and speed of separation that can be achieved by capillary zone electrophoresis (CZE) and its applicability to nonvolatile and thermally labile species, so far the technique is not widely accepted for routine analyses. A major drawback of CZE in many practical analyses is its poor quantitative capability.

The two most commonly practiced and accessible sample introduction methods in CZE are hydrodynamic (HD) and electrokinetic (EK) injection. While HD injection is quite insensitive to variations in sample solution composition and is thus relatively free of sampling biases, it necessitates the construction of complicated instruments due to the need of a precise mechanism to control pressure. As discussed by Gordon *et al.* (1) and Dose *et al.* (2), the simplicity of EK injection equipment should render it more reliable than HD injection. In fact, efforts have been expended on automating EK injection (3,4) as well as utilizing one (2,5-9) and two (2) internal standards to improve quantitative precision. In general, the use of internal standards offers better precision than without standards. However, several disadvantages accompany the use of internal standards. First, with the single internal standard method, it may not be convenient to find an internal standard with a migration time distinct from but similar to that of the analyte. This is because precision degrades as the difference between the migration times of the analyte and standard increases (2). With the two-internal standard technique (2), the requirement that the migration times of the standards sandwich those of the analytes makes the selection of the standards arduous and lengthens the run time. Secondly, in practical analyses, there exists the possibility of unknown impurities in the sample co-migrating with the internal standard, thereby affecting the quantitative accuracy for

all analytes. Thirdly, the necessity to accurately introduce internal standards to all sample solutions in known quantities complicates sample preparation, especially when dealing with small samples. Finally, one will also need to be concerned with loss of sensitivity due to dilution and possible interactions with the analytes (e.g., pH changes) when adding internal standards. As a consequence, it is important to further understand EK injection and explore new ways to improve its quantitative capability.

Many applications of CZE consist of determining analytes in sample matrices of different or unknown compositions. This presents a special problem for EK injection. The pH of the sample solution greatly influences ionization and thus the mobilities of the analytes during injection. For simplicity, we will neglect pH effects in this discussion. It has been identified that the quantity of analytes injected depends on the conductivity of the sample solution (10-12). While this can be alleviated by diluting a small amount of sample in a large volume of the running buffer, the ensuing loss of detectability may be intolerable in some cases, especially with the popular ultraviolet-visible absorbance detector. Use of the two-internal standard technique represents a solution to the problem (2). However, the use of internal standards may not always be desirable, as discussed earlier. Hence, it becomes necessary to investigate new alternatives to correct for sampling biases resulting from distinct sample solution conductivities.

In the present work, we present a method which improves the quantitative precision of CZE with EK injection by monitoring the electrophoretic current during injection and separation. Also, we show that the effects of sample conductivities on the amounts of analytes introduced with EK injections are nullified by proper corrections with the measured conductivities of the sample and buffer solutions

together with the migration times of the analyte and a neutral marker.

MATERIALS AND METHODS

The CZE apparatus employed resembles the one described earlier with several modifications (13). A model CV^4 variable wavelength ultraviolet-visible absorbance detector (Isco, Inc., Lincoln, NE) operating at 230 nm and a 65-cm long (42-cm working length), 77-μm i.d. fused-silica capillary tubing (Polymicro Technologies, Inc., Phoenix, AZ) were used. The analytes, used as received, were reagent grade acetophenone (analyte 1, neutral marker), *N*-benzoylphenylalanine (analyte 2), *p*-hydroxycinnamic acid (analyte 3) and benzoic acid (analyte 4) (Sigma Chemical Co., St. Louis, MO) present in all sample solutions at 0.60, 1.90, 4.00 and 4.30 mM respectively such that the peaks were all baseline-resolved, of about the same height and of similar appearance to those in ref. 2. The running buffer (40.0 mM sodium phosphate) and all sample solutions (100, 77, 55, 33 and 10 mM sodium phosphate) were at pH 7.67. The capillary was flushed with a 50 mM NaOH solution for 6 hours and then equilibrated with the running buffer for at least 4 days before use. Conductivity measurements were made with a model CDCN-36 conductivity detector equipped with a model CDCN-36-EP-K electrode (Omega Engineering, Inc., Stamford, CT) and all the readings reported were those at 25.0 °C. Although the present electrode requires at least 5 mL of solution, as little as 7 μL is feasible with the use of micro-electrodes which are available commercially. Semi-automated EK injections were controlled by an electronic timer in the control circuit (14) while manual EK and HD injections were timed by visual reference to a digital stopwatch. The injection times for EK and HD injections were 5 and 90 s respectively. HD was performed by raising the level of the sample vial 2 cm above that of the buffer vial. The separation and injection potentials for all runs were 15 kV. A/D conversion of

the running current and the detector output was via a 16-bit interface board (Data Translation, Marlborough, MA, DT2827) at 600 and 7.7 Hz for injection and separation respectively. Conversion is based on a sample-and-hold rather than a true integration mode. All computations were performed with a BASIC program on an IBM PC/AT (Boca Raton, FL) and the temporal location of the centroid of each peak was taken to indicate the analyte migration time.

RESULTS AND DISCUSSION

When an analyte is present at concentrations much lower than those of the buffer ions such that the conductivity of the sample zone is essentially identical to that of the running buffer, the migration velocity of analyte a (v_{ma}) during electromigration can be described by (13,15,16)

$$v_{ma} = K_a \frac{I}{A} \tag{1}$$

where A is the cross-sectional area of the capillary and K_a a constant determined by the buffer pH, dielectric constant, ionic strength, viscosity, size and shape of analyte a as well as wall and analyte ζ potentials. The crucial point is that v_{ma} is linearly proportional to the electrophoretic current (I) and not the applied electric field in the presence of temperature variations (13). Thus, I, which is easily measured, can be used to provide an accurate indication of v_{ma}. It follows that the amount of analyte a moving past axial location x at time t in a small increment of time is

$$dn_a(x,t) = K_a c_a(x,t) I(t) dt \tag{2}$$

where $n_a(x,t)$ and $c_a(x,t)$ denote, respectively, the amount and concentration of analyte a at x and t. Hence, the amount of analyte a passing through the detection region located at D is

$$n_{aD} = K_a \int_0^\infty c_a(D,t) I(t) dt \tag{3}$$

where in practice the integration is performed over a finite interval determined by the appearance of the analyte peak at the detector. Eq. 3 allows for temporal

fluctuations in v_{ma} through I(t) and, as discussed by Huang and co-workers (17), distinct analyte electrophoretic mobilities through K_a. This then accounts for variations in the migration velocity of each analyte passing the detector, which give rise to different peak areas for a given amount injected (17). Eq. 3 is more reliable, however, than simply using the total migration time, since only the individual velocities right at the moment of appearance at the detector are relevant. We have experimentally determined that I and, hence, V_{ma}, fluctuate by 0.36% over the time scale of a few minutes. This is explicitly accounted for in eq. 3.

EK injection of samples with conductivities similar to that of the running buffer

Because of the small i.d. and, thus, large resistance of the capillary, the electric field outside the capillary is typically negligible relative to that inside during electromigration (14). During EK injection, the sample solution is driven toward the capillary from the bulk by electroosmotic pressure (18) and, hence, no bias based on distinct analyte electrophoretic mobilities is expected initially. But, at the instant when the analytes cross the capillary-sample solution interface, in addition to electroosmotic flow, the analytes experience electrical forces whose magnitudes depend on, among other factors, their electrophoretic mobilities. The electroosmotic flow and electrical forces during EK injection should be identical in nature to the ones during separation because the conductivities and the pH's are identical. Therefore, from eq. 2, the amount of analyte a injected is

$$n_{ai} = K_a c_a^s \int_0^{t_i} I(t)dt \qquad (4)$$

where t_i is the time when I is non-zero during injection and c_a^s (= $c_a(0,t)$) the concentration of analyte a in the sample solution. Eq. 4 is valid if electromigration is

the only mode of analyte introduction. In eq. 4, K_a accounts for EK sampling biases resulting from distinct analyte electrophoretic mobilities (10,19) while I(t) compensates for variations in injection potential, injection time and temperature. Similar equations have been derived using the electric field or potential rather than I (2,10,11,19). However, since the relation between v_{ma} and electric field or potential is not linear whereas that between v_{ma} and I is linear (20-23), the use of I should provide more accurate results. Besides, treating the injection I as time-variant is more realistic than otherwise, as both the injection I-t (17) and injection zone-t (14) profiles are not plug-like, with or without a shunt resistor.

Now, provided that no irreversible adsorption of analytes occurs and sample solvent evaporation is not serious, the parameter of interest, c_a^s, which is constant from run to run and independent of variations in injection and separation conditions caused by changes in potential, injection time and temperature, can be obtained by combining eq. 3 and 4 (based on mass conservation) to give

$$c_a^s = \frac{\int_0^{\infty} c_a(D,t)I(t)dt}{\int_0^{t_i} I(t)dt} \qquad (5)$$

According to eq. 5, correcting the detector peak area with the temporal profile of I during separation and during injection should improve the quantitative precision of EK injection, if the errors concerned are significant. Noteworthy is that K_a is absent from eq. (5). This implies that sampling biases in EK injection due to the distinct electrophoretic mobilities of analytes are nullified in the relative sense. Even though less of the slower-migrating analytes are injected, they also give rise to wider peaks in the electropherogram. From this perspective, analyte quantitation with EK injection

in CZE is actually a closer analogy to that in high-performance liquid chromatography than is the case with HD injection, since analyte migration times are typically not used to correct for the different migration velocities of analytes having distinct electrophoretic mobilities (17).

Table I lists the precision of (a) integrated injection I, (b) raw, (c) injection I-corrected, (d) migration I-corrected, and (e) injection and migration I-corrected peak areas as well as corrected areas from the (f) one- and (g) two-internal standardization methods (2). Except for manual EK injections, the RSD's for all the parameters are at the 1 to 2% level. This corresponds to the better group of precision values found in the literature, as summarized in ref. 2. A probable reason for the low RSD's is the long equilibration time between the capillary surface and the buffer (at least 4 days) employed in the present work. Other researchers (3,4) have already shown that the amount of analyte introduced during EK injection is roughly proportional to the injection potential and to the injection time. Here, manual EK injections are used to simulate variations in potential, temperature and time during injection. The higher RSD's for raw peak areas with manual compared to semi-automated EK injections are expected, and the lower RSD's for manual HD compared to manual EK injections can be explained by the longer injection time (90 s) used in the former in comparison to that in the latter (5 s). Since the RSD's for the migration I-corrected peak areas are only slightly lower than those for the raw peak areas with all three schemes, we can conclude that v_{ma} drifts between runs and v_{ma} fluctuations during separation are negligible compared to other sources of errors, even without forced-air or liquid temperature control. This is confirmed by the fact that the migration times in these experiments were reproducible to $< 0.3\%$.

On the other hand, for manual EK injection, correcting the raw peak areas

Table I: Quantitative Precision[a] with HD, Manual and Semi-automated EK Injection

Injection Scheme[b]	Manual HD[c]				Manual EK[d]				Semi-automated EK[d]			
Analyte	1	2	3	4	1	2	3	4	1	2	3	4
Integrated Injection I	-	-	-	-	3.6				0.8			
Raw Peak Area	1.3	1.1	0.9	1.6	3.6	3.2	3.7	4.3	0.7	1.1	1.0	2.0
Injection I-Corrected Peak Area	-	-	-	-	1.8	0.8	1.2	1.5	1.4	1.7	1.5	2.8
Migration I-Corrected Peak Area	1.1	0.9	0.9	1.3	3.5	3.0	3.8	4.1	0.3	0.8	0.8	1.9
Inj. & Mig. I-Corrected Peak Area	-	-	-	-	1.6	0.8	1.1	1.2	0.9	1.4	1.4	1.7
One Internal Standard[e]	-	1.7	1.7	2.2	-	1.6	0.8	1.2	-	1.1	1.5	2.0
Two Internal Standards[f]	-	0.2	1.1	-	-	1.4	0.7	-	-	1.0	1.4	-

[a]In % RSD.
[b]Four consecutive runs were performed to obtain the data for each injection scheme.
[c]Injection time: 90 s; vertical displacement: 2 cm.
[d]Injection time: 5 s; injection potential: 15 kV.
[e]Analyte 1 was the internal standard.
[f]Analytes 1 and 4 were the internal standards.

with the integrated injection I lowers the RSD's from the 3-4% to 1-2% level. The errors in the raw data are thus due wholly to the imprecision in timing 5-s intervals. This is not surprising as the observed RSD for the integrated injection I of 3.6% is similar to those for the raw peak areas and could obviously account for the poor precision of the latter. However, the same is not true with semi-automated EK injection where correction with the integrated injection I actually degrades the precision slightly. We note that the precision for semi-automated EK injection is already very good. This implies that the errors in the raw peak areas and the integrated injection I are not correlated at this level of precision. Three successive semi-automated EK injection current-time profiles are shown in Fig. 1. The step-like behavior present during the rising and falling edges of the pulses is characteristic of this and another power supply used. A third power supply however provided a smooth profile on both edges. Neither the step heights, as judged from Fig. 1, nor the step intervals (RSD = 3.6%) are reproducible. The start-stop intervals, on the other hand, show negligible variations (RSD < 0.04%). The observed RSD of 0.8% in the integrated I for semi-automated EK injection in Table I thus reflects variations in the pulse shape. Even poorer reproducibility can be expected if the matrix changes, affecting the conductivity of the system. Monitoring the current during injection from different matrices can therefore aid in quantitation.

It can be seen in Table I that correcting the raw peak area with both the integrated injection I and migration I is useful when the precision is poor (manual EK) but not when the precision is already good (semi-automatic EK). It is interesting to note that at this level of precision, the RSD's obtained with one, two or no internal standard (current-corrected) are all comparable in magnitude. The relatively poor signal-to-noise ratio for absorbance measurements in these small capillaries is

Fig. 1. Time profiles of the current pulse for 3 consecutive EK injections in the semi-automated mode set for 5 s each.

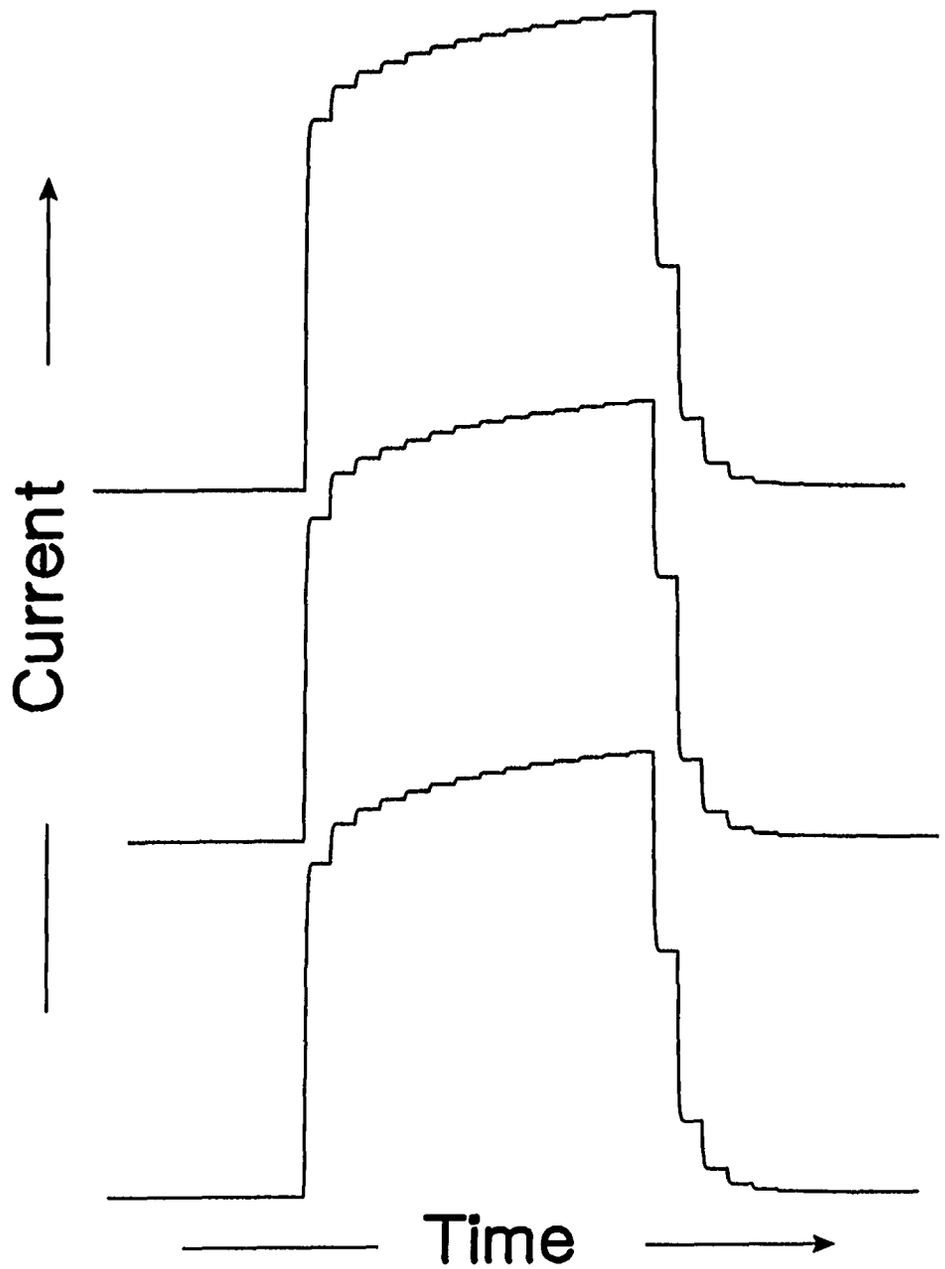
Current
Time

well recognized. The limiting factor here is probably imprecision attributable to the determination of the peak area, detector response or the presence of "ubiquitous" injection (24,25).

EK injection of samples with conductivities different from that of the running buffer

EK injection of sample solutions having conductivities different from that of the running buffer can be likened to field-amplified capillary electrophoresis (18). Depending on the relative magnitudes of the electroosmotic flow velocities of the running and sample buffers, the ensuing electroosmotic pressure induces viscous flow in the injection zone in a direction which either reinforces or opposes the bulk flow. In all practical situations, however, the length of the injection zone (~1 mm) is much smaller than that of the capillary (~50 cm). Thus, the bulk velocity (v_b) during EK injection is simply the electroosmotic flow velocity when the capillary is totally filled with the running buffer. Hence, the migration velocity of analyte a during EK injection is

$$v_{ai} = v_b + v_{aei} \tag{6}$$

where v_{aei} represents the electrophoretic velocity of analyte a in the injection zone. It should be emphasized that v_{ai} is independent of the electroosmotic flow of the sample solution in the injection zone for all typical cases. However, the analytes in the injection zone experience an electric field different in magnitude from that in the running buffer, as the conductivities of the running and sample buffers are not identical (10-12). Again, since the length of the injection zone is much smaller than

that of the capillary, the electric field in the injection zone can be approximated by $(k_r/k_s)V_i/L$ and v_{ai} becomes (18)

$$v_{ai} = [\mu_{eo} + (k_r/k_s)\mu_{aei}]V_i /L \quad (7)$$

where μ_{eo} denotes the electroosmotic mobility of the running buffer, μ_{aei} the electrophoretic mobility of analyte a in the sample solution, V_i the applied potential during injection, L the length of the capillary, k_r the conductivity of the running buffer and k_s the conductivity of the sample solution. Eq. 7 is valid in the absence of isotachophoretic effects. Experimentally, μ_{eo} can be determined from t_b, the migration time of a neutral, unretained species under identical conditions, since v_b is dictated by the electroosmotic flow of the running buffer. Because the time that analyte a takes in leaving the sample buffer zone during separation is small compared to its migration time (t_{ma}) (26) and, to a first degree of approximation, the μ_{aei}'s in the running and sample buffers can be treated as identical if the temperatures during injection and separation are similar (27), v_{ai} can be expressed as

$$v_{ai} = \left[\frac{1}{t_b} + \left(\frac{k_r}{k_s}\right)\left(\frac{1}{t_{ma}} - \frac{1}{t_b}\right)\right]\frac{V_i L}{V_r} \quad (8)$$

where V_r is the applied potential during separation. Since n_{ai} and, hence, peak area, is proportional to c_a^s and v_{ai}, the peak areas resulting from the injection of analyte a from sample solutions 1 and 2, which may possess distinct conductivities, with EK injection can be related by the following expression:

where A_{aj}, c_{aj}^s and k_{sj} represent the peak area from analyte a dissolved in sample

$$\frac{A_{a2}}{A_{a1}} = \frac{c^s_{a2}}{c^s_{a1}} \left[\frac{1/t_b + (k_r/k_{a2})(1/t_{ma} - 1/t_b)}{1/t_b + (k_r/k_{a1})(1/t_{ma} - 1/t_b)} \right] \quad (9)$$

solution j, the concentration of analyte a in sample solution j and the conductivity of sample solution j respectively. Eq. 9 is valid if the injection times, injection potentials, running potentials and temperatures of the operating conditions are reproducible from run to run. As shown in Table I, this does not present a problem in the present work with semi-automated EK injection. In addition, it is assumed that exposure of the capillary wall to the small amounts of sample solutions different in composition from that of the running buffer does not result in permanent alteration of the overall wall ζ potential.

Qualitatively, the linear dependence of peak area on sample solution resistance with EK injection has been observed for cations (10). In Fig. 2, we present the plot of peak area against $1/k_s$ for anions. The positive and negative slopes of the plots for cations and anions respectively are expected on the basis of eq. 9, as t_{ma}/t_b for cations is less than unity and *vice versa* for typical directions of electroosmotic flow and applied potentials. Since neutral species are not affected by electrical forces, the insensitivity of the peak areas corresponding to analyte 1 upon sample solution conductivity in Fig. 2 is not surprising. From eq. 9, it can be seen that the dependence of the peak area from a neutral marker upon sample solution conductivity vanishes as t_{ma} and t_b are identical. This provides support for the contention that v_b and, therefore, the amount of neutral species injected, is practically

Fig. 2. Relationship between the amount of analyte injected and the conductivity of the sample solution.

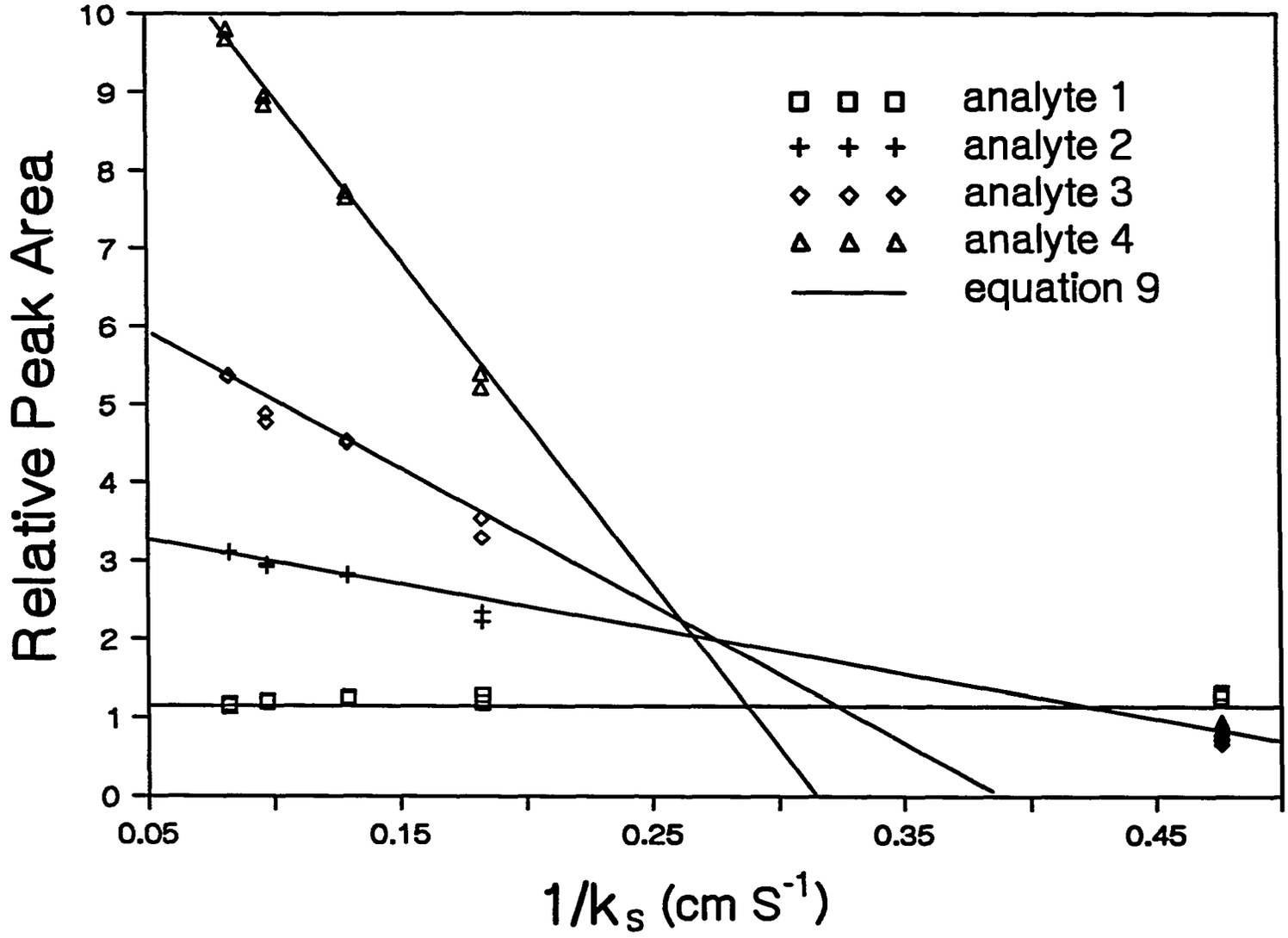
Relative Peak Area
10
9
8
7
6
5
4
3
2
1
0
0.05
0.15
0.25
0.35
0.45
1/k_s (cm S^-1)
analyte 1
analyte 2
analyte 3
analyte 4
equation 9

independent of the electroosmotic flow in the injection zone, whose magnitude depends on the ionic strength, and, hence, conductivity, of the sample solution (20,21). It is interesting to note from eq. 8 and 9 that for a sample with high conductivity relative to that of the running buffer, the second term within each set of square brackets becomes negligible, and no sampling bias is expected in EK injection. This results from the fact that the electric field within the injection zone becomes negligible. In other words, the vertical-intercepts in Fig. 2 should correspond to values obtained from HD injection for identical bulk volumes introduced. A similar correspondence exists in the case of cations. This explains the non-zero intercepts in Fig. 2 of ref. 10.

In Fig. 2, we have plotted the measured peak areas (data points) as well as the predicted peak areas (lines) for 4 different analytes in 5 different sample matrices. The lines are not least-square fits of the data. Rather, the first sample matrix (100 mM phosphate, extreme left) provides the calibration factors for differences in responses and differences in concentrations for the 4 analytes. Eq. 9 then allows one to predict all other peak areas based on the experimentally determined t_b, t_{ma}, k_r and k_j. Except for analytes 3 and 4 from the sample solution with the lowest conductivity, the agreement between theory and experiment is excellent. We also note that t_b varied by only 0.43% (RSD) even though the buffer concentrations changed by an order of magnitude. The RSD's for t_{ma} of the other analytes were 0.55%, 0.64% and 0.68% respectively. So, little additional error is introduced in using eq. 9 as a result of variations in migration velocities past the detector. If

necessary, eq. 3 can be employed to correct for the A's in eq. 9. The small RSD's for t_b and t_{ma} also confirm that exposure of the capillary wall to this set of sample solutions did not significantly alter the overall wall ζ potential. However, the same may not be true if the sample solutions contain a potential-determining species more dominant than the one in the running buffer (28).

The $1/k_s$-intercepts in Fig. 2 correspond to the points at which the anionic analytes employed here would cease to be injected by electromigration as k_s decreases further. Rather unexpected, however, are the non-zero peak areas from analytes 3 and 4 in the sample solution with the lowest conductivity. Since the local electric field in the injection zone becomes so large that the electrophoretic velocities of analytes 3 and 4 in such a low-conductivity medium actually exceed the bulk velocity in magnitude during injection (12), none of analytes 3 or 4 is expected to enter the capillary by electromigration. Since meticulous attention has been paid to ensure that no significant height differential between the injection and detection ends of the capillary as well as between the levels of the sample and the two running buffer solutions exists during both injection and separation, HD injection could not have been responsible for this phenomenon.

One explanation is based on the so-called "ubiquitous" injection (24), where the mere insertion and withdrawal of the capillary into and from the sample solution would give rise to analyte introduction. Indeed, we have confirmed this hypothesis by doing just that (data not shown). The amounts of analytes thus introduced give rise to peak areas that are around 5-10% of those shown in Fig. 2. However, there does

not seem to be any particular correlation between the *percentage* of the areas due to ubiquitous injection and the sample conductivity or the analyte ζ potential. Unfortunately, the inadequate sensitivity of the present detection system for the analytes presents an obstacle to detailed quantitative studies along this avenue. We plan to carry out further work in characterizing and elucidating the mechanism of this injection process in the future. Fortunately for this study, however, the small percentage of analytes introduced in each case through "ubiquitous" injection does not cause uncertainties beyond the 1% level (see Table I), which would hamper the application of eq. 9. Fig. 2 clearly shows there is sample introduction beyond "ubiquitous" injection for the last (10 mM phosphate) sample solution. This can be explained by the fact that electroosmotic flow has a large time constant (~ ms) relative to ionic migration (~ ps). Thus, when the electric field is switched off, some analytes will be carried into the capillary by the slowly decaying electroosmotic flow. This type of hysteresis thus constitutes a secondary correction factor to eq. 9.

The utility of various parameters in relating analyte concentrations in sample solutions having different conductivities with EK injection are outlined in Table II. Since the concentrations of each analyte in all sample solutions are identical, the peak areas from the injection of the sample solution containing 100 mM sodium phosphate are arbitrarily taken to indicate the correct analyte concentrations with which calculated values from other sample solutions are compared. A value of 1.00 implies an error-free determination. As discussed earlier, the behaviors of the raw peak areas are expected. Because the raw peak area of analyte 1 remained nearly

Table II: Calculated Analyte Concentrations[a] in Sample Solutions of Different Conductivities with EK Injection[b] by Various Methods

Sample Buffer Concentration[c]	Sample Solution Conductivity[d]	Analyte	Methods				
			Raw Peak Area	Eq. 10	One Internal Standard	Two Internal Standards	Eq. 9
77	10.3	1	1.05	0.88	1.10	--	--
		2	0.95	0.80	--	1.01	0.98
		3	0.90	0.76	1.73	1.05	0.95
		4	0.91	0.77	1.93	--	0.98
55	7.75	1	1.08	0.68	1.18	--	--
		2	0.91	0.58	--	0.98	1.03
		3	0.84	0.54	1.00	0.99	1.01
		4	0.79	0.50	1.01	--	1.01
33	5.49	1	1.07	0.48	1.45	--	--
		2	0.74	0.33	--	1.01	0.99
		3	0.64	0.29	1.00	1.01	0.98
		4	0.54	0.24	1.01	--	1.00
10	2.10	1	1.12	0.20	4.78	--	--
		2	0.24	0.04	--	0.97	0.40
		3	0.13	0.02	0.60	1.05	-1.97
		4	0.09	0.02	0.46	--	-6.55

[a]In mM. Two injections were made for each sample studied. All results are relative to the raw areas obtained from a sample containing 100 mM sodium phosphate. There, the solution conductivity is 12.2 S cm^{-1}.
[b]As in Table I for semi-automated EK injection.
[c]In mM sodium phosphate.
[d]In S cm^{-1}.

unchanged from one sample solution to another while those for the charged analytes varied, using the area of the former as the reference in the single-internal standard technique is unfair. Nonetheless, even when the anionic analyte 2 was used as the reference in calculating the relative peak areas (Table II), they still failed to relate the results from sample solutions of distinct conductivities. An explanation for this can be found in eq. 9 where dividing the peak area of an analyte with that from another analyte in the same sample solution but with a different migration time does not eradicate its dependence upon k_s. It has been proposed that the sample size resulting from EK injection is given by (11)

$$\text{sample size} = \frac{c_a^s \, v_c \, t_i \, V_i \, k_r}{t_{ma} \, V_r \, k_s} \qquad (10)$$

where v_c is the capillary volume to the detector and t_i the injection time (assuming plug injection). Eq. 10 indicates that the correction factor is simply the product of A_{a1}/A_{a2} and k_{s2}/k_{s1}. With c_a^s, v_c, t_i, V_i and V_r remaining invariant using the semi-automated injection of the present experimental setup, the concentration values calculated from eq. 10 still fail to relate the results from sample solutions of different conductivities. This can be explained by the fact that eq. 10 does not take into account the presence of bulk flow and is valid only in its absence. On the contrary, eq. 9 is able to relate the results from all sample solutions at the 0 to 5% level, which is close to the accuracy permitted by the precision shown in Table I, with the exception of the last (10 mM sodium phosphate) solution. This is expected because eq. 9 is devised on the condition that electromigration is the only injection mechanism in operation. As discussed earlier, the presence of "ubiquitous" injection and hysteresis in migration renders this assumption inappropriate and contributes significantly when little or no analyte is injected by electromigration, such as when a

very low-conductivity sample solution is involved. The negative values for analytes 3 and 4 reveal the fact that the magnitude of the electrophoretic velocity for each of the analytes exceeds that of the electroosmotic flow rate, corresponding to the case where no analyte injection by electromigration is expected. Interestingly, the two-internal standardization technique (2) succeeds in relating the results from all sample solutions at the 0 to 5% level, including the last (10 mM sodium phosphate) solution. This shows that that method is not only insensitive to the relative contributions from hydrodynamic flow and electromigration, but is also valid in the presence of "ubiquitous" injection and hysteresis in migration.

Nevertheless, in many situations, the use of eq. 9 may prove to be advantageous because only the migration time of a neutral species and not its concentration or response factor is required. This means that its quantity in the sample solution need not be known with a high degree of accuracy, thus simplifying sample preparation. Besides, migration times can generally be determined with a higher degree of precision (13) compared to, for example, absorption signals. As a matter of fact, if the samples concerned already contain neutral species, addition of the neutral marker would not even be necessary. Furthermore, since neutral species are not amenable to separation in CZE, their presence in the sample would not have adverse effects on the resolution of the analytes of interest. Therefore, no additional effort is needed to select internal standards with suitable migration times in method development. Finally, since bulk flow is dictated by the running buffer when the injection zone is small, *vide supra*, one can even determine t_b in separate experiments and not manipulate the sample solution at all.

In short, correction based on the integrated injection current (eq. 4) raises the quantitative precision of CZE with manual EK injection to the levels attained with

semi-automated EK and manual HD injections. The use of eq. 9 nullifies sampling biases based on distinct sample solution conductivities without the need to utilize any quantitative internal standards. However, correcting for matrix effects in EK injection resulting from large differences in viscosity and pH amongst sample solutions remain untenable thus far.

REFERENCES

1. Gordon, M. J.; Huang, X.; Pentoney, S. L.; Zare, R. N. Science 1988, 242, 224-228.
2. Dose, E. V.; Guiochon, G. A. Anal. Chem. 1991, 63, 1154-1158.
3. Rose, D. J.; Jorgenson, J. W. Anal. Chem. 1988, 60, 642-648.
4. Schwartz, H. E.; Melera, M.; Brownlee, R. G. J. Chromatogr. 1989, 480, 129-139.
5. Huang, X.; Luckey, J. A.; Gordon, M. J.; Zare, R. N. Anal. Chem. 1989, 61, 766-770.
6. Fujiwara, S.; Honda, S. Anal. Chem. 1987, 59, 2773-2776.
7. Honda, S.; Iwase, S.; Fujiwara, S. J. Chromatogr. 1987, 404, 313-320.
8. Otsuka, K.; Terabe, S.; Ando, T. J. Chromatogr. 1987, 396, 350-354.
9. Fujiwara, S.; Honda, S. Anal. Chem. 1986, 58, 1811-1814.
10. Huang, X.; Gordon, M. J.; Zare, R. N. Anal. Chem. 1988, 60, 375-377.
11. Smith, R. D.; Udseth, H. R.; Loo, J. A.; Wright, B. W.; Ross, G. A. Talanta 1989, 36, 161-169.
12. Huang, X.; Ohms, J. I. J. Chromatogr. 1990, 516, 233-240.
13. Lee, T. T.; Yeung, E. S. Anal. Chem. 1991, 63, 2842-2848.
14. Kuhr, W. G.; Yeung, E. S. Anal. Chem. 1988, 60, 2642-2646.
15. Tsuda, T. J. Liq. Chromatogr. 1989, 12, 2501-2514.
16. Hjerten, S. Chromatogr. Rev. 1967, 9, 178.
17. Huang, X.; Coleman, W. F.; Zare, R. N. J. Chromatogr. 1989, 480, 95-110.
18. Chien, R.-L.; Helmer, J. C. Anal. Chem. 1991, 63, 1354-1361.

19. Lukacs, K. D.; Jorgenson, J. W. J. High Resolut. Chromatogr. Chromatogr. Commun. 1985, 8, 407-411.

20. Jorgenson, J. W.; Lukacs, K. D. Anal. Chem. 1981, 53, 1298-1302.

21. Tsuda, T.; Normura, K.; Nakagawa, G. J. Chromatogr. 1983, 264, 385.

22. Terabe, S.; Otsuka, K.; Ando, T. Anal. Chem. 1989, 61, 251-260.

23. Issaq, H. J.; Atamna, I. Z.; Metral, C. J.; Muschik, G. M. J. Liq. Chromatogr. 1990, 13, 1247-1259.

24. Grushka, E.; McCormick, R. M. J. Chromatogr. 1989, 471, 421-428.

25. Dose, E. V.; Guiochon, G. A. Anal. Chem. 1991, 63, 1063-1072.

26. Mikkers, F. E. P.; Everaerts, F. M.; Verheggen, Th. P. E. M. J. Chromatogr. 1979, 169, 1-10.

27. Overbeek, J. Th. G.; Wiersema, P. H. In Electrophoresis. Theory, Methods and Applications; Bier, M., Ed.; Academic Press: New York, 1967; Vol. 2, Ch. 1.

28. Adamson, A. W. Physical Chemistry of Surfaces, 4th ed.; John Wiley & Sons: New York, 1982; pp. 193-195.

PAPER III.

HIGH-SENSITIVITY LASER-INDUCED FLUORESCENCE DETECTION OF NATIVE PROTEINS IN CAPILLARY ELECTROPHORESIS

INTRODUCTION

The high efficiency and speed of capillary electrophoresis (CE) in the resolution of biomolecules have attracted much attention (1). However, efficient separation is not sufficient unless coupled to adequate detection. In this regard, CE presents a challenge as the nL cell volume and on-column arrangement render traditional detectors designed for high performance liquid chromatography (HPLC) unsuitable.

The analysis of biological materials and the determination of biomolecules are of indispensable importance to the field of biotechnology. Despite the prominent role of proteins in biotechnology, the detection of proteins in CE is far from satisfactory. So far, amperometric detection (2) is hampered by electrode fouling while conductometric (3) and mass spectrometric detection (4) are unreliable and insensitive. Radiochemical detection (5), though quite sensitive, requires labeling as well as handling and disposing of hazardous materials with short shelf-lives. Although widely used and convenient, the best ultraviolet-visible absorption detectors with the cross-beam arrangement (6) offer a limit of detection (LOD) in the μM range because of the inherently short pathlength provided by the capillary tubing. This represents a major drawback for CE in the analysis of proteins in biological matrices where the demand for concentration detection sensitivity is far more stringent (7). Besides, it excludes CE from the realm of trace analysis where HPLC is still the method of choice in spite of the poor separation efficiency of the latter.

In general, fluorescence detection in CE exhibits the best performance in sensitivity, linearity and selectivity. Even though conventional excitation sources have been used (8), the achievable sensitivity is offset by the inherent difficulty in focusing

a large amount of light from a divergent light source into the nL detection region while minimizing light scattering. Utilization of the laser as a fluorescence excitation source reduces such problems and defines the state-of-the-art in CE detectors today (9). Unfortunately, implementation of this approach to the detection of proteins is by no means straightforward because usually it is necessary to label the analytes with fluorescent tags. Because of differences in the extent of incorporation of the tags into each protein molecule, pre-column labeling gives rise to multiple peaks for each type of protein in the electropherogram (10,11). On-column labeling of proteins with laser-induced fluorescence (LIF) detection offers slightly better sensitivity than absorbance, but at the expense of separation efficiency due to the slow kinetics of inter-species conversion (11,12). The advantages gained in the 100-fold improvement in sensitivity over absorbance afforded by a post-column labeling scheme with LIF are largely offset by instrumental complexity as well as the dependence of peak efficiency upon reagent flow rate and reaction distance (10). A technique retaining the sensitivity of post-column labeling with LIF while avoiding derivatization is indirect fluorescence detection (13). However, the need to work at low buffer concentrations renders practical applications difficult.

Swaile *et al.* (11) have demonstrated LIF detection of native, underivatized proteins in CE based on the fluorescence of tryptophan and tyrosine residues. In their study, an argon-ion laser operating at 514 nm was frequency-doubled to 257 nm with a harmonic generator. But instrumental instability and poor match between the excitation wavelength and excitation maxima of the fluorophores limited the sensitivity of the technique to no better than post-column labeling with LIF (10).

Nevertheless, the ability to detect proteins at trace levels remains attractive and, in the case of assuring the purity of biopharmaceticals, essential. According to a

"Points to Consider" draft issued by the FDA on biopharmaceuticals, the analytical goal for protein impurities and contaminants are in the 1 to 100 ppm range (14). However, it is possible that a highly immunogenic protein impurity present at the ppm level can elicit an allergic response in a high percentage of human recipients (15,16). Hence, the current analytical goals set forth by the FDA merely reflect the sensitivity limits of existing technologies. This is supported by a more recent draft in which the term "analytical goals" has replaced by phases such as "as free as possible" (17). On this note, the impact realized through coupling the high separation efficiency of CE to nM-detection sensitivity for proteins would be dramatic in the development and proliferation of biopharmaceuticals.

Despite the unparalleled performance of LIF detection in CE (9-11,13,18,19), there have only been a limited number of applications reported. The need for the separation scientist to acquire the expertise in designing, assembling, operating and/or maintaining an LIF detector may be a deterrent. Hence, there is a need for an easily constructed, user-friendly and rugged LIF detector which the non-specialist can build and use without having to expend too much effort or resources. In the present work, a highly sensitive LIF detection scheme for CE based on native protein fluorescence is reported and various aspects of it are discussed. In addition, a compact, rugged and user-friendly instrumental arrangement is described.

MATERIALS AND METHODS

The experimental setup used in the present work resembles the one described previously (18) with several modifications. First, an argon-ion laser (Spectra Physics, Mountain View, CA, model 2045) was optimized for deep UV operation. A prism was used to isolate the 275.4 nm line (utilized to excite protein fluorescence) from the total output. Secondly, 2 UG-1 band pass filters (Schott Glass Technologies, Duryea, PA) were used to selectively pass the fluorescence. Thirdly, a compact, rugged LIF detector housed in a light-tight plexiglas box (25 cm × 35 cm × 10 cm) was constructed. A diagram of the detector arrangement is shown in Fig. 1.

As depicted in Fig. 1, the device represents a simple and rugged design for LIF detection. It consists of 8 main components: a quartz 1-cm focal length lens (L), capillary holder (CH), 20X microscope objective (MO), microscope objective holder (MOH), mirror (M) and mirror mount (MM), photomultiplier tube (PMT) with filter (F), plexiglas box (PB) and 2 light shields (LS). The laser beam enters the otherwise light-tight box PB through a 3-mm hole. L is rigidly mounted to PB so that the focal point of the excitation beam is uniquely defined and used as the reference point for all the other components. The capillary with a small section of its coating removed is mounted on a 2-dimensional stage CH capable of 10-μm resolution. Two short pieces of quartz capillary 350 μm o.d. and 250 μm i.d. glued to CH serve to guide the separation capillary through the optical region. This can hold the common 150 μm o.d. capillary tubing. Alternatively, 350 μm o.d. separation capillaries can be inserted directly into CH. The mounted capillary is at about 20° with respect to the incident laser beam to minimize scattering off the capillary walls. We find that this

Fig. 1. Experimental arrangement of LIF detector for CE.

TOP VIEW

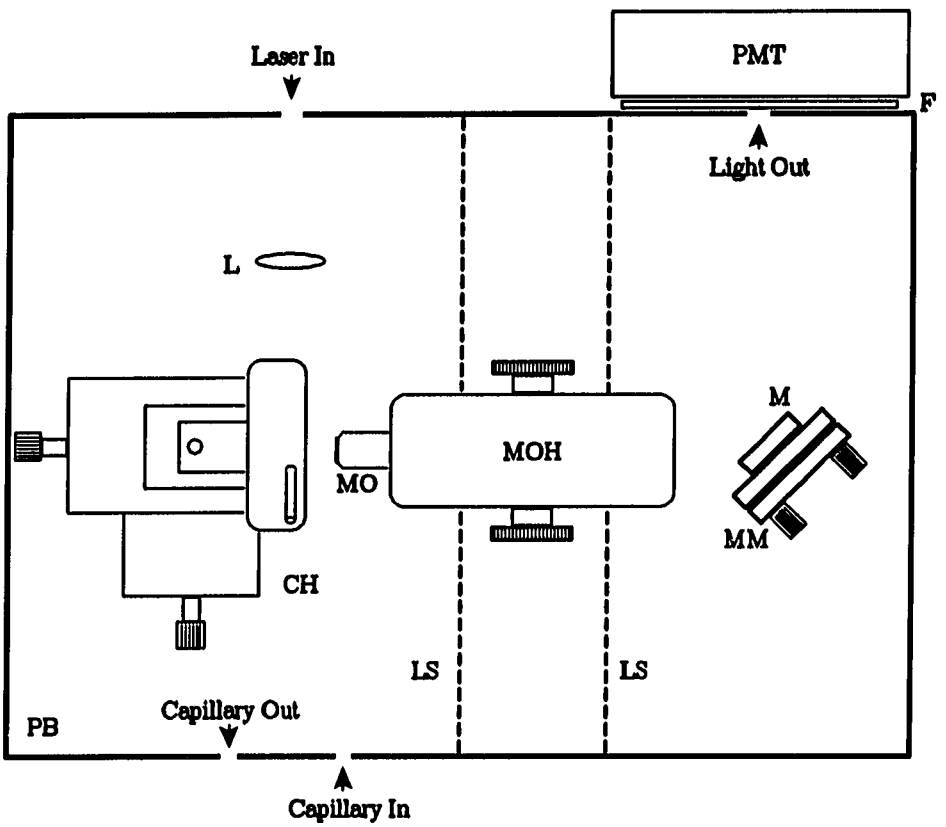

Side View of CH

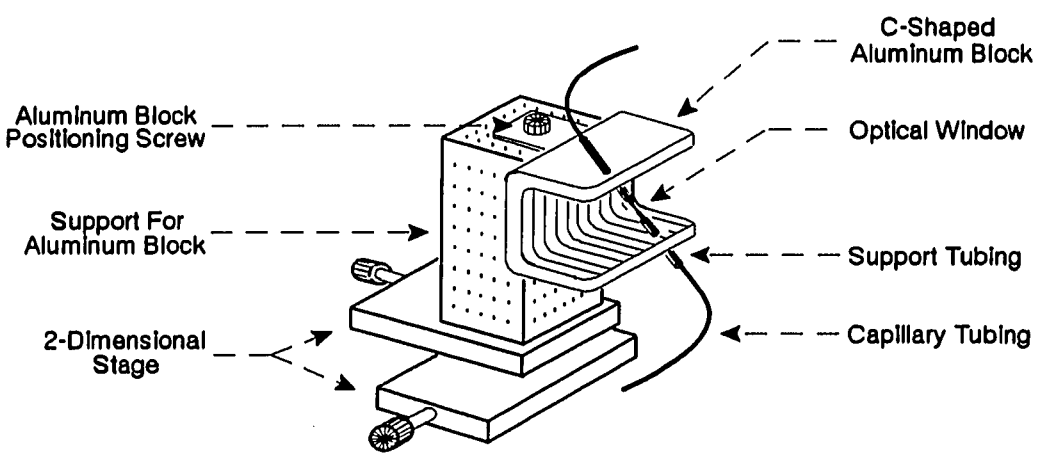

configuration is rigid enough with regard to noise from mechanical vibrations. With this design, capillary change can be accomplished in less than 5 min.

By examining the diffraction image of the transmitted light while translating CH, the incident light can easily be focused tightly into the center of the capillary. With a fluorophore (e.g., 10^{-5} *M* fluorescein solution at pH 8) running through the capillary, MO, positioned roughly such that its focal point is at the same height as the capillary window and pointing toward the excitation region, is translated with MOH so that the fluorescence image can be focused onto the exit plane of PB. By judging the sharpness of the image on the wall behind which PMT is located, the optimal location of MO is determined. Finally, the angle of M relative to PMT and MO is adjusted with MM such that the fluorescence image clears the hole on the wall of PB that is just large enough to allow passage of the fluorescence spot while excluding light scattered off the capillary walls. F can then be used to selectively pass light of the appropriate wavelengths onto the PMT. The LS's are effective in excluding stray light from passage from the region around CH into PMT. With this arrangement, we are able to routinely obtain detection limits within an order of magnitude of the state-of-the-art (9). With the top of PB in place, one can generally work in moderate room light without additional shielding.

In other studies in our laboratory, an air-cooled Ar ion laser was used. The laser and the rest of the optical components can then be bolted together on a 3/4" plexiglas base plate. A single 488 nm interference filter is mounted at the entrance to PB to eliminate room light. The components shown in Fig. 1 only cost a total of $2,000.

All separations were performed using a 5 mM sodium phosphate buffer at pH 10.2 and the analytes were dissolved in the same buffer just before use unless

specified otherwise. An electric field strength of 286 V/cm and a 77-cm long 50 μm i.d., 150 μm o.d. untreated fused-silica capillary was used throughout.

RESULTS AND DISCUSSION

The high sensitivity of LIF detection of native proteins is shown in Fig. 2 where the peak results from the injection of conalbumin present at 5×10^{-10} *M* in the sample. The LOD (S/N = 2) of 1×10^{-10} *M* here represents a 140-fold improvement over the one reported for the same analyte previously (11). The major reason for this is the simplicity and ruggedness of the present optical setup. Frequency-doubling is instrumentally elegant and requires a smaller argon ion laser, but produces light which is inherently noisy because of the quadratic dependence in the intensity of the frequency-doubled light on the intensity of the source. Temperature stability of the doubling crystal is also a problem. Besides, the excitation wavelength of 275.4 nm in the present system is a much better match with the fluorescence-excitation maxima of most proteins (20) than the 257 nm in ref. 11. Moreover, the high power used there prescribes long warm-up times. Since practical LIF detection is flicker noise limited, a frequency-doubled light source directly restricts the performance of the detector. However, the factors discussed above are not a concern in the present optical arrangement and, as a result of the much smaller source flicker, a drastic improvement in performance is realized. It is interesting to note that the fused-silica of the capillary tubing exhibits luminescence that can be visually discerned upon excitation at 275.4 nm. Even with 2 UG-1 band pass filters in place, this background luminescence cannot be totally eliminated, thereby providing an indication of the large spectral width of the luminescence. Consequently, the LOD of the present detector is limited by source-induced background luminescence flicker noise. Accordingly, increasing the dynamic reserve of the laser light or reducing the quantity of luminescent impurities in the fused-silica of the capillary tubing would

Fig. 2. Electropherogram of 5 X 10^{-10} M conalbumin injected.

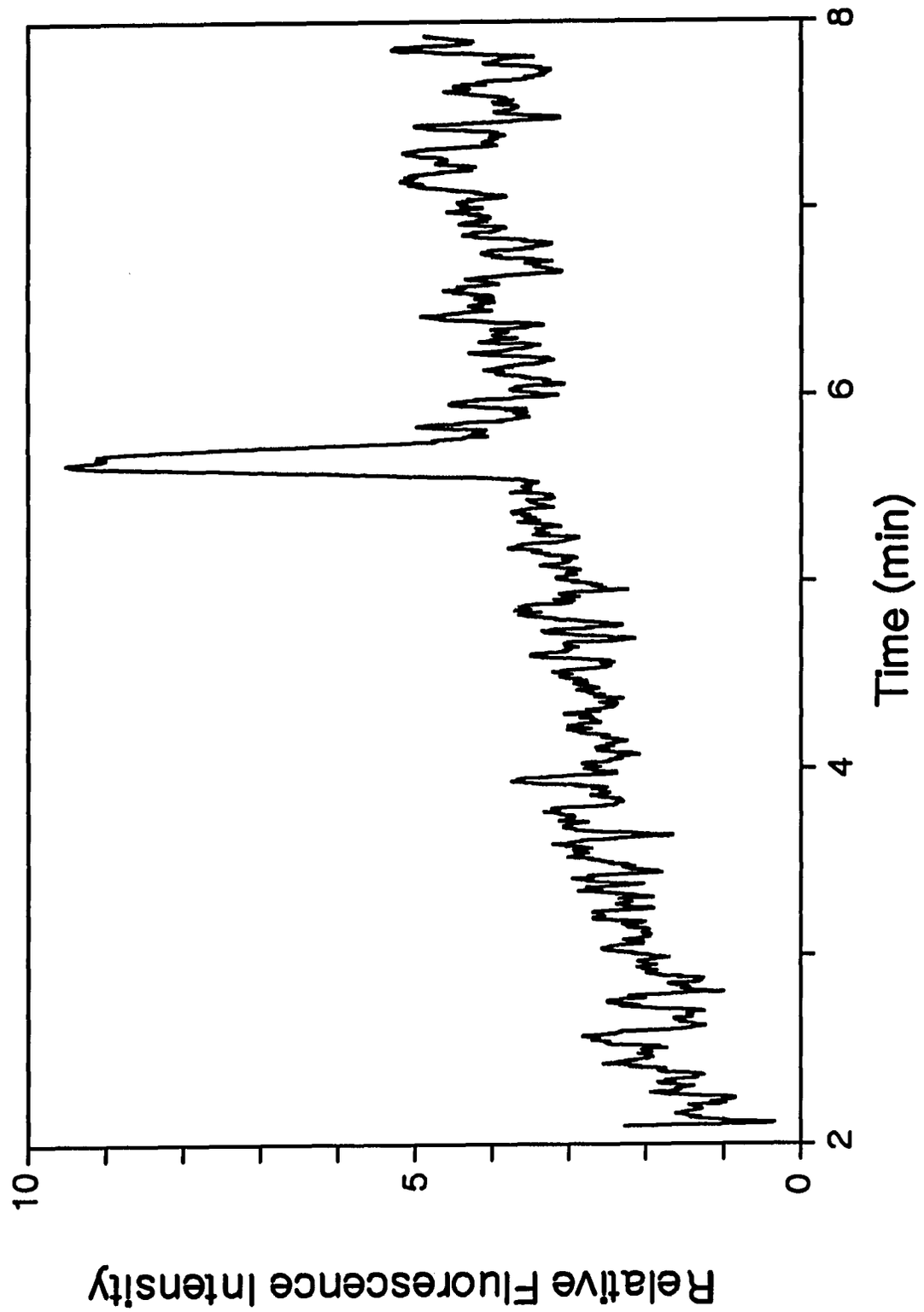
Relative Fluorescence Intensity
10
5
0
2
4
6
8
Time (min)

further lower the LOD attainable with the present detector. We note that 10^{-10} *M* is an actual injected LOD and not one extrapolated from runs at high concentrations. This is important since adsorption of analytes onto the capillary walls can prevent one from taking advantage of the high sensitivity of LIF for studying small samples at low concentrations. The actual mass LOD (injection volume = a few nL) is around 10^{-14} g, which is quite impressive. As shown in Figs. 3 and 4, the present detector shows a linear dynamic range of at least 5 and 4 orders of magnitude for tryptophan and BSA respectively. The correlation coefficient for each set in linear plots is better than 0.999. This is the first time that good quantitation is shown for LIF over a large concentration range. This highlights the stability of the present optical system over a series of runs. The linearity of data in Fig. 4 also shows that adsorption of BSA is not a problem even at these low concentrations. Although the high cost of argon-ion lasers that can produce deep UV light is a disadvantage of the present detection scheme, it will eventually gain popularity as laser technology advances in the future.

Table 1 is a summary of the reported limits of detection for proteins in CE by using various LIF techniques. Indirect fluorescence, native fluorescence excited at 257 nm, on-column and post-column labeling with LIF all offer higher LOD's than native fluorescence excited at 275 nm. The LOD achievable with indirect fluorescence detection is limited by the dynamic reserve of the laser light (13) and the difficulty in selecting a well-behaved fluorophore with an electrophoretic mobility close to that of the analyte (21). On-column labeling LIF detection is hampered by the large flicker noise on the fluorescence background resulted from the presence of unbound fluorophores in the eluent (11). The performance of post-column labeling LIF is compromised by the short reaction time at the optimal reagent flow rate and

Fig. 3. Log-log plot of tryptophan calibration curve.

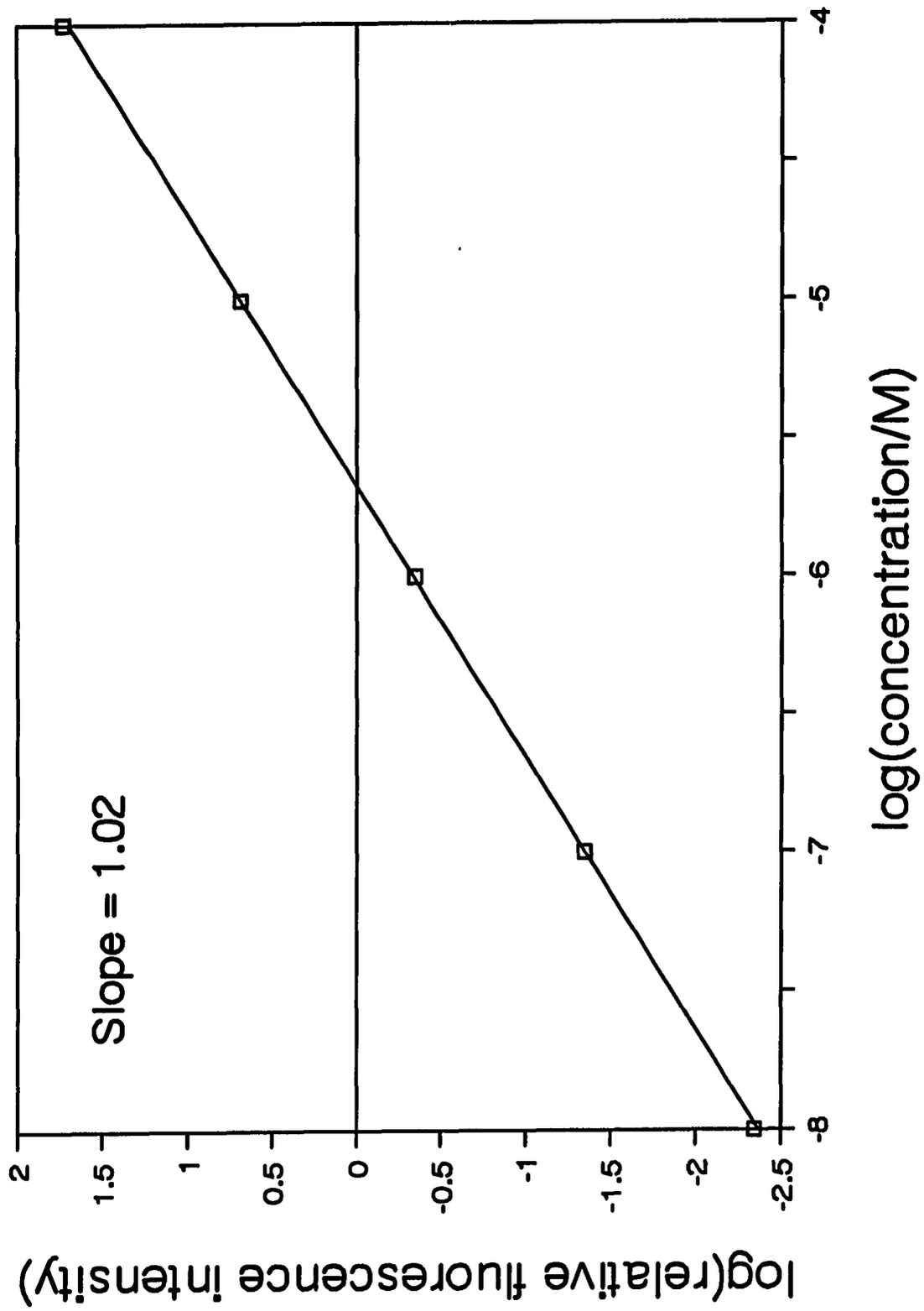
log(relative fluorescence intensity)
2
1.5
1
0.5
0
-0.5
-1
-1.5
-2
-2.5
Slope = 1.02
-8
-7
-6
-5
-4
log(concentration/M)

Fig. 4. Log-log plot of BSA calibration curve.

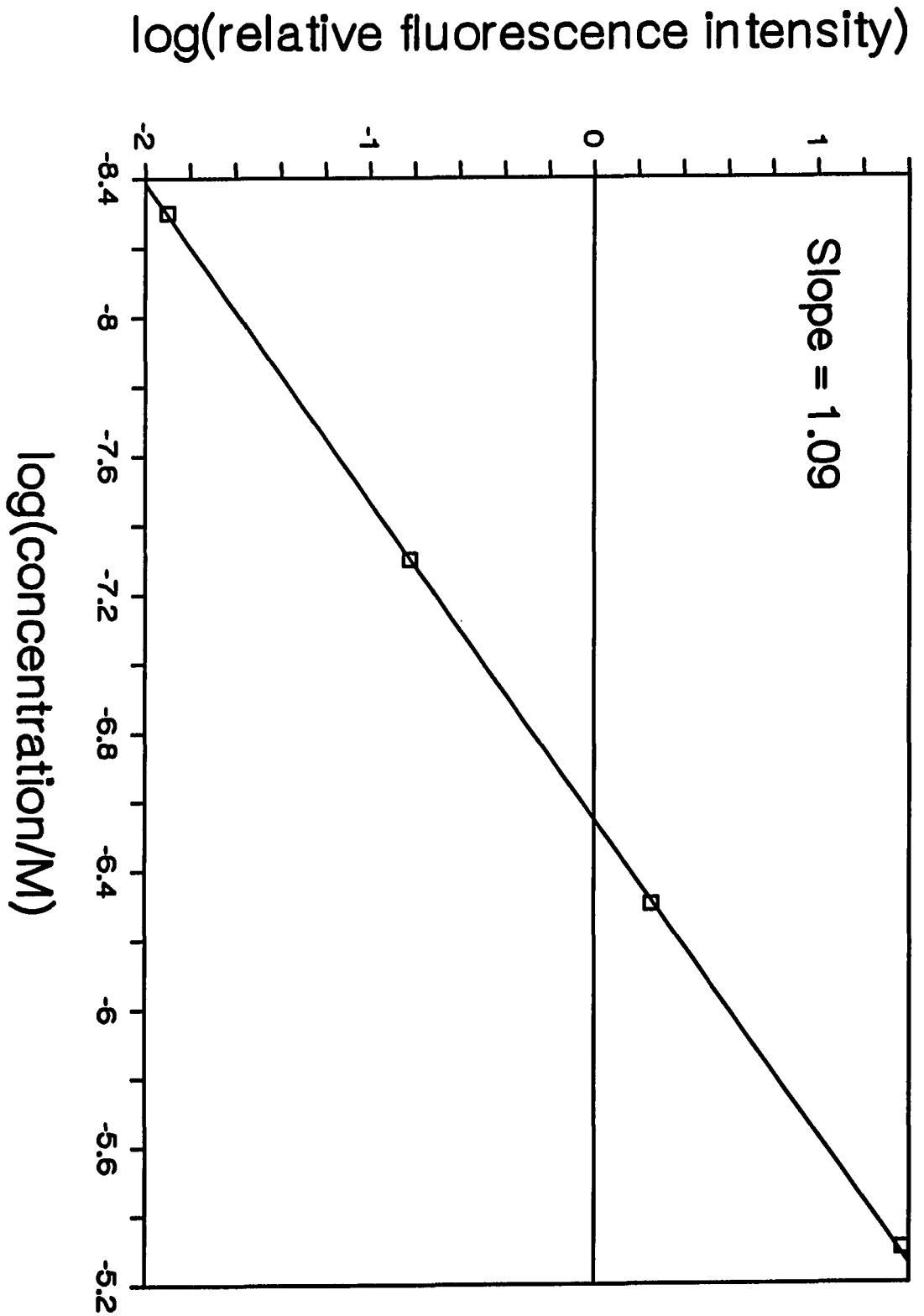
log(relative fluorescence intensity)
-2
-1
0
1
Slope = 1.09
log(concentration/M)
-8.4
-8
-7.6
-7.2
-6.8
-6.4
-6
-5.6
-5.2

Table 1: Limits of Detection for Proteins in CE by LIF[a]

Detection Scheme	LOD (*M*)			
	Conalbumin	Horse Heart Myoglobin	Bovine Serum Albumin	Lysozyme
Native Fluorescence (257 nm excitation)	1×10^{-8}[b]	--	--	--
Indirect Fluorescence	--	--	--	5×10^{-6}[c]
Pre-column Labeling with FITC[d]	1×10^{-10}[b]	--	--	--
On-column Labeling with TNS[e]	3×10^{-7}[b]	--	--	--
Post-column Labeling with OPA[f]	--	1×10^{-8}[g]	--	--
Native Fluorescence (275 nm excitation)	1×10^{-10}[h]	--	2×10^{-10}[h]	--
Native Fluorescence with stacking (275 nm excitation)	3×10^{-12}[h]	--	1×10^{-11}[h]	--

[a]calculated from signal-to-noise (S/N) of 2
[b]from ref. 11
[c]from ref. 13
[d]fluorescein isothiocyanate
[e]2-*p*-toluidinonapthalene-6-sulfonate
[f]*o*-phthalaldehyde
[g]from ref. 10
[h]this work

flow distance (10). Rather surprisingly, pre-column labeling LIF with FITC for conalbumin, which contains 102 side chain amine groups (22), offers an LOD no better than native fluorescence detection excited at 275 nm. This is in contrast to reports that FITC-derivatized amino acids can be detected in the 10^{-12} *M* range (9). The probable reason for this is the formation of multiple peaks on the electropherogram with pre-column labeling, which increases the magnitude of background fluctuations close to the migration time of the major peak and decreases the size of the major peak (11). Consequently, the use of native fluorescence as a detection principle for proteins in CE surrenders little in detection sensitivity. One gains in the simplicity and speed of analysis compared to fluorescence derivatization, which may not even be feasible at these low concentrations and small amounts. The sample is also preserved for further studies or use. One may even be able to implement fluorescence-detected circular dichroism (23) to study protein conformations. A drawback of the present detection scheme is that only tryptophan- or tyrosine-containing proteins are amenable to detection. Therefore, some peptides and small proteins may escape detection.

The LOD's of 1×10^{-10} and 2×10^{-10} *M* for, respectively, conalbumin and BSA were obtained with the analytes dissolved in buffers identical in composition to the running buffer (5 m*M* sodium phosphate at pH 10.2). Interestingly, when a 5 m*M* sodium phosphate solution at pH 6.68 was used as the sample buffer, the LOD's for the same analytes decreased to 3×10^{-12} and 1×10^{-11} *M* respectively with a small loss of separation efficiency. The phenomenon bears some similarity to electrophoretic concentration (or stacking). The lower ionic strength of the pH 6.68 sample buffer also increases the effective injection potential. Electrophoretic concentration has been applied to the analysis of dilute peptide samples with CE

where the pH of the sample buffer is higher than that of the running buffer and with that, it has been claimed the LOD can be lowered by at least 5 times (24). Therefore, electrophoretic concentration, when optimized and coupled to LIF detection of native proteins, possesses tremendous potential in protein determination at the trace level. The present enhancement should be applicable to physiological samples, which are near neutral pH. Further work on this is now under way.

Fig. 5 depicts an electropherogram showing tryptophan present at 1×10^{-8} *M* in the sample. The estimated LOD (at S/N of 2) for tryptophan is 2×10^{-9} *M*. Conalbumin, which contains 15 tryptophan and 21 tyrosine residues (22), does not show a linear increase in detection sensitivity as expected from the number of tryptophan residues. There are several explanations for this. First, the quantum yield of fluorescence of tryptophan residues in a hydrophobic microenvironment is about 3 times smaller than that for residues in a hydrophilic microenvironment (25). Hence, it is possible that most or all of the tryptophan residues in conalbumin are located in the hydrophobic core of the protein. Secondly, a variety of functional groups such as peptide bonds (26) and protonated amine groups (27) are effective in quenching the fluorescence of tryptophan residues in proteins. Thirdly, the fluorescence and fluorescence-excitation spectra of tryptophan and proteins differ (20). The present optical arrangement might favor tryptophan fluorescence over conalbumin fluorescence. However, the LOD of BSA (2×10^{-10} *M*) is only twice that for conalbumin, even though the former possesses only 1 tryptophan and 16 tyrosine residues (28). The hydrophilic microenvironment of the tryptophan residue in BSA might serve as an explanation. Another reason is that energy-transfer from the tyrosine and phenylalanine residues to the tryptophan residue in BSA might increase

Fig. 5. Electropherogram of 1 X 10^{-8} M tryptophan injected.

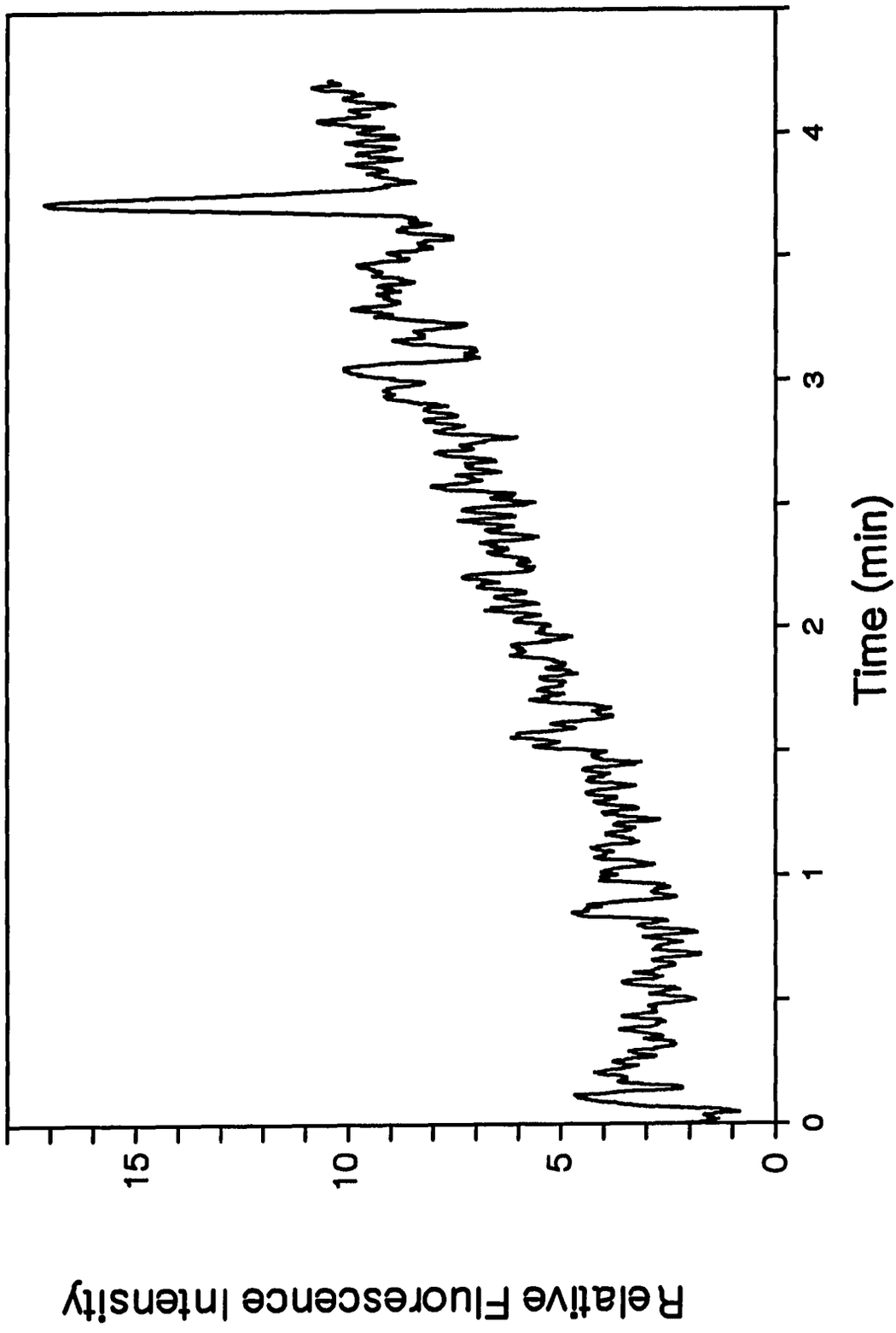
Relative Fluorescence Intensity
0
5
10
15
0
1
2
3
4
Time (min)

the effective fluorescence quantum yield of the tryptophan residue (20). Why this energy-transfer phenomenon occurs selectively in BSA but not conalbumin is unclear.

REFERENCES

1. Kuhr, W. G. Anal. Chem., 1990, 62, 403R.
2. Wallingford, R. A.; Ewing, A. G. Anal. Chem., 1988, 60, 258.
3. Huang, X.; Luckey, J.; Gordon, M.; Zare, R. Anal. Chem., 1989, 61, 766.
4. Caprioli, R.; Moore, W.; Martin, M.; Dague, B.; Wilson, K.; Moring, S. J. Chromatogr., 1989, 480, 247.
5. Pentoney, S.; Zare, R.; Quint, J. Anal. Chem., 1989, 61, 1642.
6. Jorgenson, J. W.; Wahlbroehl, Y. J. Chromatogr., 1984, 315, 135.
7. Briggs, J.; Panfili, P. R. Anal. Chem., 1991, 63, 850.
8. Green, J.; Jorgenson, J. J. Chromatogr., 1986, 352, 337.
9. Cheng, Y.-F.; Dovichi, N. J. Science (Washington, D.C.), 1989, 242, 562.
10. Nickerson, B.; Jorgenson, J. W. J. Chromatogr. 1989, 480, 157.
11. Swaile, D. F.; Sepaniak, M. J. J. Liq. Chromatogr. 1991, 14, 869.
12. Swaile, D.; Sepaniak, M. J. Anal. Chem., 1991, 63, 179.
13. Kuhr, W. G.; Yeung, E. S. Anal. Chem. 1988, 60, 2642.
14. Points to Consider in the Production and Testing of New Drugs and Biologicals Produced by Recombinant DNA Technology (draft). Office of Biologics Research and Review, Food and Drug Administration, Bethesda, MD, 1983.
15. Tron, F.; Degos, F; Brechot, C.; Courouce, A.-M.; Goudeau, A.; Marie, F.-N.; Adamowicz, P.; Saliou, A.; Laplanche, A.; Benhamon, J.-P.; Girard, M. J. J. Infect. Dis. 1989, 160, 199.
16. Powers, D. C.; Sears, S. C.; Murphy, B. R.; Thumar, B.; Clements, M. L. J. Clin. Microbiol., 1989, 27, 2666.

17. Points to Consider in the Manufacture and Testing of Monoclonal Antibody Products for Human Use (draft). Office of Biologics Research and Review, Food and Drug Administration, Bethesda, MD, 1987.

18. Lee, T.; Yeung, E. S.; Sharma, M. J. Chromatogr. (Biomed. Appl.), 1991, 565, 197.

19. Gozel, P.; Gassmann, E.; Michelsen, H.; Zare, R. N. Anal. Chem., 1987, 59, 44.

20. Teale, F. W. J. Biochem. J., 1960, 76, 381.

21. Mikkers, F. E. P.; Everaerts, F. M.; Verheggen, Th. P. E. M. J. Chromatogr., 1979, 169, 1.

22. Williams, J.; Elleman, T.; Kingston, I.; Wilkens, A.; Kuhn, K. Eur. J. Biochem., 1982, 122, 297.

23. Christensen, P. L.; Yeung, E. S. Anal. Chem., 1989, 61, 1344.

24. Aebersold, R.; Morrison, H. D. J. Chromatogr., 1990, 516, 79.

25. S. V. Konev Fluorescence and Phosphorescence of Proteins and Nucleic Acids, Plenum Press, New York, 1967, p.83.

26. Cowgill, R. W. Biochim. Biophys. Acta, 1963, 57, 272.

27. Teale, F. W. J. Photoelect. Spectrometry Group Bull., 1961, 13, 346.

28. Meloun, B.; Moravek, L.; Kostka, V. FEBS Letters, 1975, 58, 134.

PAPER IV.

QUANTITATIVE DETERMINATION OF NATIVE PROTEINS IN INDIVIDUAL HUMAN ERYTHROCYTES BY CAPILLARY ZONE ELECTROPHORESIS WITH LASER-INDUCED FLUORESCENCE DETECTION

INTRODUCTION

Recently, the chemical analysis of individual cells has attracted much attention (1-13). The ability to determine the levels of biochemically interesting species on a cell-by-cell basis promises to answer many long-standing questions in the biological and medical sciences. Some prominent examples include the chemical bases of cellular differentiation and inter-cell communication. With the availability of detailed chemical information, researchers could elucidate the functions and, hence, understand the roles of specific cells in a heterogeneous population of cells. In addition, the use of single-cell analytical technologies opens up the possibility of studying the effects of external stimuli, such as drugs and toxins, on the chemical contents of individual cells, thereby contributing valuable information which would otherwise be inaccessible. The identification of chemical markers for diseases in rare cell types (e.g., cancerous cells) can also be performed so that early diagnosis and a better understanding of the diseases are possible. Finally, since only a single cell is involved, many of the legal and moral difficulties associated with the utilization of human and animal tissues for the purposes of scientific research and drug-testing are alleviated.

Although electron microscopy (13), immunoprecipitation (12), enzymatic radiolabeling (11), micro thin-layer chromatography (TLC) (10), high-performance liquid chromatography (HPLC) with amperometric detection (9), gas chromatography/mass spectrometry (GC/MS) (8) and fluorescence microscopy (7) have been used to analyze individual cells, they suffer from either inadequate sensitivity, poor quantitative capability or the inability to determine multiple components. So far, microcolumn separation techniques coupled to electrochemical (1,3-6) or laser-

induced fluorescence (LIF) (2,4) detection offer the best performance in terms of sensitivity as well as quantitative and multi-component capabilities. The results obtained through microcolumn HPLC in the open-tubular (2-4,6) and packed (1) column formats with amperometric, voltametric and LIF detection have clearly demonstrated the quantitative determination of multiple constituents in individual cells. Likewise, Wallingford et al. (5) and Kennedy et al. (4) have succeeded in adapting capillary zone electrophoresis (CZE) with, respectively, amperometric and LIF detection to the analysis of single neurons.

However, notwithstanding the high sensitivity of amperometry and qualitative information provided by voltametry, the detection schemes are quite restrictive, as only intrinsically electroactive analytes are amenable to detection. Even though some analytes (e.g., proteins) are naturally electroactive, deterioration in performance resulting from electrode-fouling due to contamination with, in particular, high-molecular weight analytes remains problematic. LIF detection with labeling represents an alternative to electrochemical detection in the analysis of individual cells (2). Nevertheless, the need to derivatize the desired analytes within a single cell presents a daunting instrumental challenge and may degrade both the accuracy and precision of the analyses (2). Besides, derivatization is not compatible with many interesting analytes because of the absence of appropriate functional groups, interference from concomitants or variable extents of label-incorporation. Heterogeneity resulting from the last approach renders the labeling of proteins with fluorescent tags for CZE unsuitable (14,15). More recently, the determination of Na^+ and K^+ with indirect LIF/CZE (16) and monobromobimane-labeled thiol-containing peptides with direct LIF/CZE in individual red blood cells was accomplished (17). Unfortunately, the present sensitivity of indirect LIF detection is

inadequate for the quantitation of proteins whereas the derivatization of proteins is, as discussed earlier, not suitable.

Nonetheless, the ability to quantify proteins in individual cells remains attractive. As the molecules which mediate the chemical bases of life, proteins play vital roles in regulating cellular functions and behaviors (18). LIF detection of native proteins in CZE was first demonstrated by Swaile and Sepaniak (15). Since then, we have improved the sensitivity by more than two orders of magnitude through the use of the 275.4 nm line from an argon ion laser (19) so that the sensitivity of this detection scheme is now at a level where the determination of proteins in single human red blood cells with CZE is feasible.

The reasons for selecting the human red blood cell for study are four-fold. First, the size of the average human red blood cell of 86 fL is at least 15 times smaller than the smallest cell type used in other studies (1). Therefore, it is hoped that the capability of analyzing the human red blood cell would translate into the feasibility of applying LIF/CZE to most other types of mammalian cells. Secondly, the chemical contents and cell volume of the average human red blood cell have been documented by numerous other workers (20). As a consequence, the utility of the present approach can easily be assessed. Thirdly, the freedom of red blood cells from attachment to extraneous cells or tissues simplifies their isolation and injection. Finally, the wide availability of human red blood cells renders the procurement of samples straightforward.

In the present work, we demonstrate the use of LIF/CZE for the determination of several proteins in individual red blood cells and report the variations in the amounts of individual proteins from cell to cell. To the best of our knowledge, this is the smallest biological unit that has been subjected to quantitative multicomponent

chemical analysis to date and, for the first time, inter-cellular variations in the levels of multiple proteins are reported.

MATERIALS AND METHODS

Apparatus

The CZE system used in this work is similar to the one described previously (19). Briefly, a 110 cm long, 20 μm i.d. and 150 μm o.d. fused-silica capillary tube (Polymicro Technologies, Inc., Phoenix, AZ) and a high-voltage power supply (0-40 kV; EH Series; Glassman High Voltage, Inc., Whitehouse Station, NJ) were used throughout. All separations were performed at -29 kV with the injection end at electrical ground and an effective separation length of 64 cm. The capillary tubing was pressure-flushed with a (3:1/v:v) methanol:water mixture for 30 min followed by 0.1 M NaOH (aq) for the same period of time before use. The capillary however was not treated in between runs.

The LIF detector consisted of an argon ion laser (Model 2045; Spectra-Physics, Mountain View, CA) operating at 275.4 nm. An on-column detection window was created by removing a 5-mm section of polyimide coating on the fused-silica capillary tubing. A 1-cm focal length quartz lens (Melles Griot Corp., Irvine, CA) was used to focus the laser beam into the detection region while the fluorescence was collected at an angle of 90° to the beam via a 20X microscope objective (Edmund Scientific Co., Barrington, NJ). After spatial and spectral filtering, the current from the photomultiplier tube (Model IP28; Hamamatsu Corp., Bridgewater, NJ) was amplified by a Model 427 meter (Keithley Instruments, Inc., Cleveland, OH) set at a rise time of 300 ms. Data was acquired at 10 Hz via a 24-bit A/D conversion interface (Chrom Perfect Direct, Justice Innovations, Palo Alto, CA) and was stored on an IBM PC/AT computer (Boca Raton, FL).

Sample preparation

Human red blood cells were isolated from the plasma of a normal adult male. When not in use, the plasma was stored in a heparin and EDTA-containing test-tube at 5°C for up to 48 hours. After centrifugation, the supernatant serum was siphoned off and a 135 mM NaCl and 20 mM sodium phosphate solution at pH 7.4 with a volume equivalent to 4 times the volume of the red blood cells on the bottom of the test-tube was added. The mixture was mixed by gentle shaking and separated by another centrifugation which was, again, followed by the removal of the supernatant liquid. The siphoning-mixing-centrifuging cycle was repeated at least 6 times. Then the sample was remixed and ready for use. The absence of serum proteins was confirmed by the analysis of the intercellular fluids by LIF/CZE. 30-μL droplets containing a concentration of red blood cells which is approximately 1/1000th that in plasma were deposited on standard microscope glass slides. This was accomplished by touching the red blood cell solution with the tip of a needle and transferring the sample on the tip to a 30-μL droplet of the pH 7.4 solution already deposited on the glass slide.

Introduction of red blood cells

The 30-μL droplet of the red blood cell solution was examined under a microscope with a magnification of 100X. With a 5-mm section of its injection end cleared of the polyimide coating, the injection end of the capillary tubing was gently immersed in the droplet under the guidance of a 3-dimensional micromanipulator such that the opening of the tubing could clearly be seen. A single cell was introduced into the tubing by manually controlling a 20-mL piston-syringe connected to the detection end of the gas-tight buffer vial. The cell was then allowed to settle

on and adhere to the inner surface of the tubing. After the injection end of the tubing was transferred to the running buffer, electrophoresis was initiated and the cell was lysed via osmotic shock when it was exposed to the running buffer. It took about 12 hours of practice for the practitioner to become reasonably proficient at the injection procedure.

Introduction of sample solutions

The sample solutions were introduced hydrodynamically by raising the injection end of the capillary tubing to a height of 38.7 cm relative to the detection end for 60 s.

Solutions

The running buffer, 50 mM $Na_2B_4O_7$ (aq) at pH 9.1, and the sample buffer, 135 mM NaCl and 20 mM NaH_2PO_4 (aq) at pH 7.4, were brought to the appropriate pH's with NaOH (s) and were filtered with 0.22-μm cutoff cellulose acetate filters (Alltech Associates, Inc., Deerfield, IL) before use. This filtration step greatly reduces noise spikes caused by particles passing through the detection region. The stock hemoglobin A_0 (HemA), methemoglobin (Met) and carbonic anhydrase (CAH) solutions were prepared in the pH 7.4 sample buffer.

Reagents

Reagent-grade $Na_2B_4O_7$, NaCl, NaH_2PO_4 and NaOH crystals were purchased from Fisher Scientific Co. (Fair Lawn, NJ) while human HemA, human Met and CAH were from Sigma Chemical Co. (St. Louis, MO). All reagents were used as received and only deionized water was used.

Data treatment

Data were collected at 10 Hz. These are then merged into working files with a 5:1 reduction to produce an effective data rate of 2 Hz. Within a given data file there are typically 2 or 3 noise spikes resulting from microbubbles or particles passing through the laser beam. These are easily recognized because they represent sub-second events. They are therefore removed from the data files by interpolation between the adjacent points. No further smoothing of the data was performed.

RESULTS AND DISCUSSION

Separation and detection of hemoglobin and carbonic anhydrase

The average human red blood cell houses more than 100 proteins (20), with HemA (450 amol/cell) and CAH (7 amol/cell) present in sufficient quantities to render their determination by LIF/CZE feasible. Depending on the age and history of the cells, some Met, a form of hemoglobin where the Fe^{2+} in the heme group has been oxidized to Fe^{3+}, may also be present. A separation of the protein standards from commercial sources by CZE with LIF detection was attempted and the ensuing electropherogram is depicted in Fig. 1. Both CAH and HemA migrated as rather sharp zones with an average efficiency of about 58,000 plates. The peak corresponding to Met, however, appears quite broad and exhibits subtle features which indicate that many forms of the protein with similar but distinct electrophoretic mobilities are present. Several separations at other pH's were attempted, but no significant improvement was noticed (data not shown). Four consecutive injections of the same sample solution show that the migration times and peak areas are reproducible to within 1 and 3% respectively.

The mass limits of detection (signal/noise = 2) for CAH and HemA are 2 and 8 amol respectively whereas linear dynamic ranges of at least 2 orders of magnitude are found for both CAH (4×10^{-9} to 4×10^{-7} M) and HemA (9×10^{-9} to 9×10^{-7} M), with the slopes of the logarithmic calibration curves being 1.02 and 1.05 respectively. Met was not studied because of the broad and complex features of its peak. Besides, it represents only 0.4% of all hemoglobin in normal human red blood cells *in vivo* (20). The reproducible migration times and peak areas together with the large linear dynamic ranges render the use of external standardization for the

Fig. 1. Electropherogram of standard proteins. Peaks A, B and C are carbonic anhydrase (CAH), methemoglobin (Met) and hemoglobin (HemA) respectively.

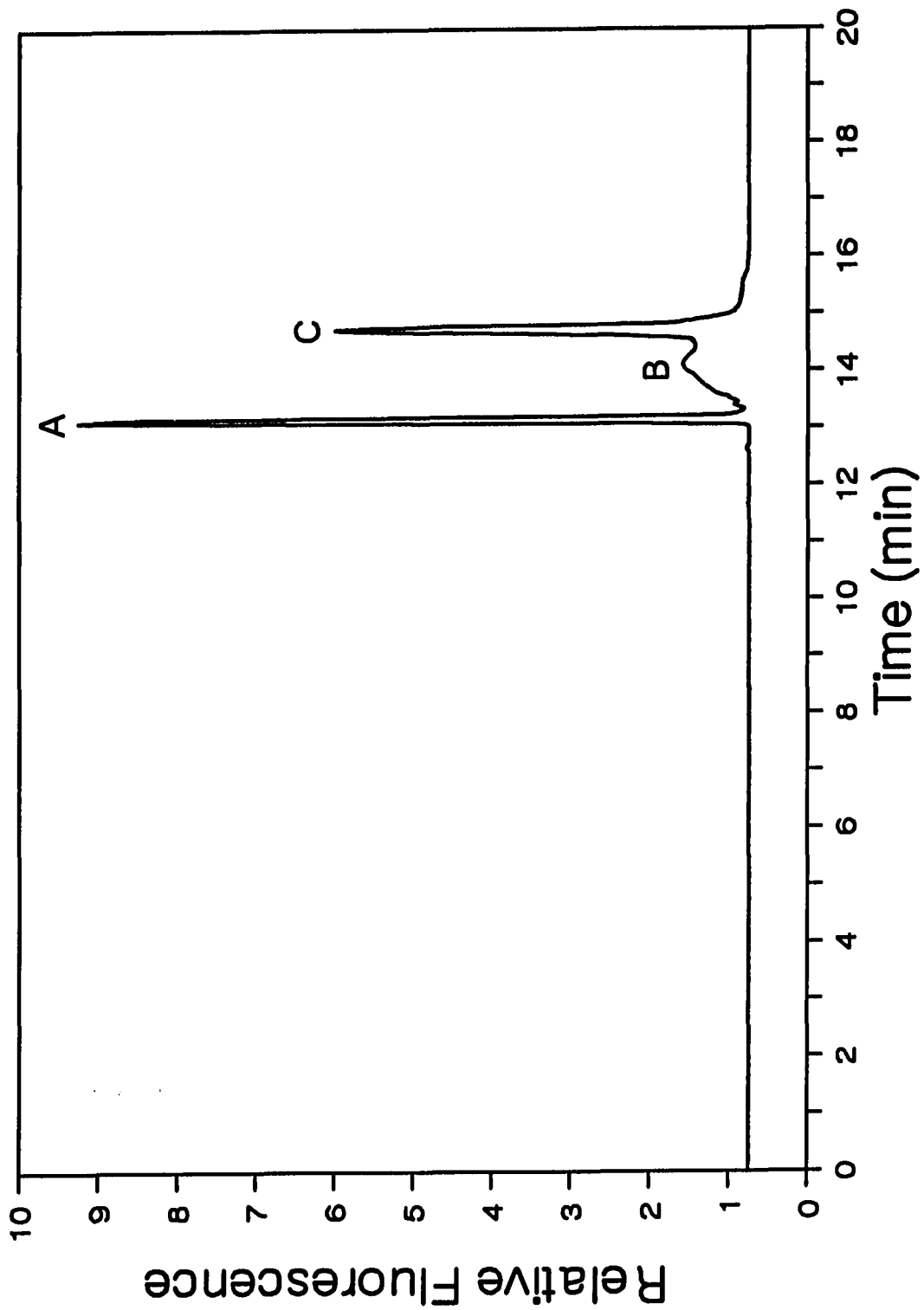
Relative Fluorescence
Time (min)
A
B
C
0
1
2
3
4
5
6
7
8
9
10
0
2
4
6
8
10
12
14
16
18
20

quantitation of CAH and HemA in biological samples suitable. This aspect is crucial, as the addition of internal standards to biological matrices may give rise to undesirable effects including pH changes, concomitant-standard interactions and dilution. When only limited amounts of samples, such as individual cells, are available, the precise and accurate introduction of internal standards to the samples involves the use of sophisticated nL-microdispensers requiring a high degree of operator-skill (1). Because of the small volumes and low analyte levels, variable extents of surface adsorption to the microvial also present a problem. Moreover, increased sample-handling increases the chance of contamination and concentration changes resulting from solvent evaporation.

Analysis of hemolysate

Fig. 2 depicts the electropherogram of the hemolysate of human erythrocytes. By comparison to Fig. 1, the presence of CAH and HemA in the hemolysate is quite obvious. In addition, several small peaks and some subtle features can be discerned throughout the electropherogram. They are probably due to the less abundant proteins in the cells (20). The most prominent unidentified feature is peak 2, which we will refer to as an unknown protein (Unk). Fig. 2 is in good agreement with the results of ref. 21 where the same running buffer was used but the analytes were detected by absorbance at 200 nm. In addition to the much better signal-to-noise ratio with native fluorescence detection, the prominent system peaks and baseline fluctuations in the electropherogram obtained with absorbance detection are also absent in Fig. 2. The latter phenomena can be explained by the high selectivity of fluorescence detection for the analytes of interest and the absence of refractive-index artifacts, thereby reducing undesirable disturbances resulting from concomitants in

Fig. 2. Electropherogram of hemolysate of human erythrocytes. The lettered peaks are as depicted in Fig. 1 while the identities of the numbered peaks are unknown. The most prominent of these, peak 2, is referred to as Unk in the text.

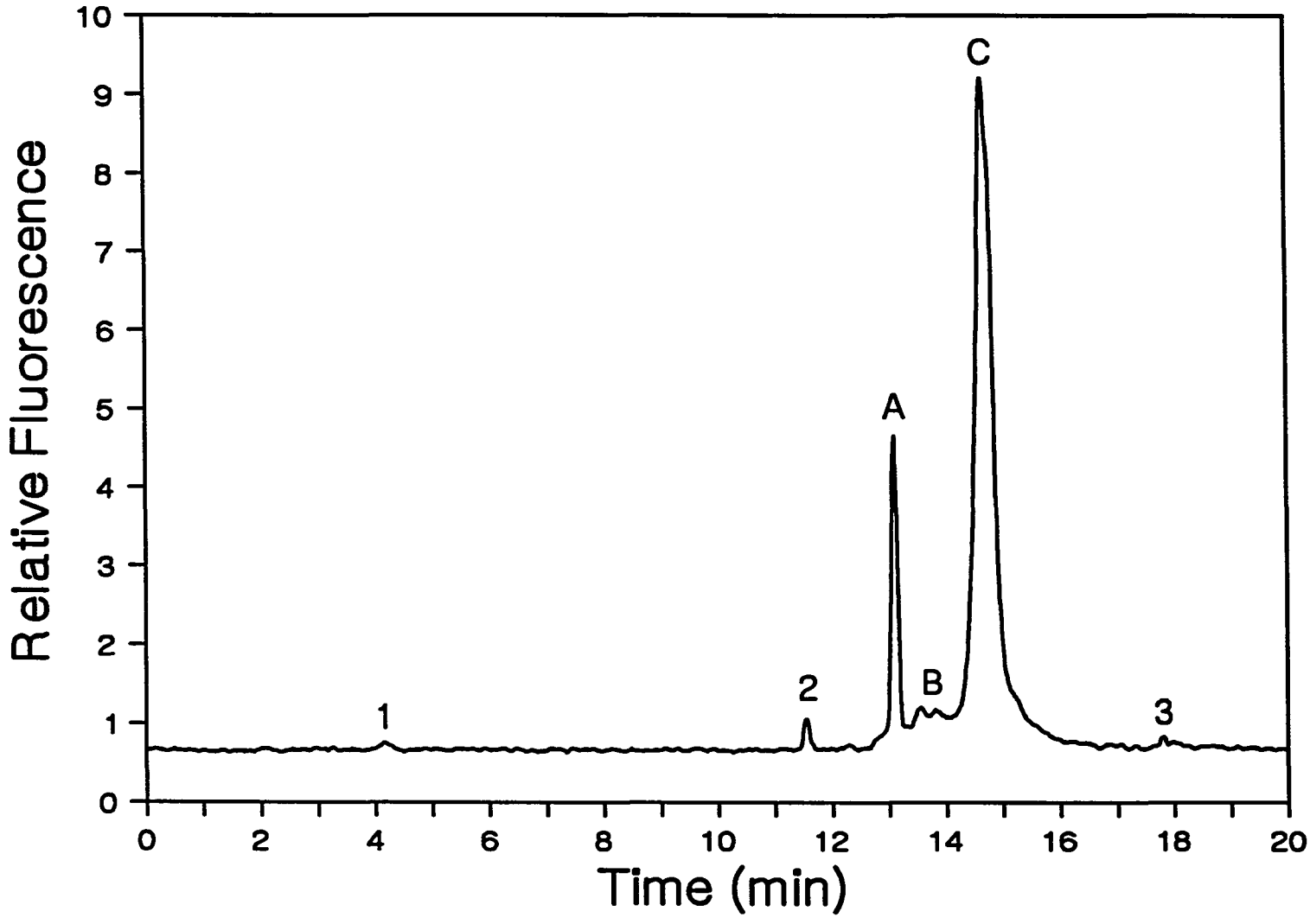
Relative Fluorescence
Time (min)
0
1
2
3
4
5
6
7
8
9
10
0
2
4
6
8
10
12
14
16
18
20
A
B
C
1
2
3

the sample matrix and simplifies the electropherogram for protein separations.

The experimentally measured values of 1.7×10^{-3} and 0.349 g/mL cells for, respectively, CAH and HemA agree well with the 2.5×10^{-3} and 0.335 g/mL for the same analytes obtained by other methods (22,23). Since the composition of human red blood cells varies with the age of the donor (24,25) and with physiological condition, the slight differences between the values from the present work and earlier studies are not surprising. Other possible sources of inaccuracies include differences in the composition of the buffers used to lyse the cells, the amount of time spent by the lysed cells in the buffer and the temperature at which lysis occurred (26). From the earlier discussion on the applicability of external standardization, we believe that instrumental contribution to the slight disagreement in the analyte levels is insignificant.

It is interesting to compare the efficiencies of the separations in Figs. 1 and 2. Except for the sample solutions, the running conditions for both separations were identical. However, it is evident that the peaks in Fig. 2 are much broader than those in Fig. 1. In fact, the average efficiency decreased from 58,000 plates in Fig. 1 to 14,000 plates in Fig. 2. This might be a consequence of a temporary change in the ζ-potential of local regions on the wall of the capillary (27) resulting from the different pH, ionic strength and composition of the hemolysate solution from those of the running buffer, as well as the adsorption of concomitants onto the wall of the capillary. This illustrates that when optimal efficiencies are desired in the analysis of biological matrices with CZE, proper sample cleanup or dilution may be necessary.

Analysis of individual cells

A total of 39 cells were analyzed consecutively. Ten of the data files contained unexpected baseline shifts, abnormally high noise levels due to scattering inclusions in the running buffer, or signal levels beyond the digitization range of the A/D converter. Therefore, only 29 files are further processed for the quantification of the individual components. The success rate clearly improved with practice, as only 1 of the last 17 runs (compared to 5 of the first 10 runs) was discarded.

Fig. 3 shows a set of runs that are representative of the data collected. The numbers refer to the chronological order of the 39 cells studied. These are plotted on a common scale to allow quantitative comparisons. An important observation is that the signal-to-noise ratios are excellent and that baseline stability is not of concern for the 29 cells included for quantitative analysis. Another striking feature is that the individual cells are very different from each other, and from the "average" cell composition depicted in Fig. 2. Cell #22 has a composition most similar to that in the hemolysate, but that is the exception rather than the rule. For all of these, one can clearly recognize the major components, CAH, HemA, Met, and Unk, which correspond to peaks A, C, B and 2 in Fig. 2. There are also other minor features which vary from cell to cell, e.g., one between CAH and Met, but because they are not fully resolved from the main components under these electrophoretic conditions, further discussion of these are not warranted. We note that a 20-μm i.d. capillary was used here. So, even better detectability can be expected for single-cell studies if a 10-μm i.d. capillary is used, albeit at the expense of more critical optical alignment and more difficult manipulation at injection.

The precision of the migration times, using CAH as the marker, degraded from <1% RSD for consecutive standard runs to ~6% RSD for the series of 39

Fig. 3. Electropherograms of proteins in several individual human erythrocytes. Numbers refer to consecutive run numbers over the entire series of 39 trials. A common scale factor is used throughout.

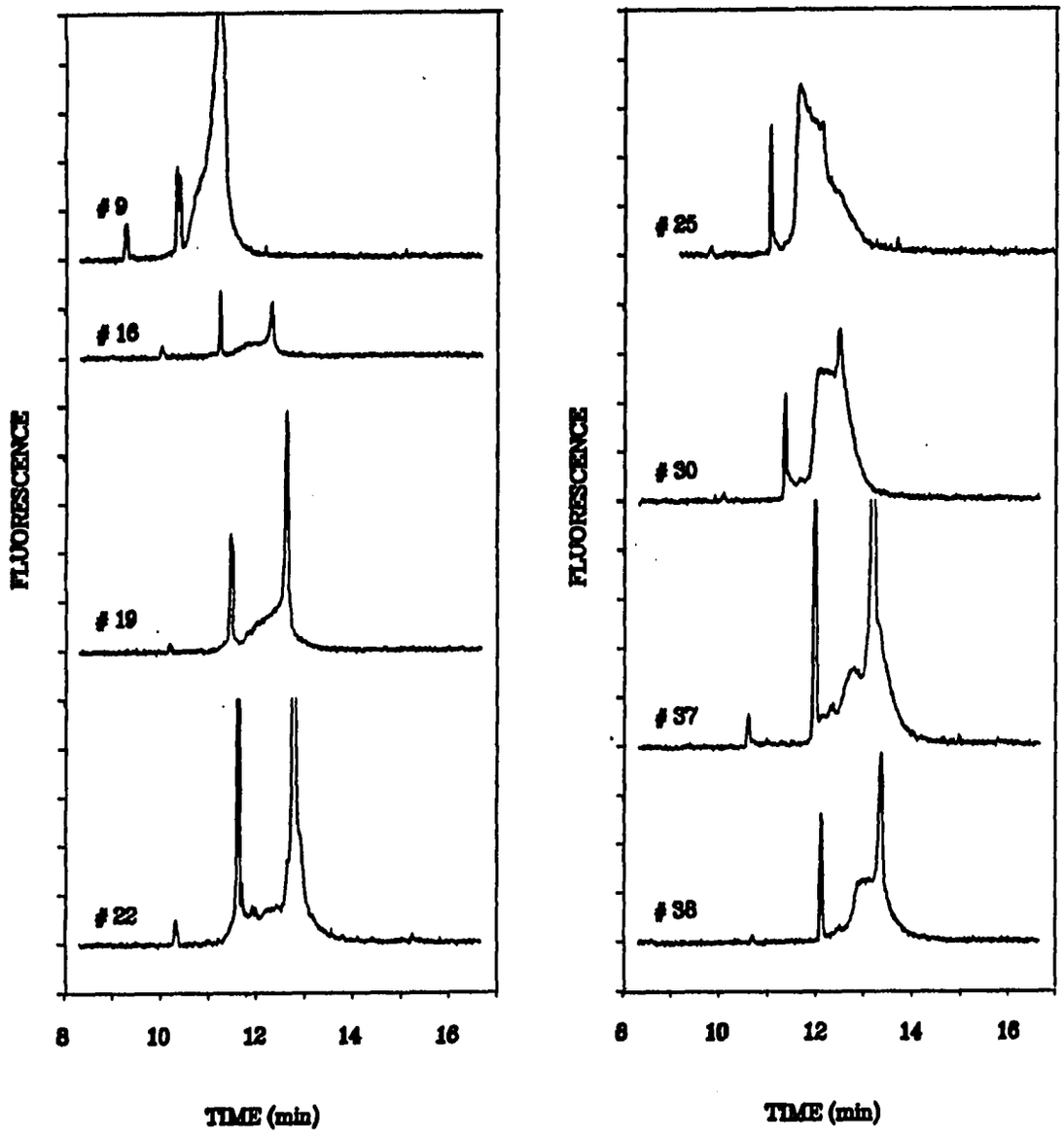
FLUORESCENCE
9
16
19
22
8
10
12
14
16
TIME (min)
FLUORESCENCE
25
30
37
38
8
10
12
14
16
TIME (min)

Fig. 4. Changes in migration time of carbonic anhydrase over the course of the entire experiment.

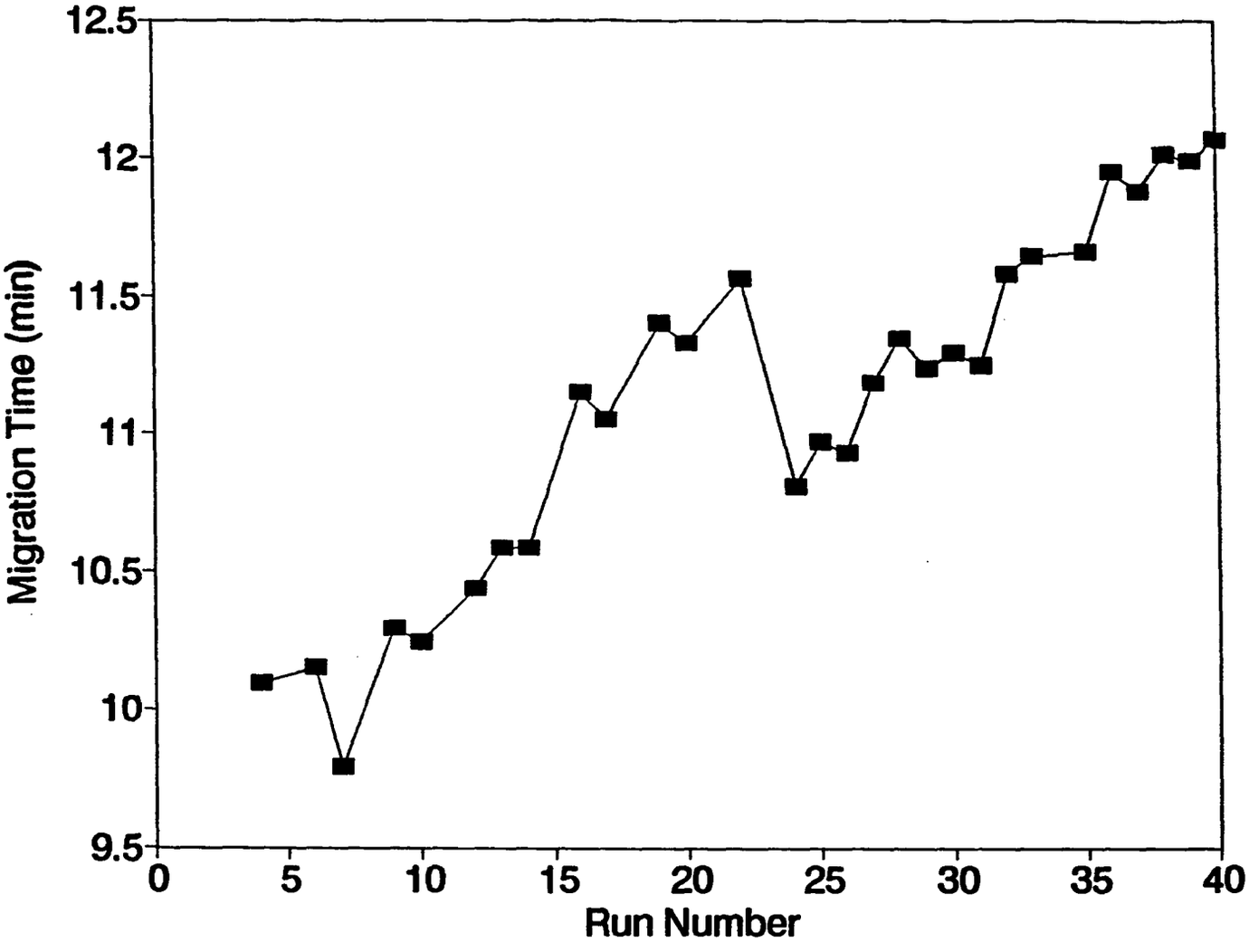
12.5
12
11.5
11
10.5
10
9.5
Migration Time (min)
0
5
10
15
20
25
30
35
40
Run Number

single-cell runs. In Fig. 4 we show the variation in migration times of CAH in this study. There is a clear drift in migration time over the 24 hour duration of the set of experiments. The correlation coefficient for the plot in Fig. 4 is listed in Table I, and is definitely significant at the 99% confidence level. Overall ζ-potential changes resulting from the contamination of the surface of the capillary wall are probably responsible for this. The drift is small because the injected quantities are small. In fact, the difference in the migration times of the CAH and HemA peaks in all the unadjusted electropherograms are found to be equal to within ~2%. This indicates that variations of the migration times result not from changes in the electric field or temperature of the separation medium, but those in the ζ-potential of the capillary wall between runs (28).

Fig. 5 shows some examples of the unusual electropherograms obtained in this study. Close examination reveals that each electropherogram involves two sets of repeating features at somewhat different signal levels. Within each set of repeating features, the migration time spacings between the features are constant. The sharp peak of CAH is quite apparent in each set. This argues against the presence of other unexpected components or the slow release (partial lysis) of proteins from a given cell. Rather, the repeating features can be explained by the injection and separate lysis of two distinct cells in a given run. Such an event will lead to uncorrelated cytoplasmic sampling times after the cells are adsorbed on the capillary wall, delaying the second set of repeating features. Throughout these studies, care was taken to provide single-cell injection as confirmed by observation under a microscope. Still, there is the possibility that the disk-shaped erythrocytes are stacked on top of each other and injected as a "single" cell. Surface area considerations favor such a geometry for coadsorption, which is difficult to identify at

Fig. 5. Electropherograms each corresponding to the injection of 2 cells with asynchronous lysis. Repeating features are clearly identifiable.

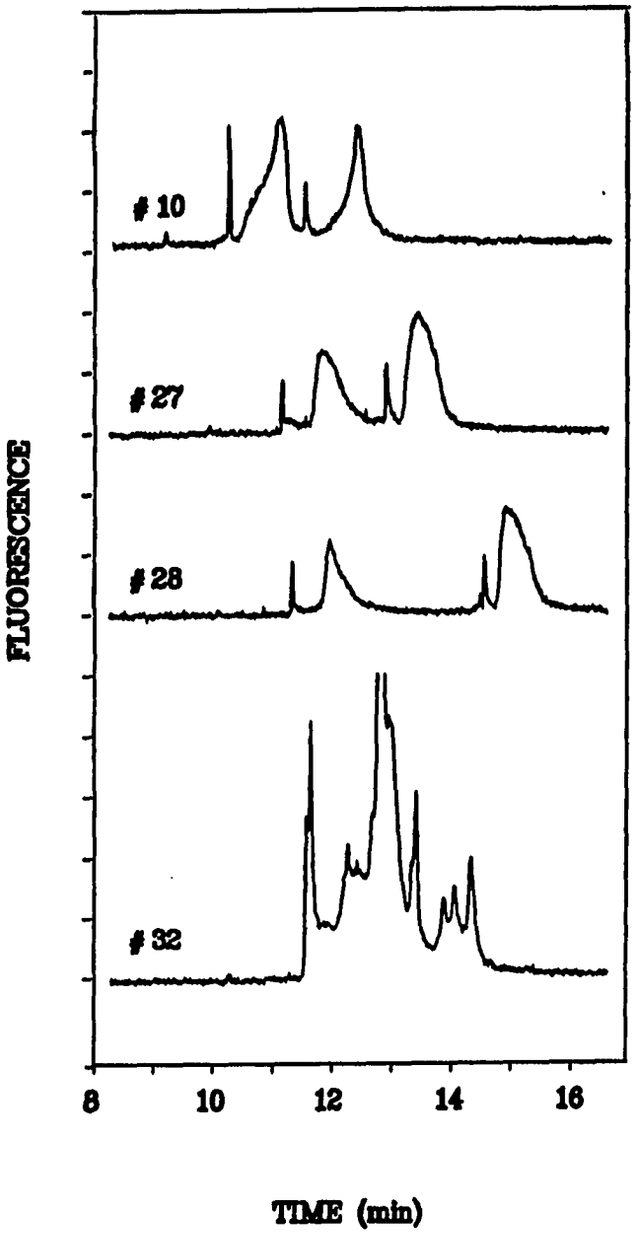
FLUORESCENCE
10
27
28
32
8
10
12
14
16
TIME (min)

this power of magnification. Since erythrocytes are not compartmentalized like certain other cells, such sets of features cannot be attributed to late release from different parts of the cell. The facts that the relative amounts are not constant and that only a few experiments reveal these repeating features further support such a conclusion. The delayed lysis after 1-2 minutes can be explained by the fact that the residual cell membrane of the top cell can act as a protective shield for the bottom cell. Fig. 5 shows that our procedure for cell injection and spontaneous lysis at the start of electrophoresis (when electroosmotic flow carries the low ionic-strength buffer past the adsorbed cell) provides an internal check on multiple-cell events. Unless the cells lyse together within a time corresponding to the peak width of CAH, the electropherogram will allow discrimination among the individual events. Future experiments with lower cell densities and at higher microscope magnification will remove such uncertainties.

The prominent peaks corresponding to CAH and HemA can be used to correct for migration time variations (Fig. 4) among all the runs. Then, 5-s intervals of all electropherograms can be binned together to form a composite electropherogram. This is shown in Fig. 6. The main features are clearly visible. In comparison to Fig. 2, the Met peak is larger, probably at the expense of the HemA peak. The possibility that some of the HemA might have been oxidized to Met during the typical storage period exists, as it is well-known that HemA is readily oxidized to Met by atmospheric oxygen (29,30). Such quantitative information should be valuable to blood bank operations, where the integrity of the HemA form is important.

Fig. 6. Composite of 29 electropherograms of single human erthrocytes. The lettered peaks are as depicted in Fig. 1.

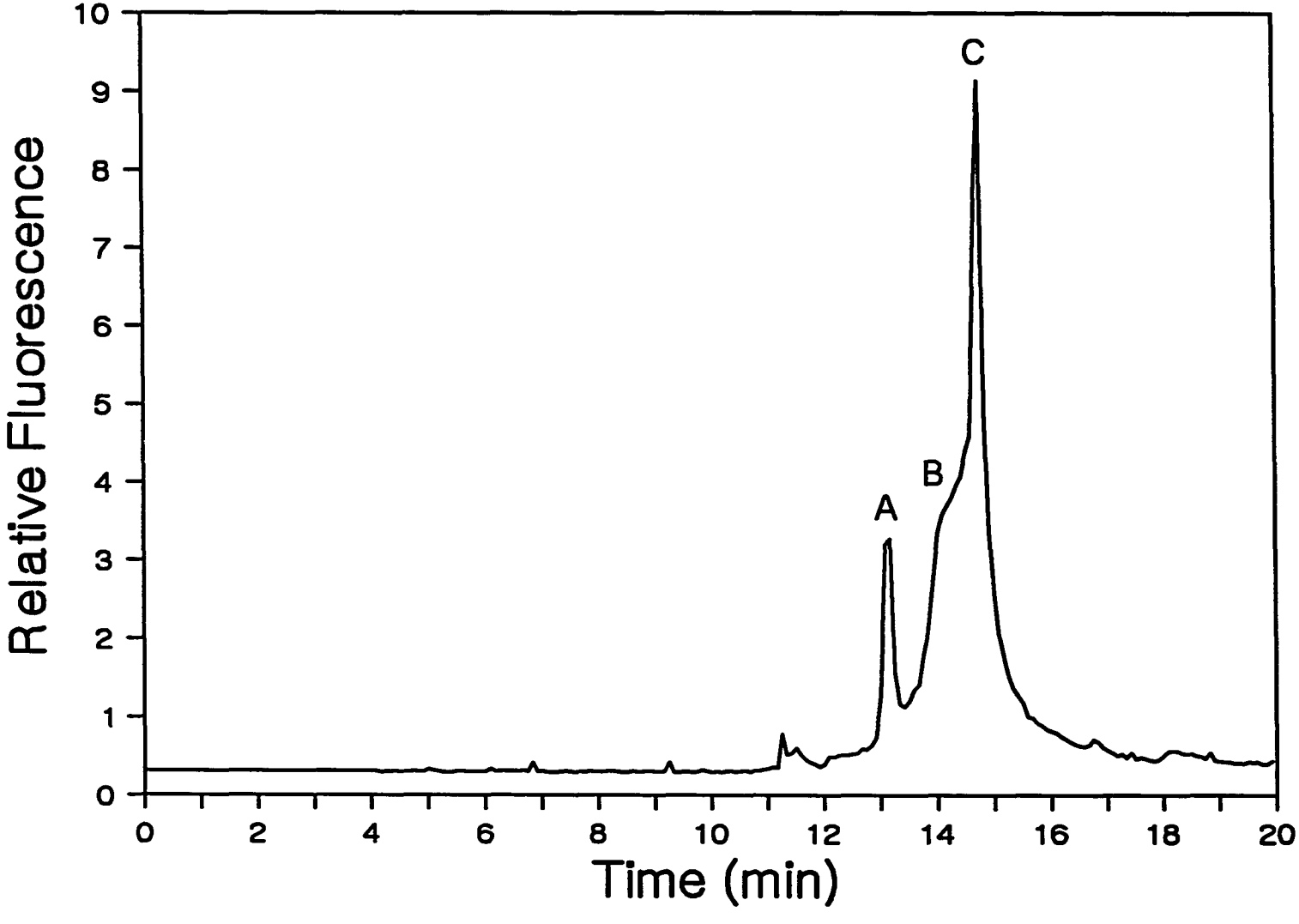
Relative Fluorescence
Time (min)
A
B
C
0
1
2
3
4
5
6
7
8
9
10
0
2
4
6
8
10
12
14
16
18
20

Quantitative correlations

Since the entire cell is injected into the capillary with no additional manipulation or derivatization reaction, one can expect superior quantitative reliability compared to previous single-cell studies. For quantitative determinations, the individual data points were first normalized with respect to the migration time of CAH for that electropherogram. This corrects for peak area determinations irrespective of the speed of migration past the detector. Then, integration is performed, with baseline correction, separately for CAH, HemA, Unk and total signal. For some electropherograms, reliable determination of every one of the first 3 may not be possible because of uncertainties in the baseline, so some of the values were not used in the following analysis. For those runs with double sets of features, individual contributions from two separate cells were assumed and integration was performed separately for each set.

The total fluorescence signal for each run is plotted for the individual cells in Fig. 7. Since over 90% of the cell proteins are known to be in one form of hemoglobin or another, this is an important quantity. Even though various forms of hemoglobin may have different molar absorptivities or fluorescence yields, the correction is not expected to be large. The total signal is then a good measure of the total hemoglobin originally in the cell, even given the possibility of changes or degradation after *in vivo* sampling. Previous determination of total hemoglobin has been reported based on the density on a photographic image of individual cells in the field of view of a microscope under 415 nm light (31). That does not take into account the large spectral shift in the heme chromophore (as opposed to the protein moieties here) between the HemA and the Met forms. Naturally, photographic images are limited in linear dynamic range and were not even calibrated in the

Fig. 7. Total (integrated) signal recorded for individual erythrocytes over the population sampled.

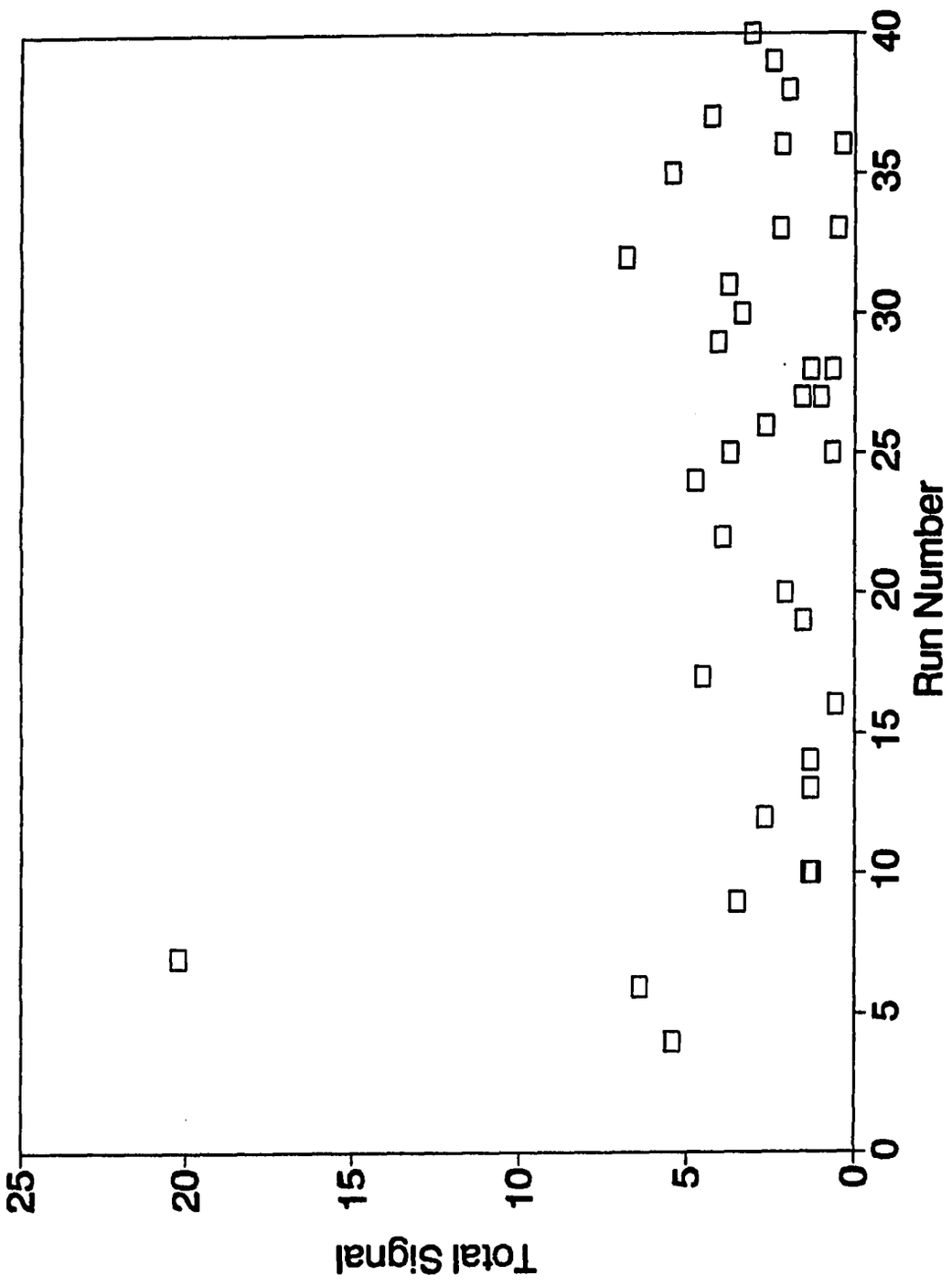
Total Signal
25
20
15
10
5
0
0
5
10
15
20
25
30
35
40
Run Number

earlier study.

Fig. 7 shows several important features. First, there is no correlation with respect to run number (see also Table I). Variations are therefore not due to changes in the column surface, drift in optical alignment, or degradation of the cells over the 24-hour measurement time, any of which would have given rise to noticeable trends in the data as plotted. Second, the distribution of values does not follow Gaussian statistics. The normal description of the data is 3.67 ± 3.59 (mean ± stardard deviation). From studies of standard, matrix-free protein samples, the experimental uncertainties in quantitation should be no larger than 3%. A histogram of the data is shown in Fig. 8. While histograms have been reported for various cell components earlier (12), our unique quantitative reliability for individual measurements allow detailed distributions to be obtained. Fig. 8 reflects true differences between cells rather than measurement and sampling errors. Indeed, erythrocytes should be fairly uniformly distributed in the blood stream with ages spanning 1-120 days (20), and an "average" is not meaningful. Third, human erythrocytes are known to be quite homogeneous in terms of cell volumes (±7%) in an individual (32-34). This is qualitatively verified under the microscope for our sample. Yet, the total signal varied by roughly an order of magnitude over the 35 cells plotted, even neglecting cell #7. Previous reports have mentioned variations of factors of 2 or 3 (12,31), but only semi-quantitative techniques were employed. In the extremely unlikely situation that we have quite a few two-cell injections with simultaneous lysis, the results would still show a factor of 5 variation in total signal. Although not quantitative, some cells do appear quite a bit darker than others within the field of the microscope, lending support to the above measurements.

In Fig. 9 we show the variations of the fraction of HemA (as a function of

Fig. 8. Histogram of total signal in individual human erthrocytes.

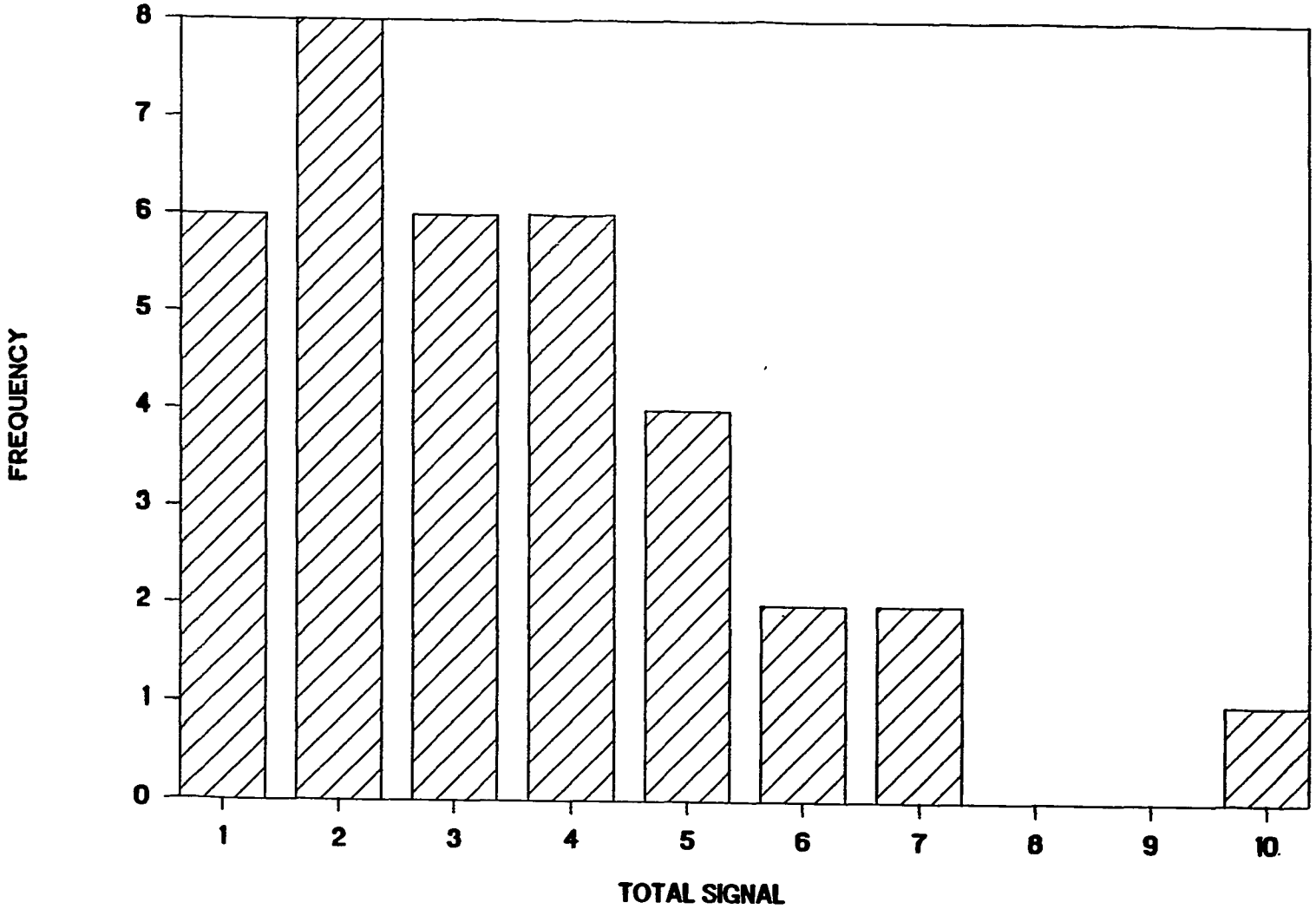
FREQUENCY
0
1
2
3
4
5
6
7
8
1
2
3
4
5
6
7
8
9
10
TOTAL SIGNAL

Fig. 9. Fraction of hemoglobin A_0 for individual erythrocytes over the population sampled.

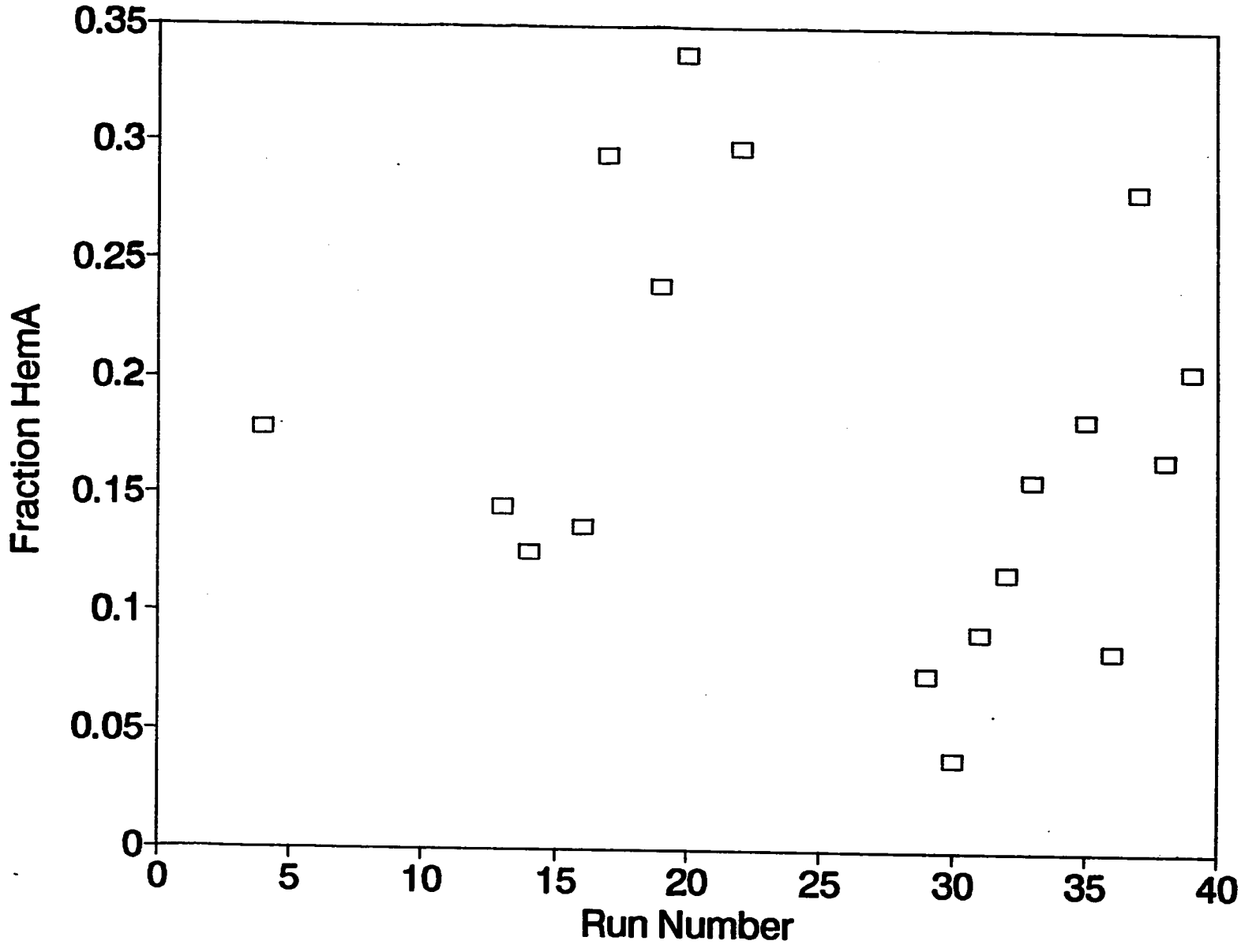
Fraction HemA
0.35
0.3
0.25
0.2
0.15
0.1
0.05
0
0
5
10
15
20
25
30
35
40
Run Number

the total signal) among cells. These values refer to fluorescence intensities and are not corrected for differences in response factors among different proteins (19). Fig. 9 is different from Fig. 7 because cell sizes, multiple injections, and optical alignment changes will all be properly corrected for. Again, we see a non-Gaussian distribution which distorts the standard representation of 0.175 ± 0.085 for the 18 cells for which HemA can be confidently measured. There is no correlation with run number or with the total observed signal (see Table I). The individual values in Fig. 9 varied by an order of magnitude. Since the majority of hemoglobin in cells *in vivo* is in the A_0 form (HemA), Fig. 9 shows degradation after *in vivo* sampling to Met. It is surprising at first sight that for such a homogeneous cell type the rate of degradation after exposure to the same *in vitro* environment can be so different. However, if the reducing environment (e.g., glutathione content) (17) and/or the activity of various reducing enzymes are different, such an observation can be expected.

Table I. Correlation Coefficients

r(N)*	t_m	Total	CAH	HemA	Unk
Run #	.92 (29)	.28 (35)	.02 (32)	.19 (18)	.04 (24)
Total			.23 (32)	.04 (18)	.01 (24)
CAH				.65 (18)†	.18 (22)
HemA					.30 (14)

*r, correlation coefficient; N, number of observations
†0.65 > 0.468 (95%)
> 0.590 (99%)
All other entries are below the statistically significant values even at the 95% confidence level (35).

Table I also lists the correlation coefficients for regression plots for the other two quantified components within single cells, fraction CAH and fraction Unk as a function of run number and as a function of total signal. None of these showed statistically significant correlations (35). Indeed, there is no *a priori* reason why they should, if our sampling and measurement procedure is not subject to systematic errors. Fraction CAH (0.083 ± 0.032) and fraction Unk (0.021 ± 0.033) also do not follow Gaussian statistics and also vary by roughly an order of magnitude over the whole data set. These results support the range of variability of chemical contents in individual cells shown in Figs. 7 and 9. The fraction Unk present in each cell is also not correlated with the fraction CAH or fraction HemA present, as indicated in Table I. We can conclude that Unk is not directly related to HemA-Met degradation, but further insight cannot be gained until positive identification (e.g., fraction collection and GC-MS analysis) is made.

The relationship between the fraction of CAH and fraction of HemA in individual cells is shown in Fig. 10. There is a positive correlation between the two as supported by Table I. At the 99% confidence level, the observed correlation coefficient of 0.65 is larger than the required value of 0.59 for this number of observations (35). Cells with a larger fraction of HemA remaining tend to also show a higher level of CAH. A reasonable explanation of this is these represent cells of different ages (20). The older cells are less likely to retain protein or enzymatic activity, since proteins are not replaced in erythrocytes once manufactured. The same factors (reducing environment, reducing enzyme activity, ATP levels) that maintain the integrity of HemA are likely to affect CAH as well. Further studies on cell populations of known age (*in vivo*) and on different individuals will elucidate this point.

Fig. 10. Relationship between the fraction of carbonic anhydrase and the fraction of hemoglobin A_0 for individual erythrocytes.

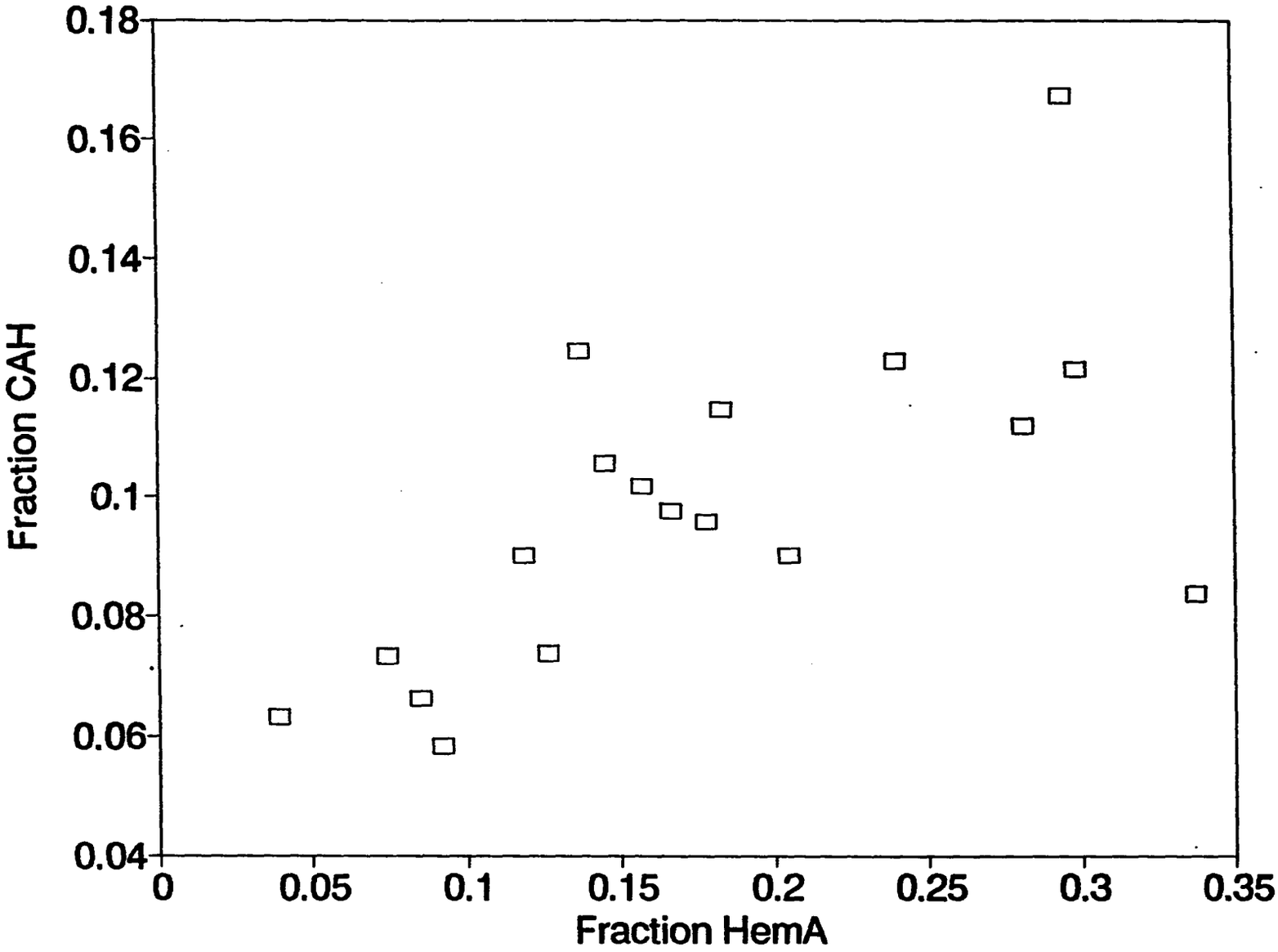
0.18
0.16
0.14
0.12
0.1
0.08
0.06
0.04
Fraction CAH
0
0.05
0.1
0.15
0.2
0.25
0.3
0.35
Fraction HemA

The same blood sample was used throughout and was collected from the experimenter. This is necessitated by the safety concern over using foreign blood samples. No abnormality is expected. The "average" levels of CAH and HemA per cell, assuming a cell volume of 86 fL, were determined from the hemolysate (Fig. 2) as calibrated by external standards (Fig. 1) and were found to be 5 amol and 0.47 fmol respectively. These are close to the literature values of 7 amol and 0.45 fmol respectively (22,23). However, it is difficult to obtain a reliable absolute calibration of the same quantities from the single-cell data (Fig. 6), since the injection volume of the standards is dependent on temperature (viscosity), capillary diameter, and injection hysteresis (36). The capillary diameter is nominally 20 μm but can deviate easily by 10-20% (37). Since single-cell studies are more valuable for noting individual differences than to replace routine blood tests to give the "average" levels, absolute calibration may not be the limiting factor in many biological applications. However, more work is needed along these lines.

CONCLUSION

We have shown that native fluorescence can be used to monitor individual proteins from single erythrocytes separated by capillary zone electrophoresis. The sensitivity is sufficient for detecting amol levels of proteins, which addresses even minor components in erythrocytes, and is likely to approach sub-amol levels if even smaller capillaries are used. Future applications to cell compartments, organelles, or to even smaller cells are certainly not out of the question. The fact that no derivatization or handling of the intracellular fluid is needed in this scheme means that quantitation will be independent of reaction efficiency, transfer (injection) efficiency, or retention on sample vials. Presumably variations in excitation/emission efficiency as a function of environment (buffer pH) can be corrected for when modifications are made to alter the selectivity of the separation to isolate other components. Our results show that Gaussian statistics are not suitable for describing these cell populations. Age is a likely factor that affects the rate of oxidation of HemA to Met, and can explain the positive correlation between fraction CAH vs fraction HemA in the cells after storage. Previous results on single-cell glutathione levels (17) also show similar non-Gaussian statistics and may in fact be related to the present observations. Unexpectedly large variations in the individual protein fractions as well as in the total signal among the cells, up to a factor of 10, highlight the importance of single-cell studies. It may be that the "outliers" are the only significant ones that will provide chemical markers for early disease diagnosis. Extension of the present work to lymphocytes and to cancer cell lines should therefore be valuable.

REFERENCES

1. Cooper, B. R.,; Jankowski, J. A.; Leszczyszyn, D. J.; Wightman, R. M.; Jorgenson, J. W. Anal. Chem., 1992, 64, 691-694.
2. Oates, M. D.; Cooper, B. R.; Jorgenson, J. W. Anal. Chem., 1990, 62, 1573-1577.
3. Kennedy, R. T.; Jorgenson, J. W. Anal. Chem., 1989, 61, 436-441.
4. Kennedy, R. T.; Oates, M. D.; Cooper, B. R.; Nickerson, B.; Jorgenson, J. W. Science, 1989, 246, 57-63.
5. Wallingford, R. A.; Ewing, A. G. Anal. Chem., 1988, 60, 1975-1977.
6. Kennedy, R. T.; St. Claire, R. L.; White, J. G.; Jorgenson, J. W. Mikrochim. Acta, 1987, II, 37-45.
7. Jessen, K. R. In Immunocytochemistry; Polek, J.; van Noorden, S., eds.; Academic Press: New York, 1974, Chapter 3.
8. McAdoo, D. J. In Biochemistry of Characterized Neurons; Chan-Palay, V.; Palay, S., eds.; Wiley: New York, 1984.
9. Lent, C. M.; Mueller, R. L.; Haycock, D. A. J. Neurochem., 1983, 41, 481-490.
10. Osborne, N. N. Nature, 1977, 270, 622-623.
11. McCaman, R. M.; Weinrich, D.; Borys, H. J. Neurochem., 1973, 21, 473-476.
12. Gitlin, D.; Sasaki, T.; Vuopio, P. Blood, 1968, 32, 796-810.
13. Bahr, G. F.; Zeitler, E. Lab. Invest., 1962, 11, 912.
14. Nickerson, B.; Jorgenson, J. W. J. Chromatogr., 1989, 480, 157-168.
15. Swaile, D. F.; Sepaniak, M. J. J. Liq. Chromatogr., 1991, 14, 869-893.
16. Kuhr, W. G.; Yeung, E. S. Anal. Chem., 1988, 60, 2642-2645.
17. Hogan, B. L.; Yeung, E. S. Anal. Chem., submitted for publication.

18. Stryer, L. Biochemistry, 3rd ed.; W. H. Freeman and Co.: New York, 1988, Chapter 2.

19. Lee, T. T.; Yeung, E. S. J. Chromatogr., 1992, 595, 319-325.

20. Pennell, R. B. In The Red Blood Cell, 2nd ed.; Surgenor, D. M.-N., ed.; Academic Press: New York, 1974, Chapter 3.

21. Lee, K.-J.; Heo, G. S. J. Chromatogr., 1991, 559, 317-324.

22. Osgood, E. E. Arch. Internal. Med., 1935, 56, 849.

23. Roughton, F. J. W.; Rupp, J. C. Ann. N.Y. Acad. Sci., 1958, 75, 156-166.

24. Markkanen, T.; Heikinheimo, R.; Dahl, M. Acta Haematol., 1969, 42, 148.

25. Hjelm, M. Advan. Exp. Med. Biol., 1970, 6, 81.

26. Dodge, J. T.; Mitchell, C.; Hanahan, D. J. Arch. Biochem. Biophys., 1963, 100, 119-130.

27. Chien, R.-L.; Helmer, J. C. Anal. Chem., 1991, 63, 1354-1361.

28. Lee, T. T.; Yeung, E. S. Anal. Chem., 1991, 63, 2842-2848.

29. Jandl, J. H.; Engle, L. K.; Allen, D. W. J. Clin. Invest., 1960, 39, 1818.

30. Eder, H. A.; Finch, C.; McKee, R. W. J. Clin. Invest., 1949, 28, 265.

31. Ambs, E. Acta Haemat., 1956, 15, 302-313.

32. Weinstein, R. S. In The Red Blood Cell, 2nd ed.; Surgenor, D. M.-N., Ed.; Academic Press: New York, 1974, Chapter 5.

33. Westerman, M. P.; Pierce, L. E.; Jensen, W. N. J. Lab. Clin. Med., 1961, 57, 819.

34. Ponder, E. Hemolysis and Related Phenomena; Grune and Stratton: New York, 1948, pp. 10-26.

35. Snedecor, G. W.; Cochran, W. G. Statistical Methods, 6th ed.; Iowa State University Press: Ames, IA, 1967, p. 557.

36. Lee, T. T.; Yeung, E. S. Anal. Chem., 1992, 64, 1226-1231.

37. From Data Sheet supplied by Polymicro Technologies for their "Flexible Fused Silica Capillary Tubing"; Polymicro Technologies, Inc.: Phoenix, AZ.

PAPER V.

SCREENING AND CHARACTERIZATION OF BIOPHARMACEUTICALS BY CAPILLARY ELECTROPHORESIS WITH LASER-INDUCED NATIVE FLUORESCENCE DETECTION

INTRODUCTION

The use of living organisms for the manufacture of pharmaceuticals by recombinant DNA technologies represents a unique approach and promises to transform numerous aspects of human health care. The novelty of biopharmaceuticals, however, renders the protocols of quality control (QC) intended for traditional pharmaceuticals inappropriate. Although many analytical techniques developed in the biological sciences have been applied to the QC of biopharmaceuticals, the necessities of high accuracy, sensitivity, resolution and speed appear to have exceeded the capabilities of many traditional methods. In fact, the vague guidelines set forth by the U.S. Food and Drug Administration (FDA) reflect an attitude of openness toward the incorporation of innovative approaches to assure the quality of biopharmaceuticals (1). To this end, the high speed and efficiency together with the automated and quantitative features of high-performance capillary electrophoresis (HPCE) in the analysis of protein mixtures represent a significant improvement over slab-gel electrophoresis and high-performance liquid chromatography (HPLC) and is bound to gain wide acceptance in the QC of biopharmaceuticals as the technology advances.

The application of HPCE with absorbance detection to the QC of biopharmaceuticals is well-documented (e.g., 2-9). For instance, peptide mapping by HPCE has been utilized to ensure the genetic stability of the organism and structural integrity of the expressed product (2,3). The quantitation of active ingredients and excipients in dosage formulations has been accomplished by HPCE (4). It has been shown that HPCE is suitable for the real-time monitoring of the major product and host cell contaminants at the various stages of product purification (5). The rapid

and high-resolution separation of slight structural variants of and probable impurities accompanying the expressed protein has been achieved by HPCE (6-8). Biopharmaceuticals with different extents of glycosylation have successfully been resolved by HPCE (7,8). HPCE has also been used to unravel the composition of a complex culture medium (9).

While the examples mentioned heretofore have clearly demonstrated the immense potential of HPCE in the QC of biopharmaceuticals, an aspect which hampers its acceptance by the industry is the poor detection sensitivity for proteins separated by HPCE. As a consequence of the short pathlength provided by the small-i.d. capillary tubing and the low extinction coefficients of most proteins in shallow ultra-violet and visible region of the electromagnetic spectrum, the detection of proteins by absorbance offers a limit of detection (LOD) in only the μM range. This drastically impairs the utility of HPCE in vital facets of the QC of biopharmaceuticals. Some prominent examples include the quantitation of trace impurities, monitoring of product yield during incubation, assurance of genetic and product stability at low protein concentrations and detailed chemical profiling of culture media. Even in situations where the proteins of interest are present at high concentrations, such as in product purity analyses via HPCE peak profiles, better precision, reduced electrophoretic band broadening and extended column-life can often by realized through the dilution of concentrated samples prior to injection. The preceding discussion underscores the importance of high detection sensitivity for proteins in HPCE.

Since many applications of HPCE to the QC of biopharmaceuticals involve the analyses of complex matrices, with all its dependencies upon concomitants, the strategy of labeling with chromophores or fluorophores to enhance detection

sensitivity is bound to be unsuccessful. Besides, the derivatization of proteins gives rise to multiple (10,11) or broad (12) peaks, further complicating the analysis. As the more elaborate electrochemical detectors (13,14) suffer from gradual deterioration in performance resulting from electrode-contamination while the sophisticated mass spectrometric detectors (15) do not yet possess the sensitivity and reliability which surpass those of absorbance detectors, their use in HPCE for proteins is unwarranted. The requirement that the analyte be tagged with radioisotopes renders the use of radiochemical detection in HPCE for the determination of proteins in production lots unsuitable (16). Hence, native fluorescence detection remains the only viable alternative for the high-sensitivity determination of proteins in HPCE.

Laser-induced fluorescence (LIF) detection of native, tryptophan-containing proteins in HPCE was first demonstrated by Swaile and Sepaniak (11). Since then, we have improved the sensitivity by more than 2 orders of magnitude through the use of the 275.4-nm line from an argon-ion laser so that most proteins can now be detected at below the nM level (17). In the present work, we report the use of HPCE/LIF to solve practical problems encountered in the screening and characterization of biopharmaceuticals. We demonstrate that the coupling of high speed, efficiency and sensitivity tremendously enhances the capability of HPCE in the QC of biopharmaceuticals. HPCE/LIF is used to monitor a vaccine purification process, quantify trace impurities in "purified" biopharmaceuticals, determine the genetic and structural stability of products at trace levels and obtain kinetic information on an enzyme-drug present at low concentrations.

MATERIALS AND METHODS

Capillary electrophoresis

The experimental setup used has been described elsewhere (17). Briefly, 50-μm i.d. uncoated fused silica capillaries of various lengths (Polymicro Technologies, Inc., Phoenix, AZ) and a voltage of +28 kV at the injection end were employed throughout. The electrode and buffer vials at the high-voltage terminal were housed in a Plexiglas box to ensure the safety of the operator. A high-voltage power supply (Glassman High Voltage, Inc., Whitehorse Station, NJ; EH Series; 0-40 kV) was used to drive the electrophoresis. The capillary was conditioned with a 1:1 (v:v) mixture of methanol and water for 30 min followed by a 0.1 M NaOH (aq) for the same period of time before use. All samples were injected hydrodynamically by raising the level of the injection end of the tubing to a height of 18.0 cm relative to that of the detection end for 40 s. Quantitative precision at the 1% RSD level has been obtained using this injection scheme (18). Data was collected via a 24-bit A/D interface (Chrom Perfect Direct, Justice Innovation, Palo Alto, CA) and stored on an IBM PC/AT (Boca Raton, FL).

Detection

The 275.4-nm line from an argon-ion laser (Spectra Physics, Inc., Mountain View, CA; Model 2035) was isolated from other lines with a prism and focused with a 1-cm focal length lens into the detection region on a part of the capillary tubing where the polyimide coating had been removed. Scattered light was prevented from passage onto the photomultiplier tube through spatial and spectral filtering. 2 UG-1 absorption filters (Schott Glass Technologies, Inc., Duryea, PA) were used. For

absorbance detection, a CV^4 variable wavelength absorbance detector (Isco, Inc., Lincoln, NE) was used.

Chemicals

Buffer solutions were prepared by dissolving the crystals of $NaH_2PO_4.H_2O$, $Na_2B_4O_7$ and NaOH (Fisher Scientific Co., Itasca, IL) in deionized water from a Waters Purification System (Millipore Corp., Milford, MA). The particulate matter in the solutions was then removed by passing the solutions through 0.22-μm cutoff cellulose acetate filters (Alltech Associates, Inc., Deerfield, IL). Trypsin and conalbumin were purchased from Sigma Chemical Co. (St. Louis, MO). α-Thrombin was kindly supplied by ZymoGenetics, Inc., Seattle, WA.

Biopharmaceuticals

All the biopharmaceuticals employed were generous gifts from various pharmaceutical and biotechnology companies. They include: recombinant hepatitis B surface antigen (rHBsAg) from Merck Sharp & Dohme Research Laboratories, West Point, PA; humanized anti-Tac monoclonal antibody (anti-TAC) from Hoffmann-La Roche, Inc., Nutley, NJ; recombinant human growth hormone (rhGH) and interferon-γ (rIFN-γ) from Genentech, Inc., S. San Francisco, CA; recombinant human interleukin-4 (rhIL-4) from Sterling Drug, Inc., Malvern, PA; recombinant human interleukin-6 (rhIL-6) from Sandoz Pharma AG, Basel, Switzerland and recombinant platelet factor XIII (rFXIII) from ZymoGenetics, Inc., Seattle, WA.

RESULTS AND DISCUSSION

Assaying biopharmaceuticals in dosage formulations

In the assay of biopharmaceuticals in dosage formulations, the importance of high accuracy and precision as well as labor- and time-saving capabilities cannot be overstated. Because of the semi-quantitative, imprecise, slow and labor-intensive features of radioimmunoassay (RIA), enzyme-linked immunosorbent assay (ELISA), bioassay, slab polyacrylamide gel electrophoresis (PAGE) and isoelectric focusing (IEF), HPLC has become the workhorse in the quantitation of biopharmaceuticals in dosage formulations (19,20). However, reliable assays must be based on multiple methods with orthogonal separation mechanisms. In this respect, HPCE possesses tremendous potential as a fast and high-resolution technique which complements HPLC. In many situations, high detection sensitivity is needed in order to take advantage of the speed and efficiency of HPCE in the quantitative determination of biopharmaceuticals in dosage formulations. An example is shown in Fig. 1 where rHBsAg(S), a vaccine used in the prevention of diseases caused by the hepatitis B virus produced in bakers' yeast and the active ingredient of Recombivax HB®, is depicted in electropherograms obtained with absorbance and LIF detection. The much better signal-to-noise ratio (S/N) with LIF detection is evident. This aspect is critical, as sufficient S/Ns are a prerequisite for accurate and precise quantitation. In addition, LIF detection affords special selectivity compared to absorbance detection. This is illustrated as the absence of the peaks at 4.0, 8.2, 8.4 and 12.2 min and the presence of the peak at 4.5 min in Fig. 1(b).

A more dramatic illustration of the differences in selectivity and sensitivity between absorbance and LIF detection is provided by Fig. 2 where a

Fig. 1 (a). Electropherogram of "pure" rHBsAg(S) (200 μg/mL) with absorbance detection at 200 nm. Condition: 25 mM sodium phosphate at pH 7.25; 70-cm capillary (55-cm working length); 28 kV running voltage at injection end.

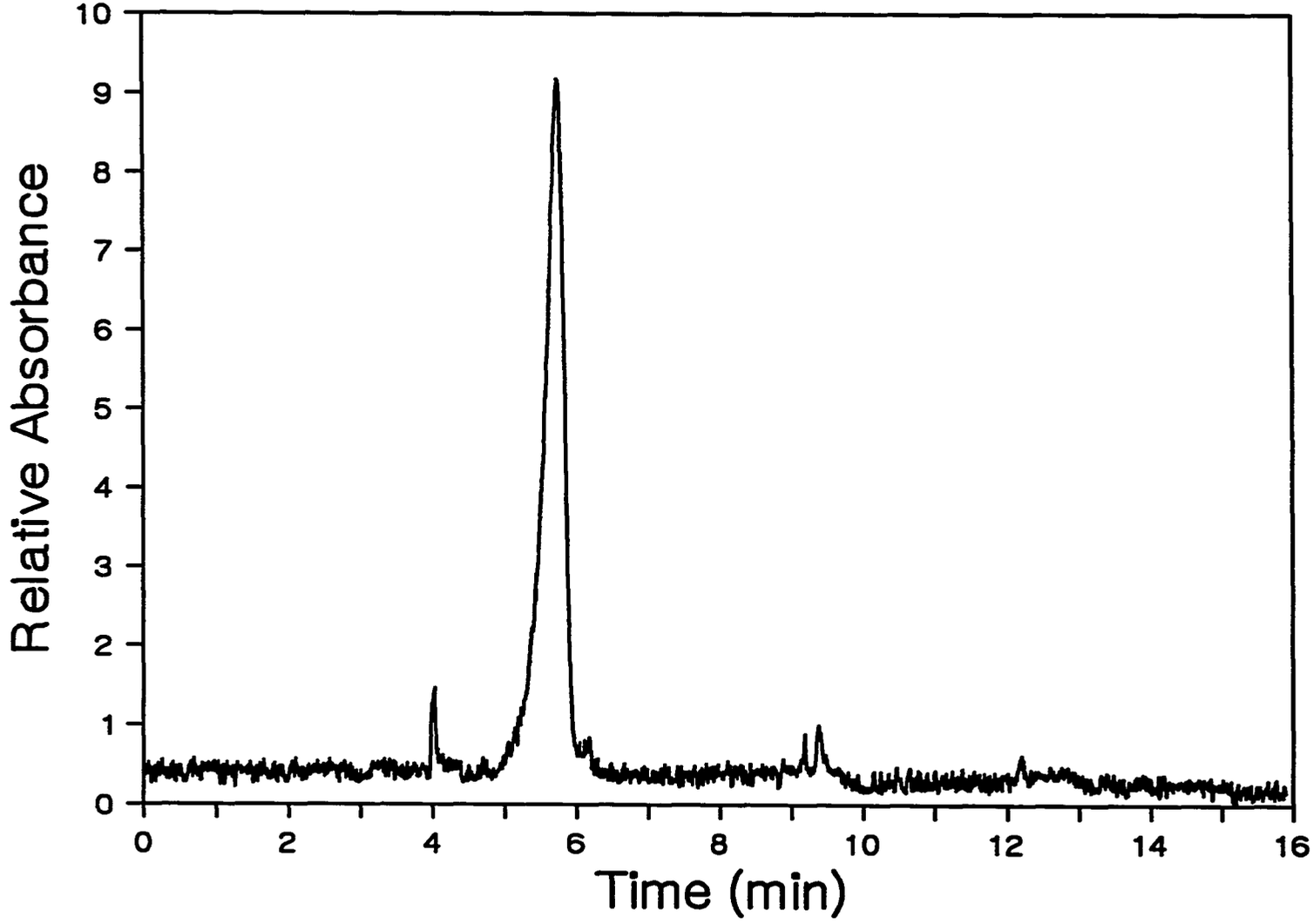
Relative Absorbance
Time (min)
0
1
2
3
4
5
6
7
8
9
10
0
2
4
6
8
10
12
14
16

Fig. 1 (b). Electropherogram of "pure" rHBsAg(S) (200 μg/mL) with LIF detection. Condition: as in Fig. 1(a).

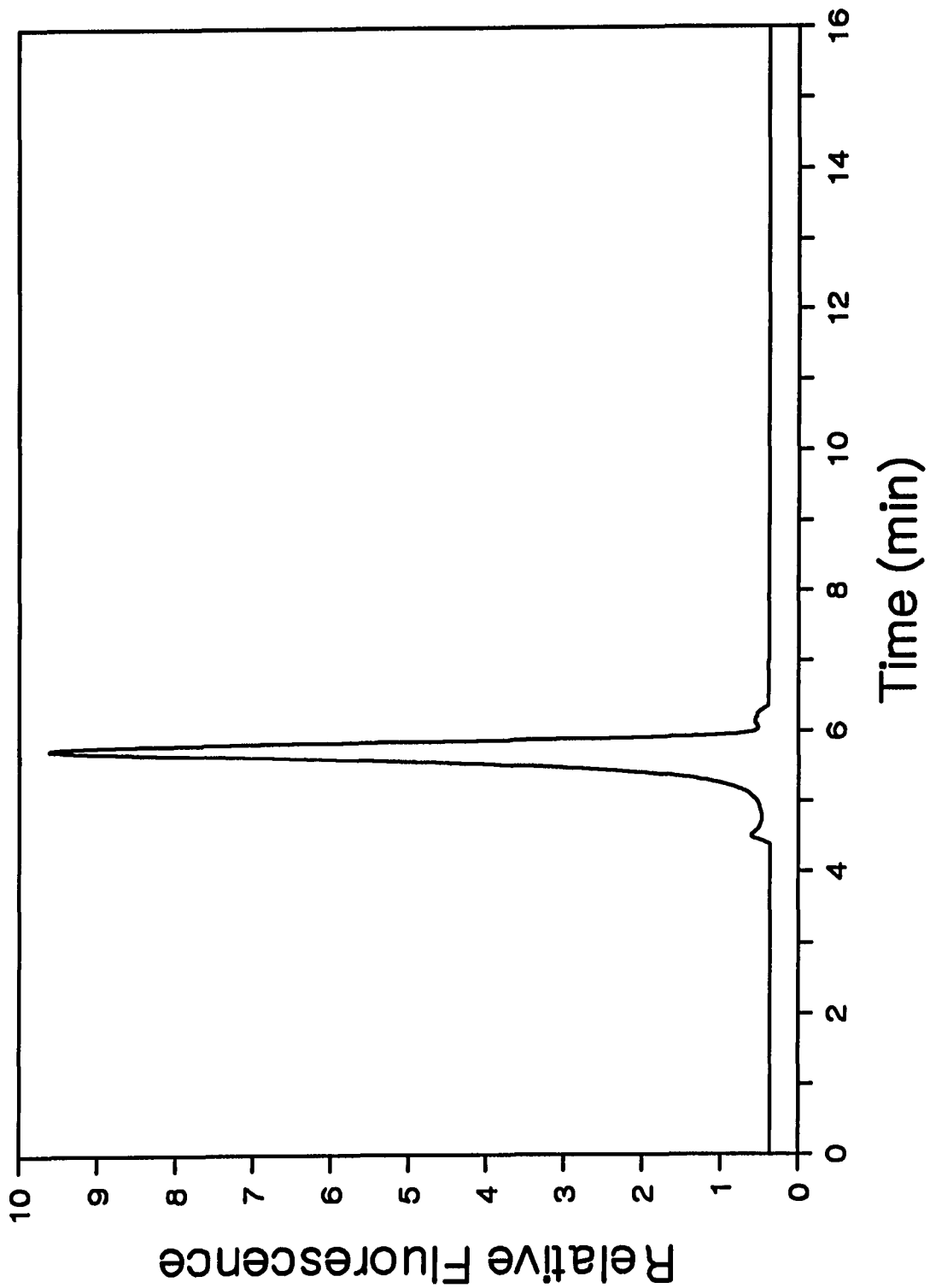
Relative Fluorescence
Time (min)
0
1
2
3
4
5
6
7
8
9
10
0
2
4
6
8
10
12
14
16

Fig. 2 (a). Electropherogram of "pure" rHBsAg(preS1+S2+S) (17 μg/mL) with absorbance detection at 200 nm. Condition: as in Fig. 1(a).

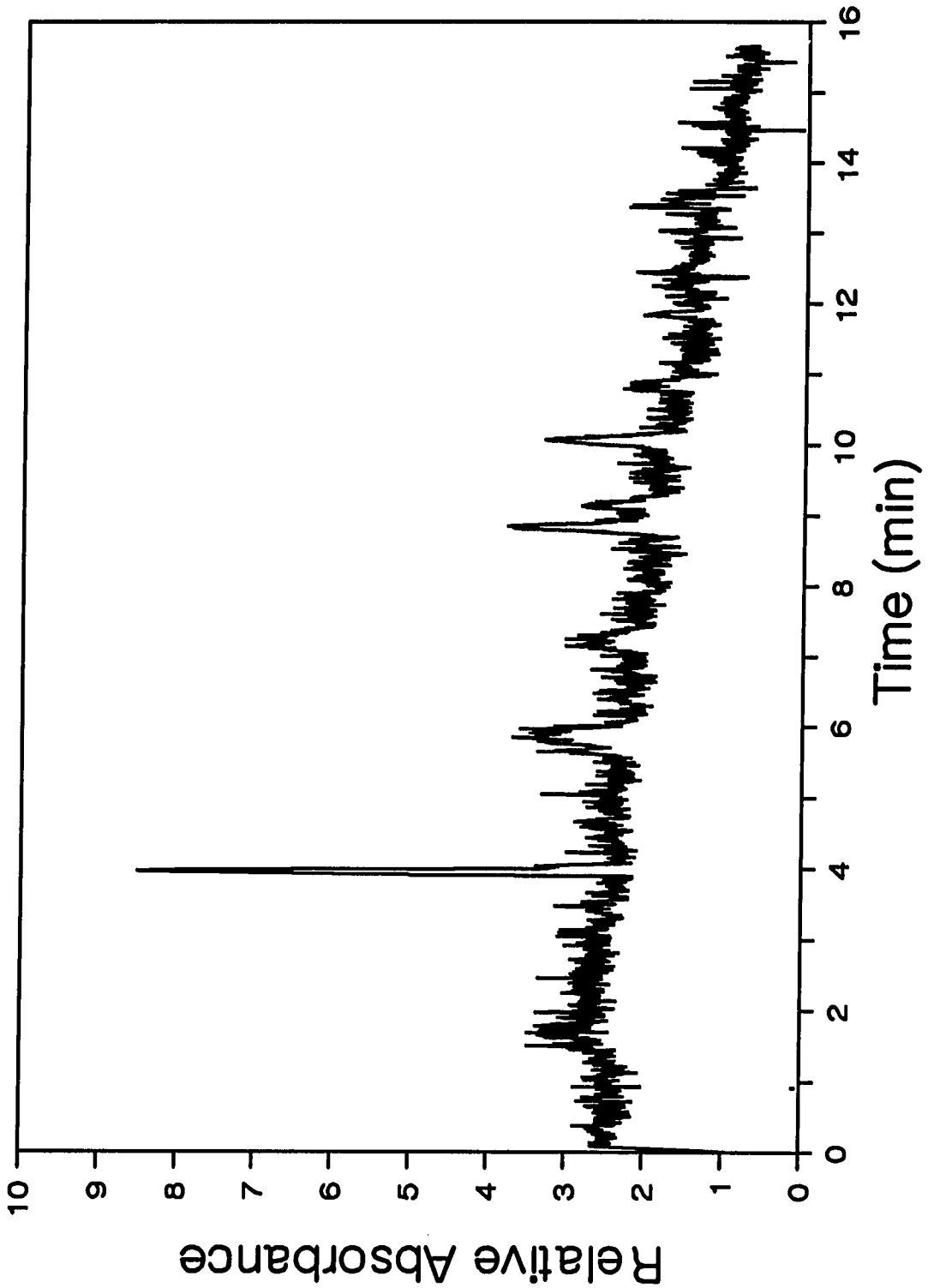
Relative Absorbance
0
1
2
3
4
5
6
7
8
9
10
Time (min)
0
2
4
6
8
10
12
14
16

Fig. 2 (b). Electropherogram of "pure" rHBsAg(preS1+S2+S) (17 μg/mL) with LIF detection. Condition: as in Fig. 1(a).

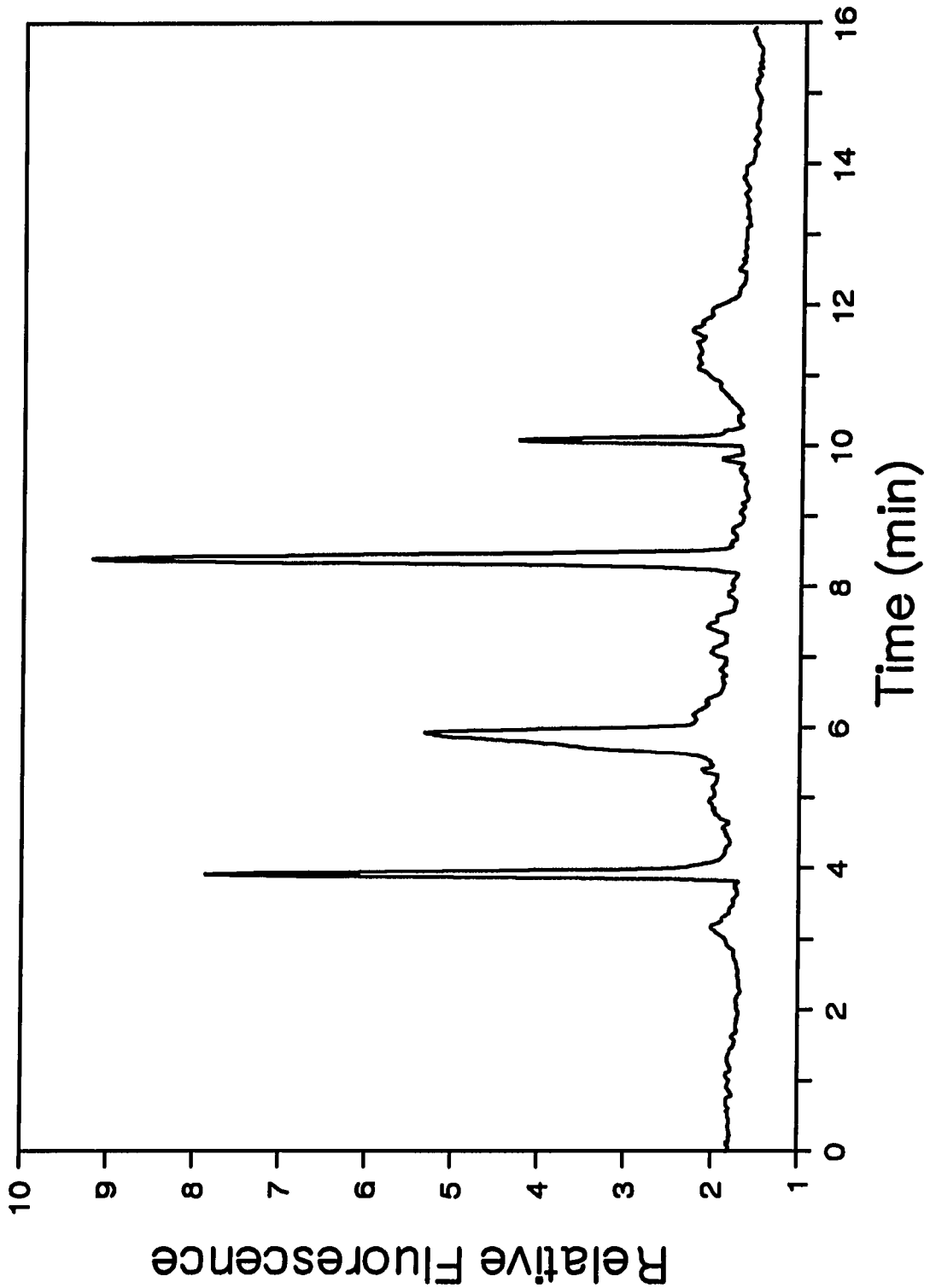
Relative Fluorescence
10
9
8
7
6
5
4
3
2
1
0
2
4
6
8
10
12
14
16
Time (min)

rHBsAg(preS1+S2+S) formulation is analyzed by HPCE. Other than the much higher S/Ns of the peaks in Fig. 2(b) than those in Fig. 2(a), the relative sizes and locations of some of the peaks are also different. Most notably, the prominent peak at 8.3 min in Fig. 2(b) is not seen in Fig. 2(a) whereas the opposite is valid for the doublet centered at 9.0 min. Many other subtle differences are readily apparent on close examination. Consequently, since the information contents afforded by absorbance and LIF detection are often different, the use of both detection schemes in tandem should provide added confidence to the analysis. We note that both of the rHBsAg formulations in this study are designated as "pure" by the manufacturer. The presence of extraneous components at low concentrations underlines the value of HPCE/LIF in the analysis of biopharmaceutical formulations.

Determination of trace impurities accompanying "purified" biopharmaceuticals

The complex culture media employed in the production of biopharmaceuticals contain many potential sources of impurities. Unfortunately, it is possible for a highly immunogenic protein impurity present at the ppm level to elicit an allergic response in a high percentage of human recipients (21,22). The use of phrases such as "as free as possible" in a draft issued by the FDA directly reflects the fact that the acceptable level of impurities is actually decided by the best technology available (1). Because slab PAGE and IEF with silver staining are insensitive and semi-quantitative at best, their use for the determination of protein impurities is unsuitable. Though quite sensitive, the utility of ELISA and RIA requires that the identities of all the impurities be known beforehand. Therefore, unidentified or unexpected impurities will escape detection. This aspect of ELISA and RIA is especially unsatisfactory in light of the lack of extensive clinical data in the brief history of recombinant DNA

technologies. Moreover, multiantigenic ELISAs are time-consuming and labor-intensive to develop as well as host cell system- and purification process-specific. Hence, a slight modification in either the culture condition or purification procedure would require the development of an entirely new set of multiantigenic ELISAs (23). Although the multicomponent capability and speed of HPLC has been utilized to quantify impurities accompanying a "purified" biopharmaceutical (24), the poor efficiency of HPLC gives rise to broad peaks, rendering the detection of trace impurities difficult. Nevertheless, because of its potential capability of determining both previously identified and unexpected impurities, HPLC remains an important method for assuring the purity of biopharmaceuticals.

As in the quantitation of biopharmaceuticals in dosage formulations, the use of multiple methods is necessary to establish the criteria of purity for a biopharmaceutical preparation. To this end, HPCE has been applied to resolve slight structural variants from the biopharmaceutical of interest (7). However, the poor sensitivity of absorbance detectors precluded the quantitation of impurities at trace levels. With sub-nM LODs, the use of LIF extends the utility of HPCE to this crucial aspect of the QC of biopharmaceuticals. Figs.3 and 4 depict, respectively, the electropherograms of "purified" rFXIII and anti-TAC where the (b) electropherograms are plotted at a sensitivity 1000 times greater than that for the (a) electropherograms. The presence of significant amounts of impurities in both rFXIII and anti-TAC is obvious. For rFXIII, the recombinant version of the last enzyme to become activated in the blood coagulation cascade produced in bakers' yeast, HPCE/LIF is the only method capable of quantifying impurities at below the 1% level at present. Assuming that the fluorescence quantum yields for the impurities are identical to that for rFXIII, the impurity present at the lowest quantity

Fig. 3 (a). Electropherogram of "purified" rFXIII (0.10 mg/mL or 670 nM). Condition: 10 mM $Na_2B_4O_7$(aq) at pH 8.1; 65-cm capillary (50-cm working length); 28 kV running voltage at injectio end.

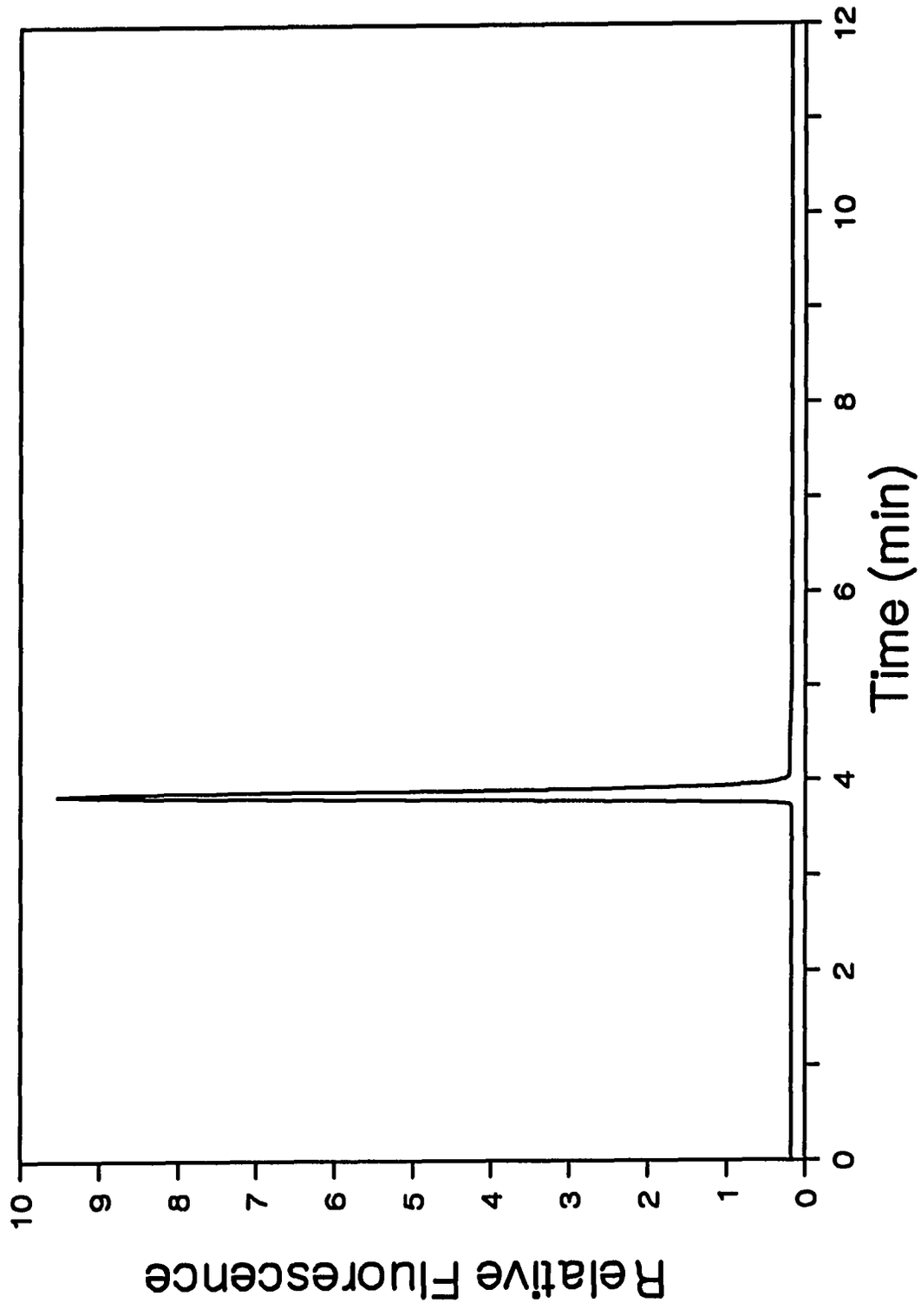
Relative Fluorescence
0
1
2
3
4
5
6
7
8
9
10
0
2
4
6
8
10
12
Time (min)

Fig. 3 (b). Electropherogram of "purified" rFXIII (0.10 mg/mL or 670 nM) at a sensitivity 1000X that oin Fig. 3(a).

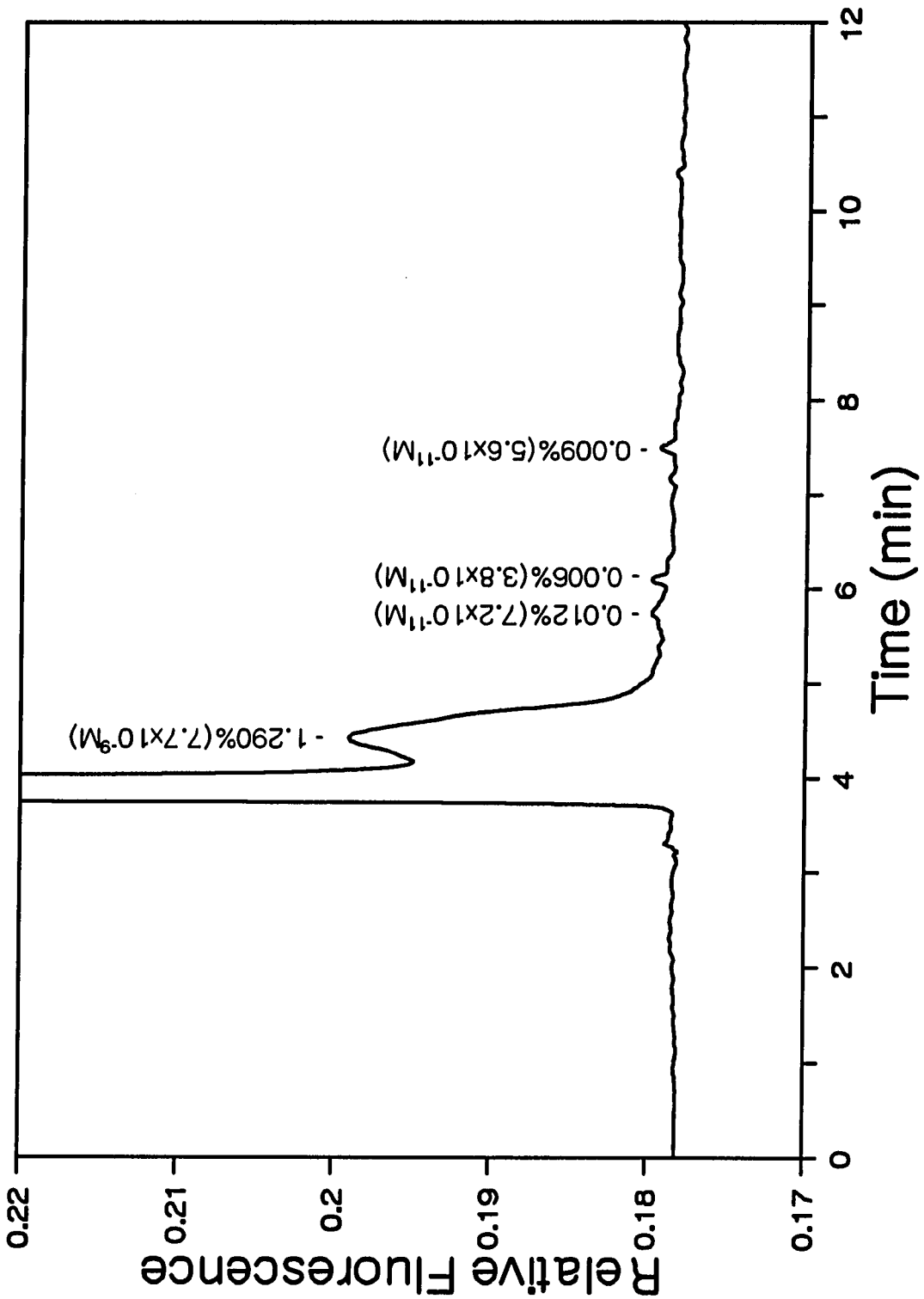
Relative Fluorescence
0.22
0.21
0.2
0.19
0.18
0.17
0
2
4
6
8
10
12
Time (min)
- 1.290%(7.7x10-9M)
- 0.012%(7.2x10-11M)
- 0.006%(3.8x10-11M)
- 0.009%(5.6x10-11M)

Fig. 4 (a). Electropherogram of "purified" anti-TAC (28 mg/mL or 180 μM).
Condition: as in Fig. 3(a).

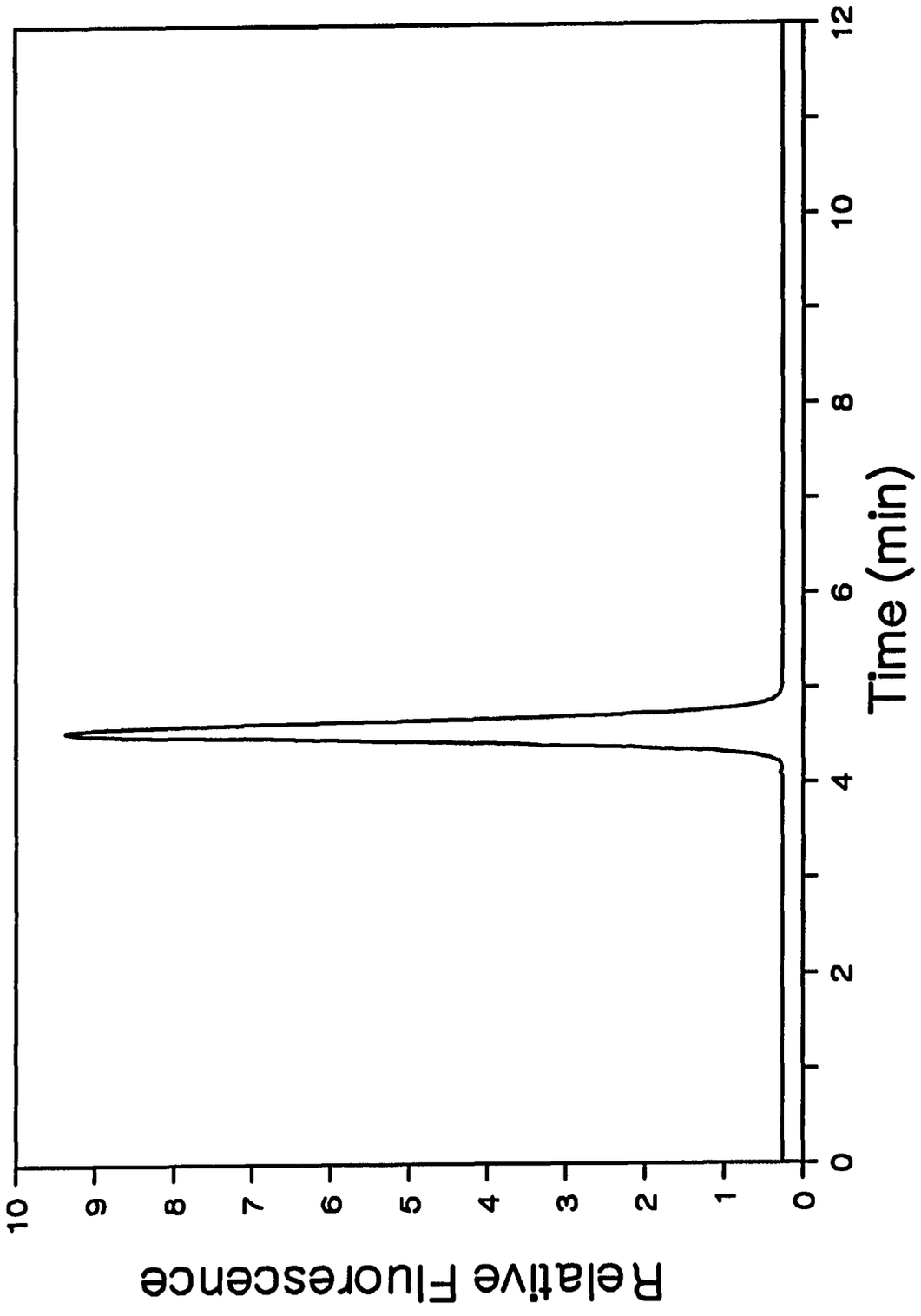
Relative Fluorescence
0
1
2
3
4
5
6
7
8
9
10
0
2
4
6
8
10
12
Time (min)

Fig. 4 (b). Electropherogram of "purified" anti-TAC (28 mg/mL or 180 μM) at a sensitivity 1000X that of Fig. 4(a).

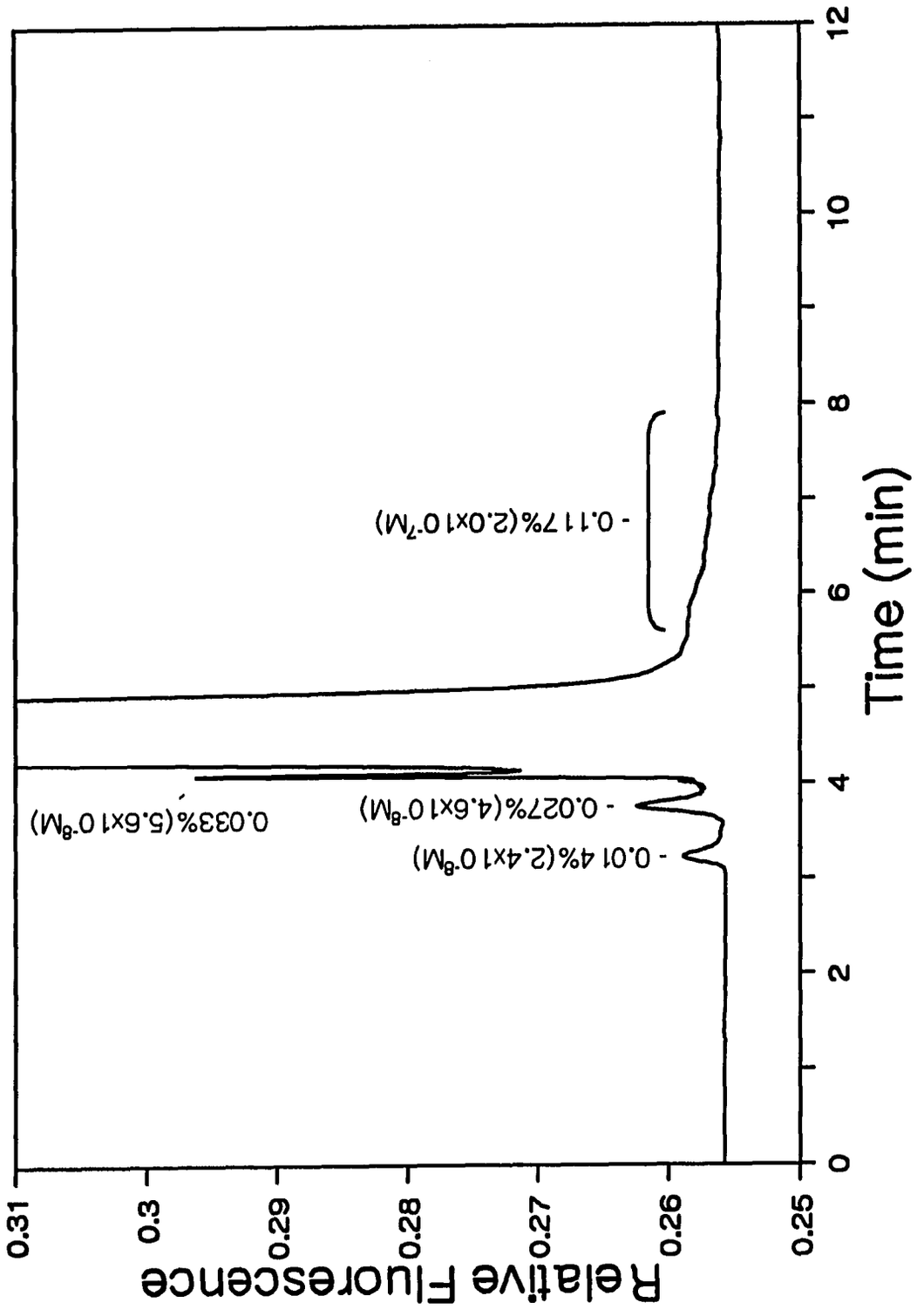
Relative Fluorescence
0.31
0.3
0.29
0.28
0.27
0.26
0.25
0
2
4
6
8
10
12
Time (min)
0.033% (5.6x10⁻⁸M)
- 0.027% (4.6x10⁻⁸M)
- 0.014% (2.4x10⁻⁸M)
- 0.117% (2.0x10⁻⁷M)

corresponds to only 0.006% of the total protein content. This translates into a concentration of merely $3.8X10^{-11}$ M. Hence, the high sensitivity of LIF detection is not superfluous, but essential to detect trace impurities resolved by HPCE. Although the sensitivity requirements for anti-TAC, an IgG1 hybrid antibody containing approximately a 9 to 1 ratio of human to murine sequence and directed against the human receptor for interleukin-2, are less stringent, HPCE/LIF is able to provide unique information, as HPCE with absorbance detection is not sensitive enough to indicate the presence of any of the impurities in Fig. 4(b). In comparison to the 4 impurity peaks observed here, reversed-phase HPLC assays yielded only 2 impurity peaks. Consequently, the orthogonal separation mechanisms of HPCE and HPLC are able to establish more stringent criteria of purity for biopharmaceuticals and, hence, redefine the meaning of "purified" biopharmaceuticals. Interestingly, the 14-s peak width-at-half-height is long for a migration time of about 4 to 5 min. This indicates the existence of structural variants amongst the IgG1 proteins comprising the monoclonal antibody. It is highly conceivable that the stringency of the criteria of purity will be extended further when other modes of HPCE, such as IEF, PAGE and electrokinetic chromatography, with LIF detection are incorporated into the analytical protocols of biopharmaceuticals in the future.

Monitoring of a vaccine purification process

Although only "well-characterized" organisms are used to produce biopharmaceuticals, the chemical description of the compositions of the production systems remains complex. This is especially valid in the case of eukaryotic cells such as bakers' yeast (*Saccharomyces cerevisiae*) utilized to manufacture rHBsAg (25). Because of the complexity and lack of long-term safety records of this expression

system, the demonstration of consistency at the various stages of the purification process is essential to assuring product integrity and purity (26). Since proteases from the host cells may "clip" the expressed product, purification must be completed as rapidly as possible. Besides, it is advantageous to be able to provide information in real-time to the recovery plant so that prompt feedback decisions can be made.

As a result, the high speed and efficiency of HPCE have been utilized to monitor the various stages in the purification of rHBsAg through acquiring electropherograms as "fingerprints" (5). However, accurate and detailed "fingerprints" are not possible with absorbance detection. Fig. 5 shows the electropherograms at an intermediate stage of a 10-step purification process of rHBsAg(preS1+S2+S) obtained by HPCE with absorbance and LIF detection. The 2 large peaks in Fig. 5(a) are from reagents introduced during purification. Noteworthy is that the peak corresponding to the component of greatest interest, rHBsAg(preS1+S2+S), appears as just a broad hump laden with noise (see Figs.1 and 2). Hence, HPCE with absorbance detection is not able to reveal qualitatively accurate "fingerprints". As shown in Figs. 5(b) and 5(c), the far richer information content of HPCE/LIF is evident. Even though the rHBsAg(preS1+S2+S) peak is not fully resolved from other components, a more detailed glimpse of the partially purified product is obtained, thereby providing a means of demonstrating consistency in the purification process. Once again, the absence of the peaks at 6.8 min as well as the difference in appearance between the peak at 4.0 min in Fig. 5(a) and that in Fig. 5(b) indicate the unique selectivity of LIF compared to absorbance detection.

Fig. 5(a). Electropherogram of partially purified rHBsAg(preS1+S2+S) (115 μg/mL protein & 15.5 μg/mL rHBsAg) with absorbance detection at 200 nm. Condition: as in Fig. 1(a).

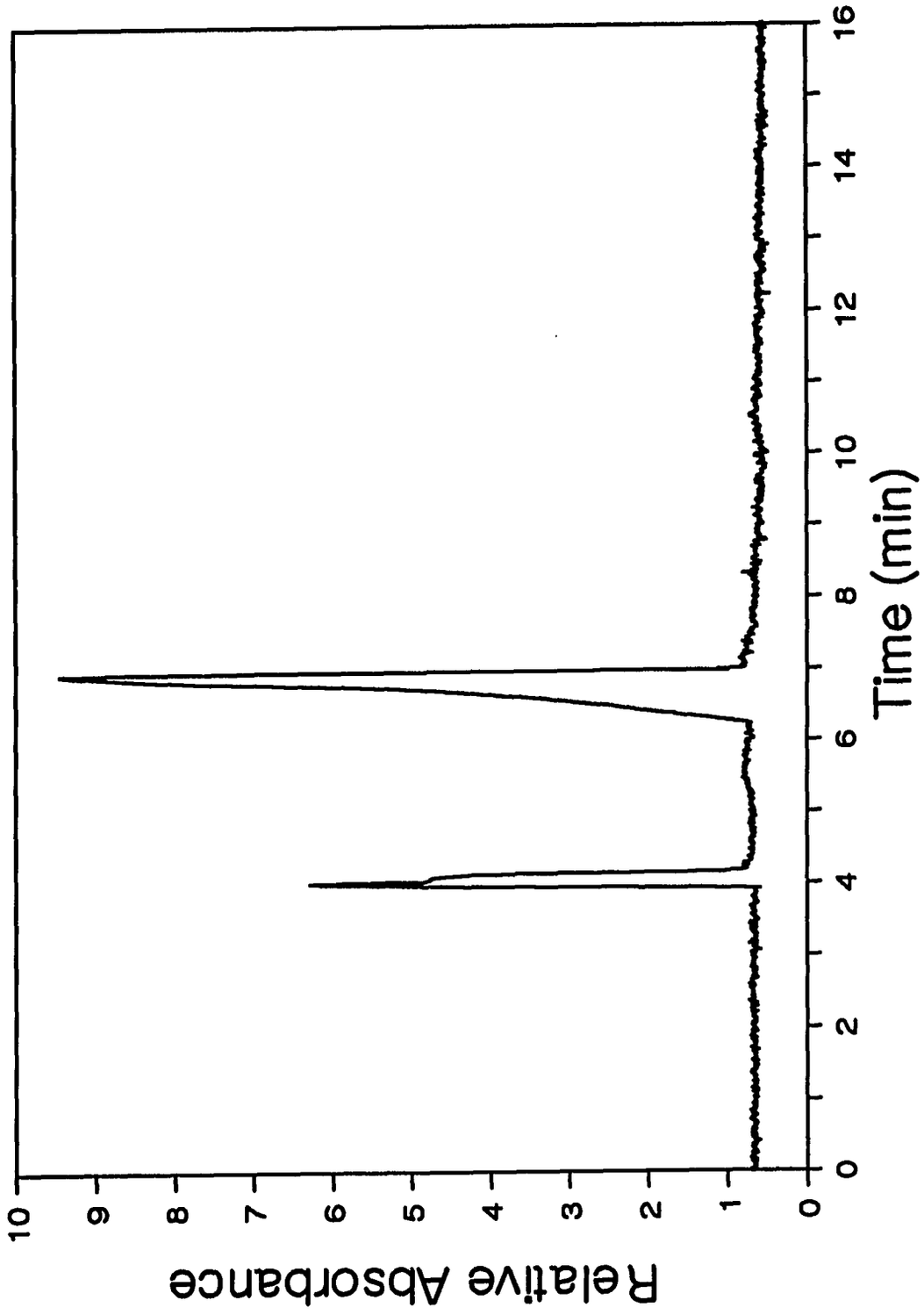
Relative Absorbance
10
9
8
7
6
5
4
3
2
1
0
0
2
4
6
8
10
12
14
16
Time (min)

Fig. 5(b). Electropherogram of partially purified rHBsAg(preS1+S2+S) (115 μg/mL protein & 15.5 μg/mL rHBsAg) with LIF detection Condition: as in Fig. 1(a).

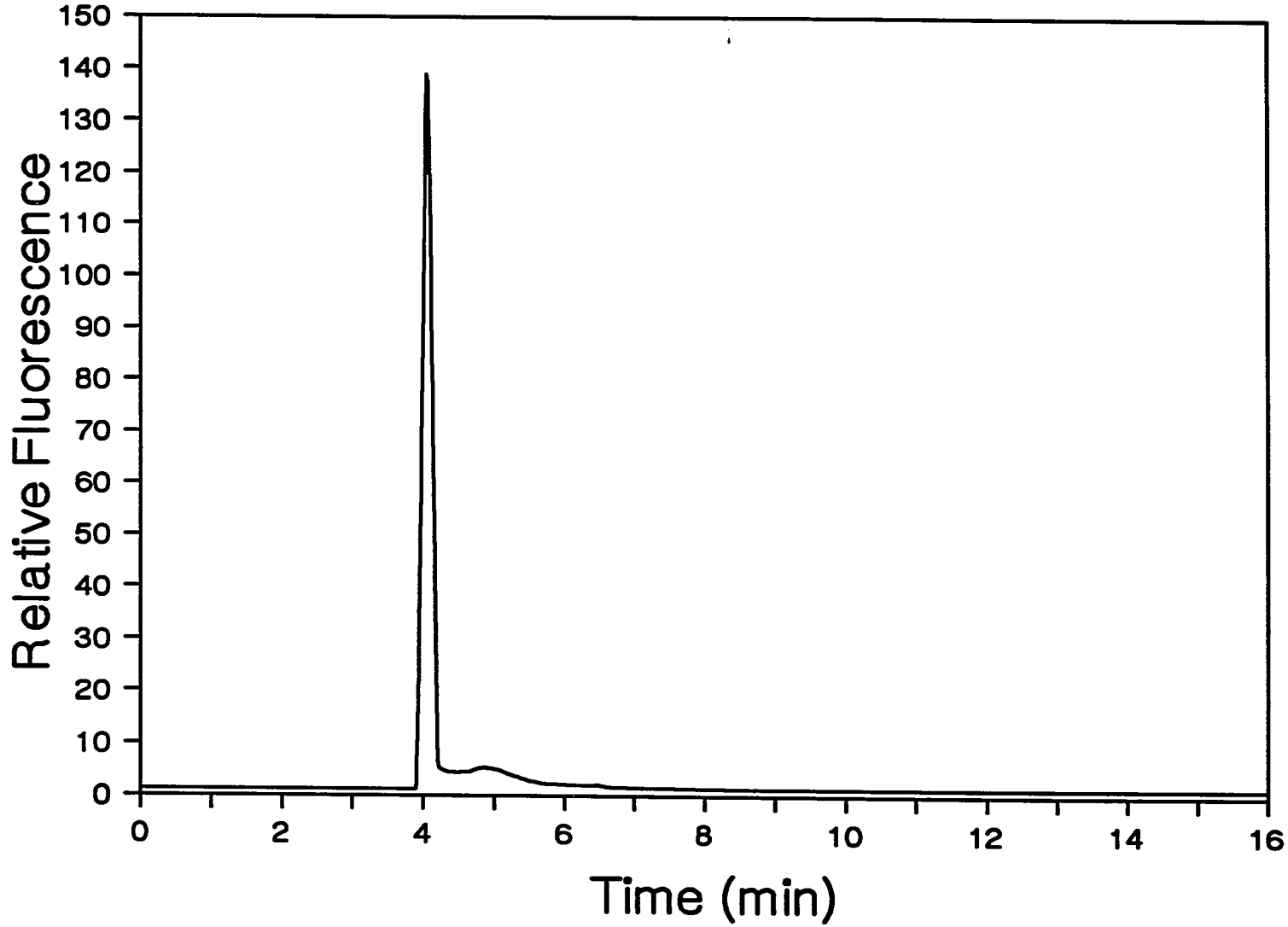
Relative Fluorescence
150
140
130
120
110
100
90
80
70
60
50
40
30
20
10
0
0
2
4
6
8
10
12
14
16
Time (min)

Fig. 5(c). Electropherogram of partially purified rHBsAg(preS1+S2+S) (115 μg/mL protein & 15.5 μg/mL rHBsAg) with LIF detection at a sensitivity 10X that of Fig. 5(b). Condition: as in Fig. 1(a).

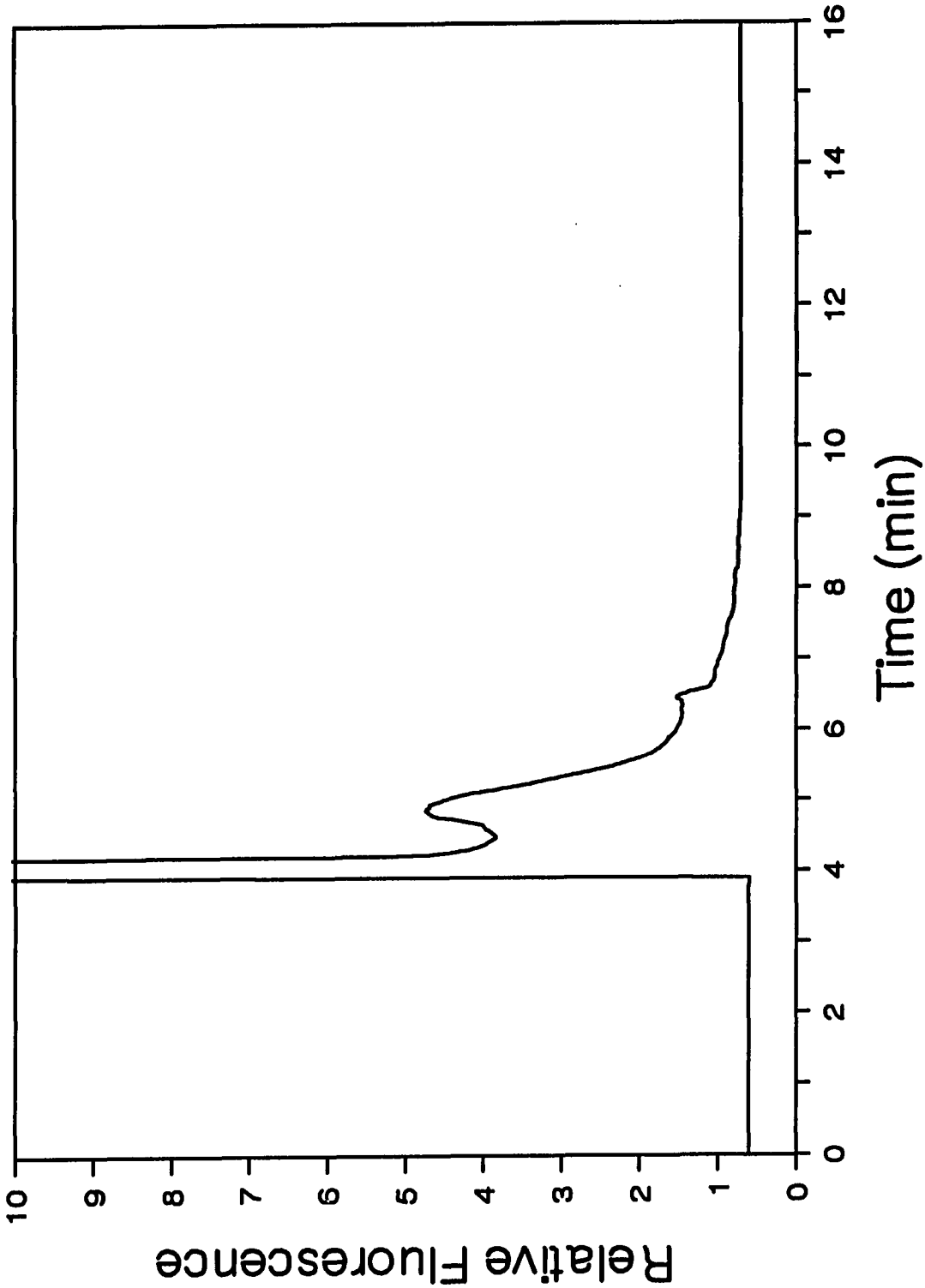
Relative Fluorescence
0
1
2
3
4
5
6
7
8
9
10
Time (min)
0
2
4
6
8
10
12
14
16

Peptide mapping of biopharmaceuticals at high sensitivity

The assurance of the genetic stability of the organism and structural integrity of the expressed product is germane to the QC of biopharmaceuticals. For simple production systems such as bacteria and yeast, nucleotide sequence analysis and peptide mapping are definitive means of detecting subtle mutations and structural modifications. In the case of mammalian cells, peptide mapping is the only method capable of such tasks, as the recombinant plasmids incorporated into the chromosomes of the cells are not easily recovered for nucleotide sequence analysis. In addition, peptide mapping is useful for monitoring changes in the positions of carbohydrate attachments in glycoproteins. Although powerful reversed-phase HPLC methods have been developed and used for separating peptide fragments from the enzymatic digestions of biopharmaceuticals (2,6,24,27), methods based on separation mechanisms distinct from that for reversed-phase HPLC and capable of resolving structural variants not recognized by reversed-phase HPLC are necessary to ensure the absence of mutations, proteolytic degradation and variances in post-translational modifications.

As mentioned earlier, the peptide mapping of biopharmaceuticals by HPCE has been described (2,3). However, the poor sensitivity of absorbance detectors renders the mapping of biopharmaceuticals present at concentrations and masses lower than, respectively, 10 μM and 1μg an impossible task. The need for low concentration and mass sensitivity in peptide mapping is necessary to minimize disturbance of the culture media or purification process during sampling and allow the expressed protein to be sequenced even if it is present at very low concentrations. The impressive results of Cobb and Novotny (28,29) have shown that the sequencing of 2 pmol (4 μM) of β-casein using a reactor column filled with a

trypsin-immobilized agarose gel followed by analysis with microcolumn HPLC or HPCE is attainable. However, the poor sensitivity of absorbance detectors and the required sample-handling prevented further decrease in sample size. Although LIF detection of labeled peptides after digestion has been attempted, derivatization necessitates dilution, thereby increasing the initial sample size compared to no derivatization (29). Recently, Amankwa and Kuhr (30) have succeeded in carrying out digestion reactions in 50-μm i.d. trypsin-immobilized open tubes and, hence, opened up the feasibility of performing online digestion and separation. Nonetheless, the need to label the peptide fragments with fluorophores in order to detect them necessitates dilution and imposes a lower limit to sample size.

The problems associated with the detection of peptides in microcolumn HPLC or HPCE can be addressed by native fluorescence detection which retains the sensitivity of LIF detection with labeling while obviating the effects of dilution during derivatization (17). As a model system, we have obtained the HPCE-separated peptide maps of conalbumin with absorbance and native fluorescence detection (Fig. 6). Not surprisingly, the electropherogram obtained with absorbance detection possesses more peaks than that with fluorescence detection (33 vs 18). This is because native fluorescence detection is selective for only tryptophan- and/or tyrosine-containing peptides whereas absorbance detection is able to detect all the fragments. Given the large size of conalbumin (MW 77,700 (31)), a complete separation of all the peptide fragments is not obtained here. Nevertheless, only 150 amol of conalbumin from a sample solution concentration of 0.13 μM is injected into the capillary. By inspection, HPCE/LIF should be able to analyze as little as 70 amol of a conalbumin digest injected. On the other hand, Fig. 6(a) shows that the LOD with absorbance detection (70 fmol) is at least 1000 times that with native

Fig. 6(a). Electropherogram of tryptic digestion of conalbumin (0.13 mM or 150 fmol injected) with absorbance detection. Condition: as in Fig. 1(a) except 25 mM sodium phosphate at pH 6.4.

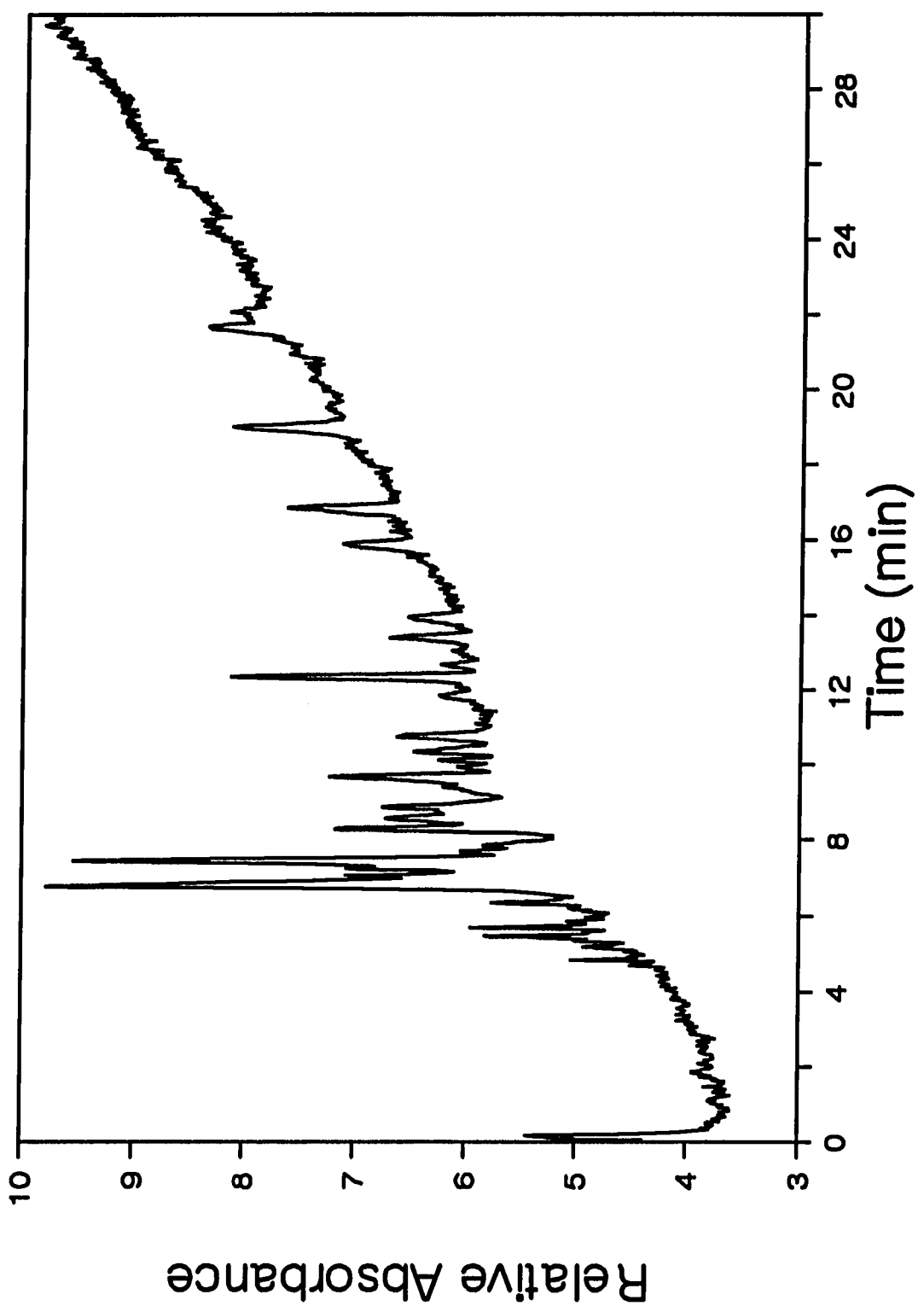
Relative Absorbance
10
9
8
7
6
5
4
3
0
4
8
12
16
20
24
28
Time (min)

Fig. 6(b). Electropherogram of tryptic digestion of conalbumin (0.13 μM or 150 amol injected) with LIF detection. Condition: as in Fig. 6(a).

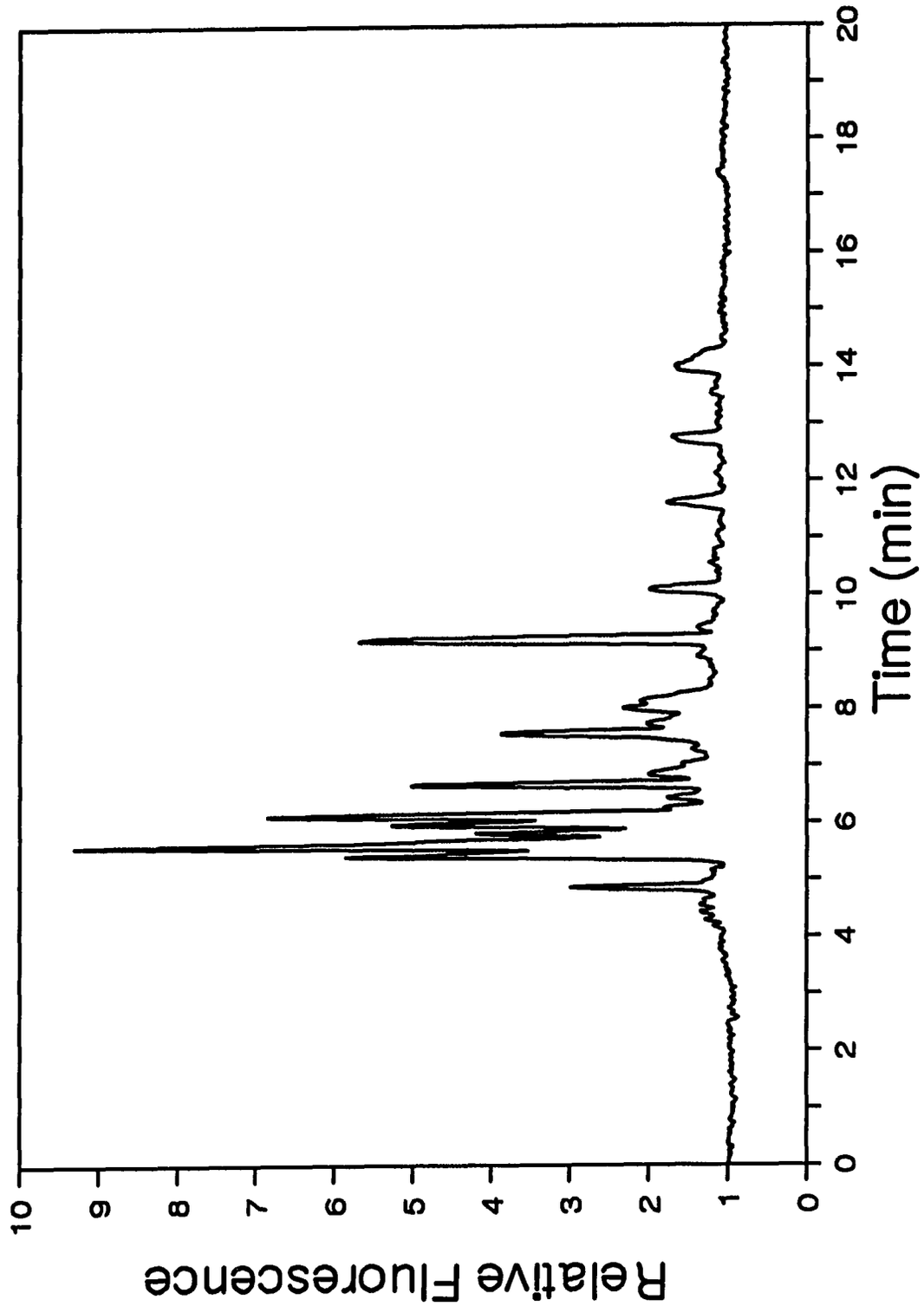
Relative Fluorescence
Time (min)
0
1
2
3
4
5
6
7
8
9
10
0
2
4
6
8
10
12
14
16
18
20

fluorescence detection. As a result, the online coupling of digestion and separation by HPCE followed by detection with native fluorescence without derivatization (30) could lower the total protein sample requirement for peptide mapping to the 10- to 100-amol level in the future. Moreover, with native fluorescence detection, the problems accompanying messy derivatization reactions are also avoided.

In order to demonstrate the utility of HPCE with native fluorescence detection to the peptide mapping of biopharmaceuticals, tryptic maps of rFXIII are shown in Fig. 7. Once again, the electropherogram obtained with absorbance detection is considerably more complicated than that with native fluorescence detection. Consequently, HPCE with native fluorescence detection not only allows the use of much smaller quantities of samples, but the peptide maps are also simplified. We note from Fig. 7(b) that the LOD for the tryptic digest of rFXIII is at worst 60 amol (or 40 nM) which is roughly 1000 times lower than that with absorbance detection (see Fig. 7(a)). Because of its selectivity for tryptophan- and/or tyrosine-containing peptides, a drawback of HPCE with native fluorescence detection is that peptides devoid of both tryptophan and tyrosine residues and, hence, any structural changes in them will escape detection. Consequently, the proper role of HPCE with native fluorescence detection in the QC of biopharmaceuticals should be that of a rapid and sensitive technique for the preliminary screening of genetic and structural changes in the expressed protein during incubation and purification. When concentration detection sensitivity is not an issue, HPLC and HPCE with absorbance detection should be the preferred alternatives.

Fig. 7(a). Electropherogram of tryptic digestion of rFXIII (80 μM or 120 fmol injected) with absorbance detection. Condition: as in Fig. 6(a).

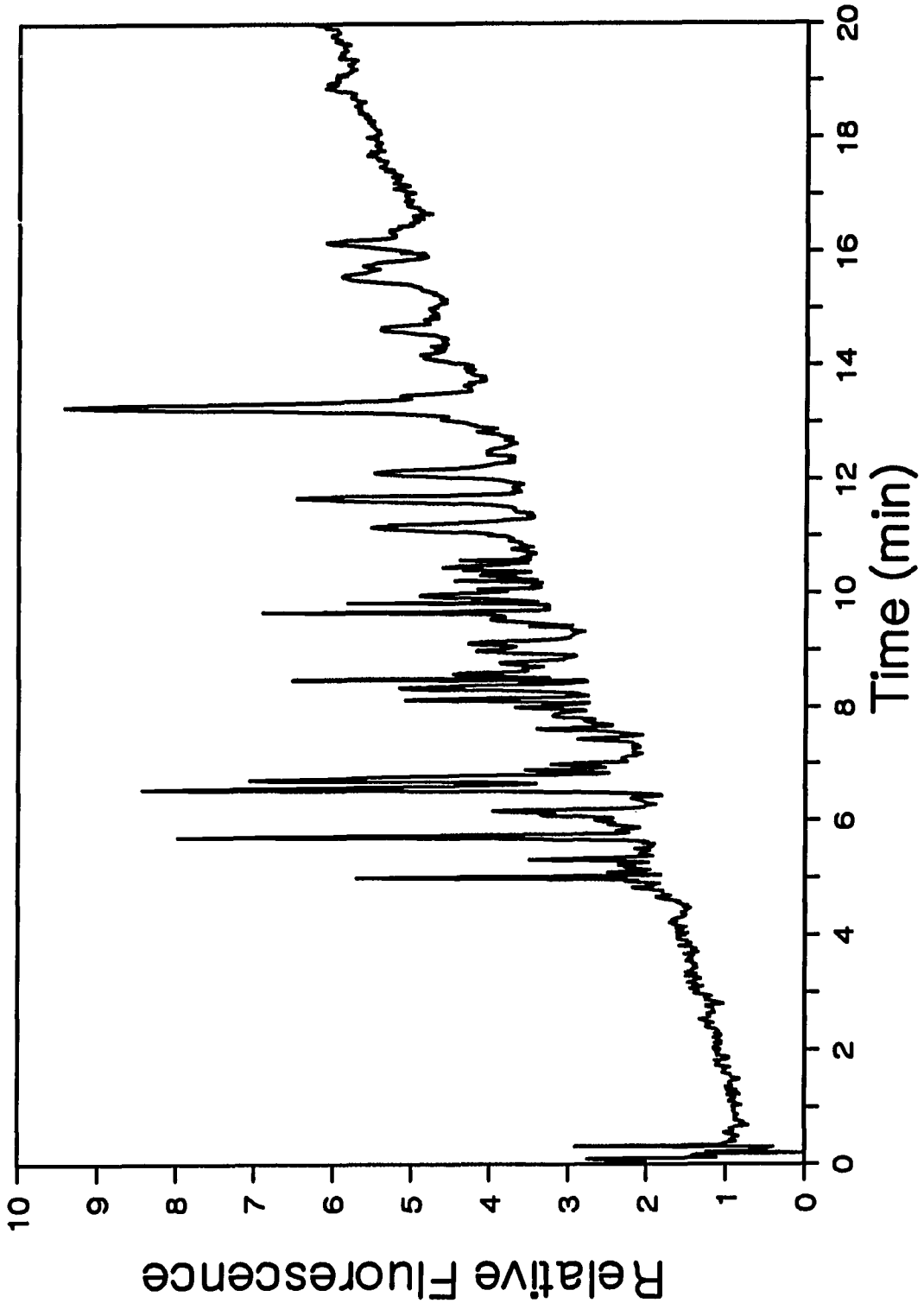
Relative Fluorescence
0
1
2
3
4
5
6
7
8
9
10
Time (min)
0
2
4
6
8
10
12
14
16
18
20

Fig. 7(b). Electropherogram of tryptic digestion of rFXIII (80 nM or 120 amol injected) with LIF detection. Condition: as in Fig. 6(a).

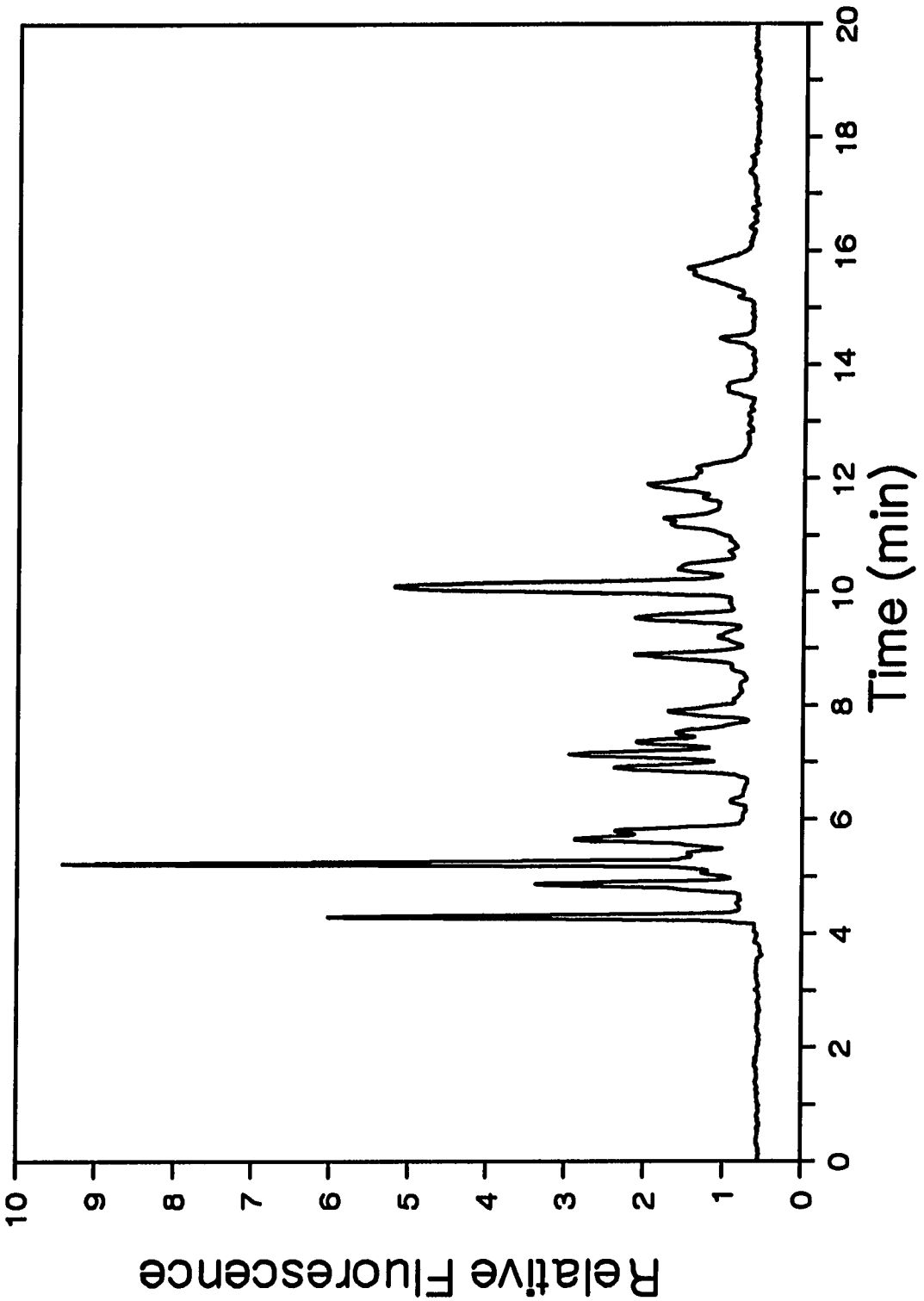
Relative Fluorescence
0
1
2
3
4
5
6
7
8
9
10
0
2
4
6
8
10
12
14
16
18
20
Time (min)

Potency assays of biopharmaceuticals

As the measurement which assesses the activity of a biopharmaceutical, potency assays determine the effectiveness of the product. While potency assays based on animal models and cell-line proliferation are expensive, time-consuming, labor-intensive and unreliable, the development of meaningful in vitro biomimetic assays, where the proposed biological effect of the drug is mimicked by other means, provides a solution to the problem of gauging the efficacy of biopharmaceuticals (23). Because of the characteristics of rapidity, simplicity and reproducibility of most chemical reactions, the chemical action of a biopharmaceutical is an obvious candidate from which biomimetic assays can be derived. Therefore, it is important to develop rapid, labor-saving, accurate and reliable methods by which biochemical reactions can be monitored.

As an example toward the development of such potency assays based on HPCE/LIF, we have studied the kinetics of rFXIII activation by α-thrombin in the presence of Ca^{2+}. The activated form of rFXIII, rFXIIIa, catalyzes the formation of γ-glutamyl-ϵ-lysyl peptide cross-links between polypeptide chains in adjacent fibrin monomers and between fibrin and other plasma proteins in the last stage of the blood coagulation cascade (32). rFXIII exists as a dimer (a_2) which, in the presence of Ca^{2+}, is catalyzed by α-thrombin to give rFXIIIa and an activation peptide (AP), as depicted in Scheme I (33,34).

Various methods have been utilized to study the kinetics of rFXIIIa formation. Precipitation (35), chromatography (36,37), PAGE (38), radioactivity assay (39) and fluorometric assay through dansylcadaverine incorporation (40) are either slow, indirect, insensitive or inaccurate. Here, HPCE with native fluorescence detection is used to study the kinetics of rFXIIIa formation in real-time. Fig. 8

Scheme 1 :

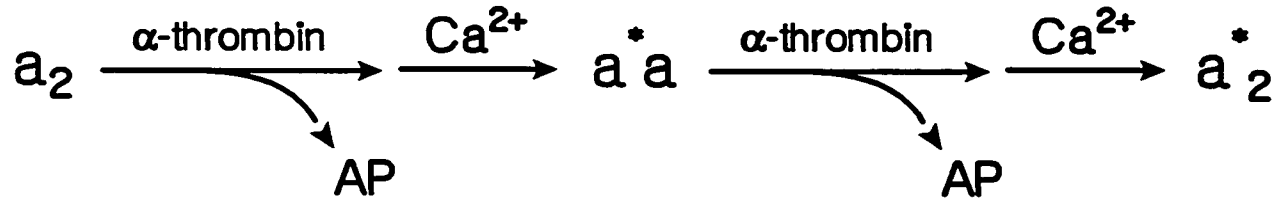

a^*_2 = rFXIIIa with both APs cleaved off

a^*a = rFXIIIa with one AP cleaved off

contains some typical electropherograms obtained by directly sampling the reacting mixture. In Fig. 8(a), the electropherogram revealing the composition of the mixture immediately after the addition of α-thrombin and Ca^{2+} to rFXIIIs is depicted. The tallest peak in the middle corresponds to rFXIII whereas the sharp peak to its left is from α-thrombin. The small hump on the right is due to an impurity in the form of rFXIIIa which forms slowly from rFXIII on storage (see Fig. 3). Even though rFXIII is present at a concentration of only 6.1 μM, the S/N is excellent with LIF detection while the same is not valid with absorbance detection (data not shown). As the reaction progresses, the size of the peaks representing both α-thrombin and rFXIII becomes smaller and smaller whereas the opposite applies to the peaks from rFXIIIa. Since rFXIII is gradually converting to rFXIIIa, the decrease and increase in the sizes of the peaks from, respectively, rFXIII and rFXIIIa are expected. Rather surprising, however, is the decreasing size of the α-thrombin peak as the reaction proceeds. An explanation for this is that the newly formed rFXIIIa catalyzes the formation of cross-links between α-thrombin and itself or other proteins, including rFXIII and rFXIIIa, thereby giving rise to species with electrophoretic mobilities similar to those of rFXIII and rFXIIIa. (This is a consequence of the fact that α-thrombin (MW 33,580) is small compared to rFXIII (MW 166,000).) The catalytic activity of rFXIIIa on itself and the other proteins resulting in the formation of polymeric species is consistent with the broad features of the slow-migrating peaks in the electropherograms obtained in the later stages of the reaction. This is because heterogeneous species often possess distinct electrophoretic mobilities and, hence, migration times (41). The fact that the peaks corresponding to rFXIIIa are not sharp indicates that species other than a^*a or a^*_2 are present.

Fig. 8(a). Electropherogram of rFXIII (6.1 μM) reaction mixture immediately after mixing. Condition: as in Fig. 3(a).

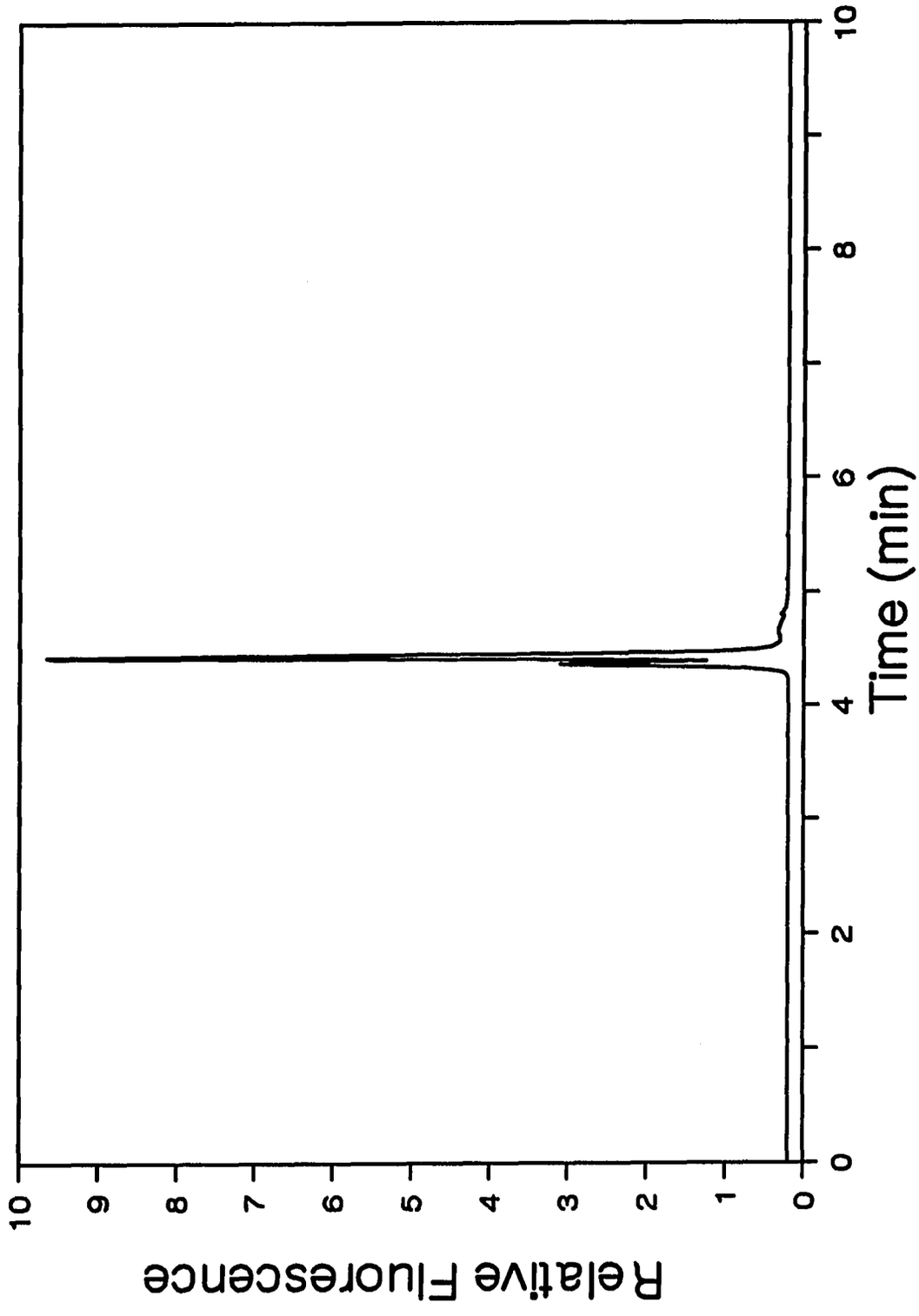
Relative Fluorescence
0
1
2
3
4
5
6
7
8
9
10
0
2
4
6
8
10
Time (min)

Fig. 8(b). Electropherogram of rFXIII (6.1 μM) reaction mixture 60 min after mixing. Condition: as in Fig. 3(a).

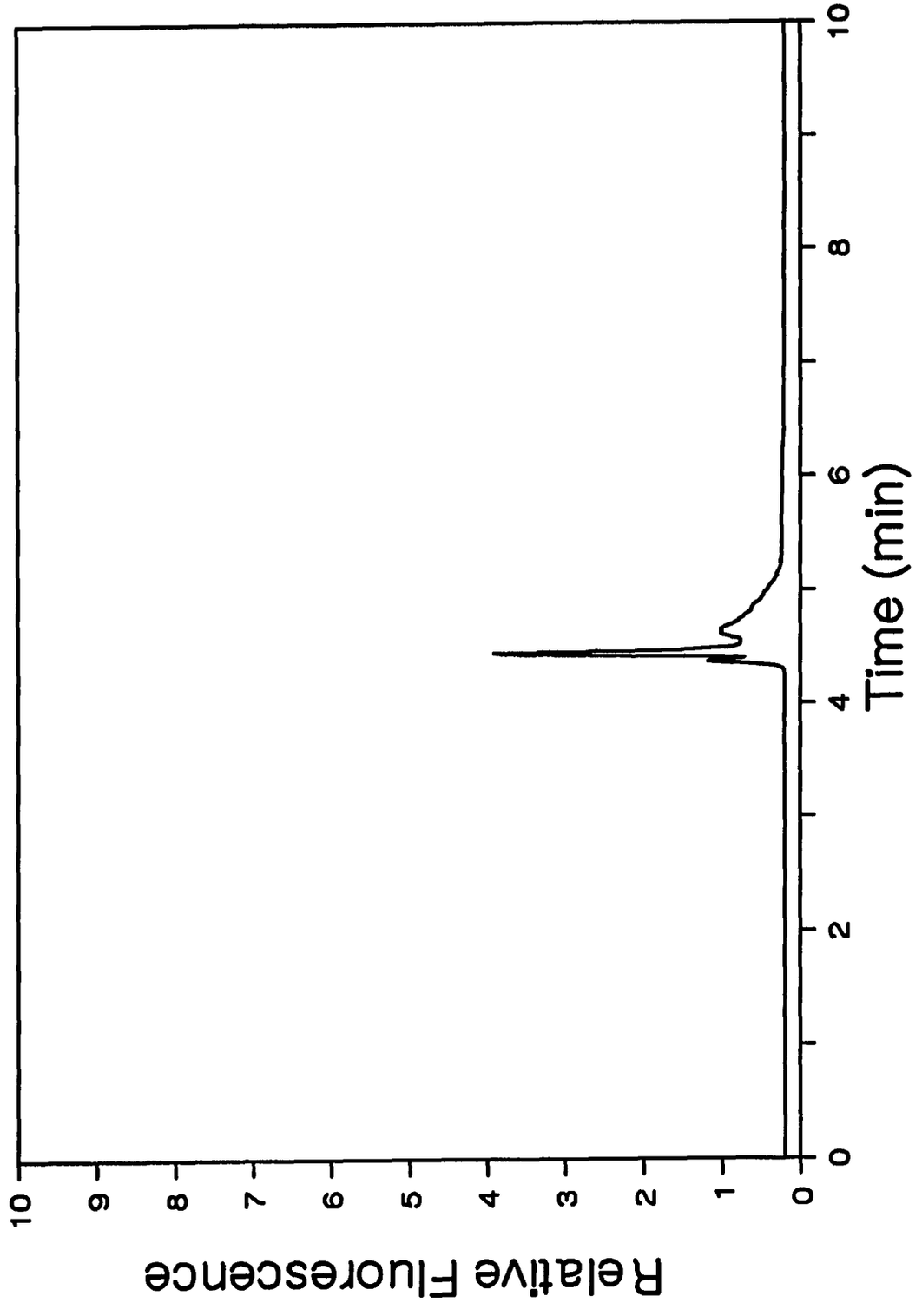
Relative Fluorescence
0
1
2
3
4
5
6
7
8
9
10
Time (min)
0
2
4
6
8
10

Fig. 8(c). Electropherogram of rFXIII (6.1μM) reaction mixture 120 min after mixing. Condition: as in Fig. 3(a).

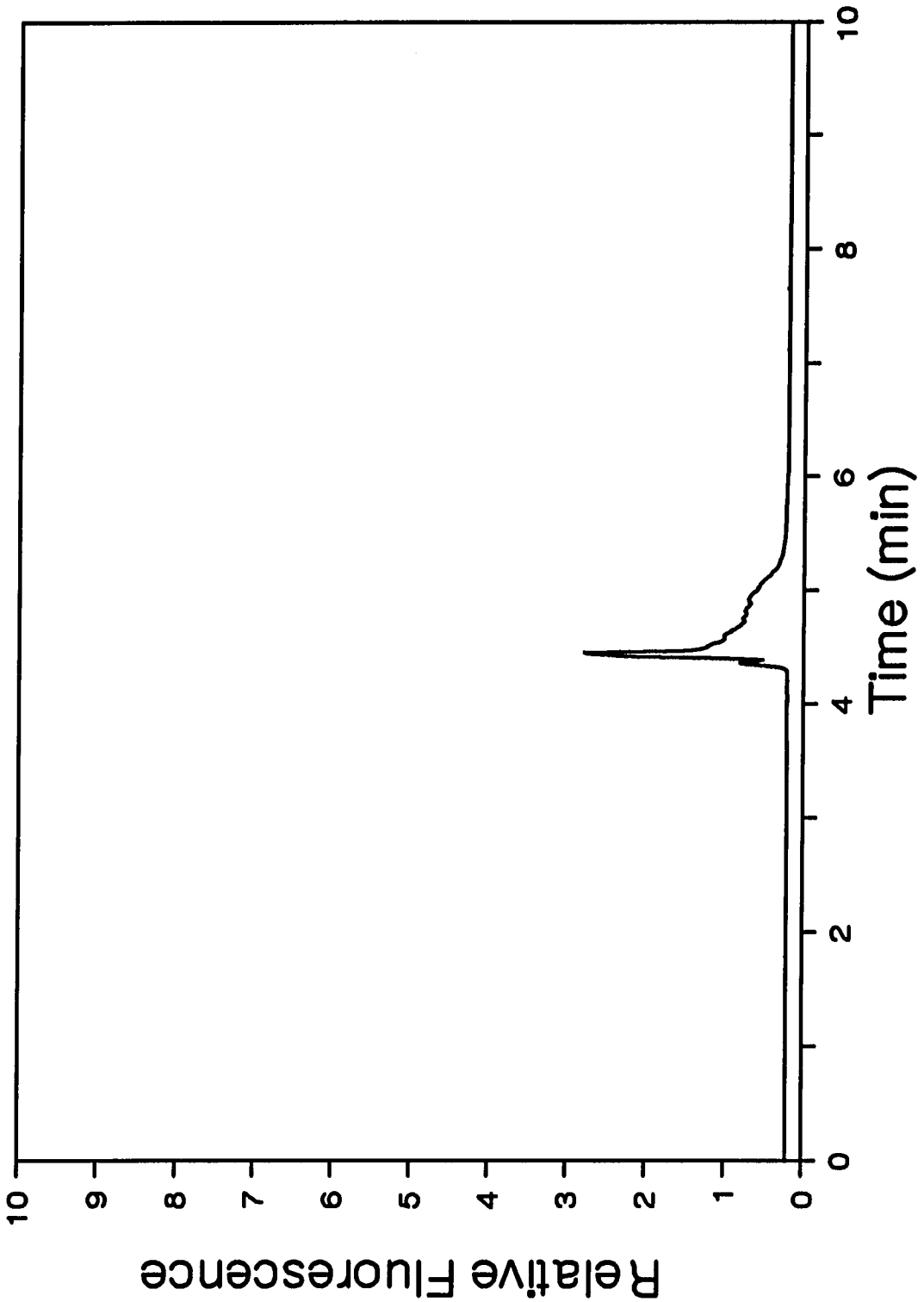
Relative Fluorescence
0
1
2
3
4
5
6
7
8
9
10
0
2
4
6
8
10
Time (min)

Fig. 8(d). Electropherogram of rFXIII (6.1μM) reaction mixture 180 min after mixing. Condition: as in Fig. 3(a).

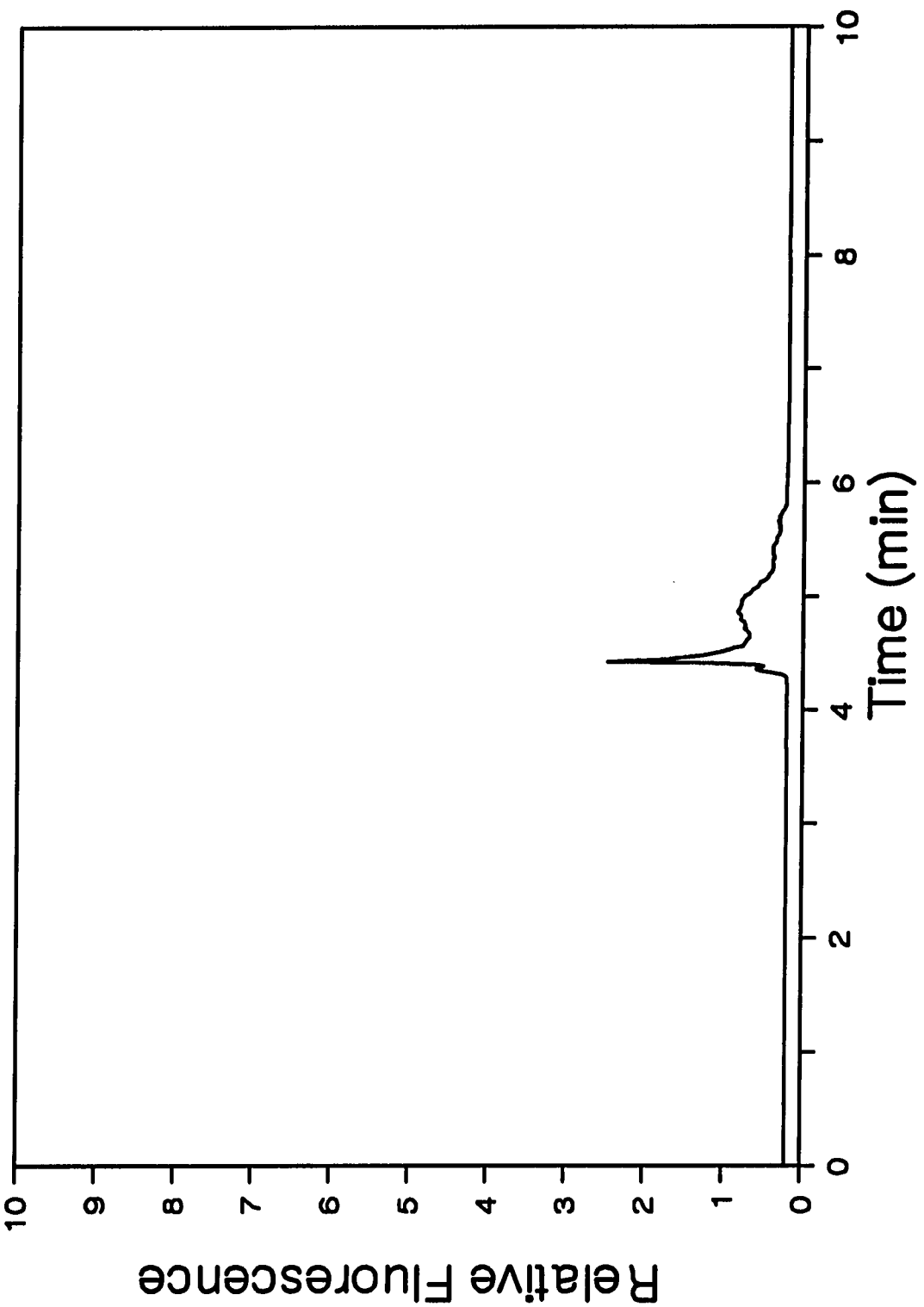
Relative Fluorescence
0
1
2
3
4
5
6
7
8
9
10
Time (min)
0
2
4
6
8
10

To demonstrate the capability of HPCE/LIF to acquire data in real-time, the peak areas from rFXIII and rFXIIIa are plotted against reaction time in Fig. 9. Because of the speed of HPCE, rapid sampling and, hence, detailed temporal profiles of the reacting mixture is possible. As it took all the components less than 6 min to migrate past the detection region, sampling intervals much shorter than the 15 min employed here are certainly feasible. We note that both sets of peak areas exhibit exponential trends and the scatter of the data in the early stages of the reaction is quite small. As the reaction time increases, however, the scatter of the rFXIII peak areas remains small while that of rFXIIIa is noticeably greater. This might be caused by increased integration errors due to the broad and irregular features of the rFXIIIa peaks in the later stages of the reaction. It is also of interest to point out that an equilibrium between rFXIII and rFXIIIa is attained as reaction time approaches infinity and that the concentration of rFXIII at infinite reaction time comprises a substantial fraction of the initial concentration.

As a^*a and a^*_2 possess identical specific activities, the observed activity (Λ) and reaction time (t) are related by (33):

$$- \ln(1 - \Lambda/\Lambda_f) = 2(k_{cat}/K_m)c_\alpha t \qquad (1)$$

where Λ_f represents the activity at infinite reaction time, k_{cat}/K_m the specificity constant of the reaction and c_α the concentration of α-thrombin. Assuming that the fluorescence quantum yields of a^*a, a^*_2 and their cross-linked species are identical, equation (1) can be expressed as:

$$- \ln(1 - A_a/A_{af}) = 2(k_{cat}/K_m)c_\alpha t \qquad (2)$$

where A_a and A_{af} denote, respectively, the areas of the peaks in the electropherogram from a^*a, a^*_2 as well as their cross-linked species during the

Fig. 9. Plots of peak areas of rFXIII and rFXIIIa versus reaction time.

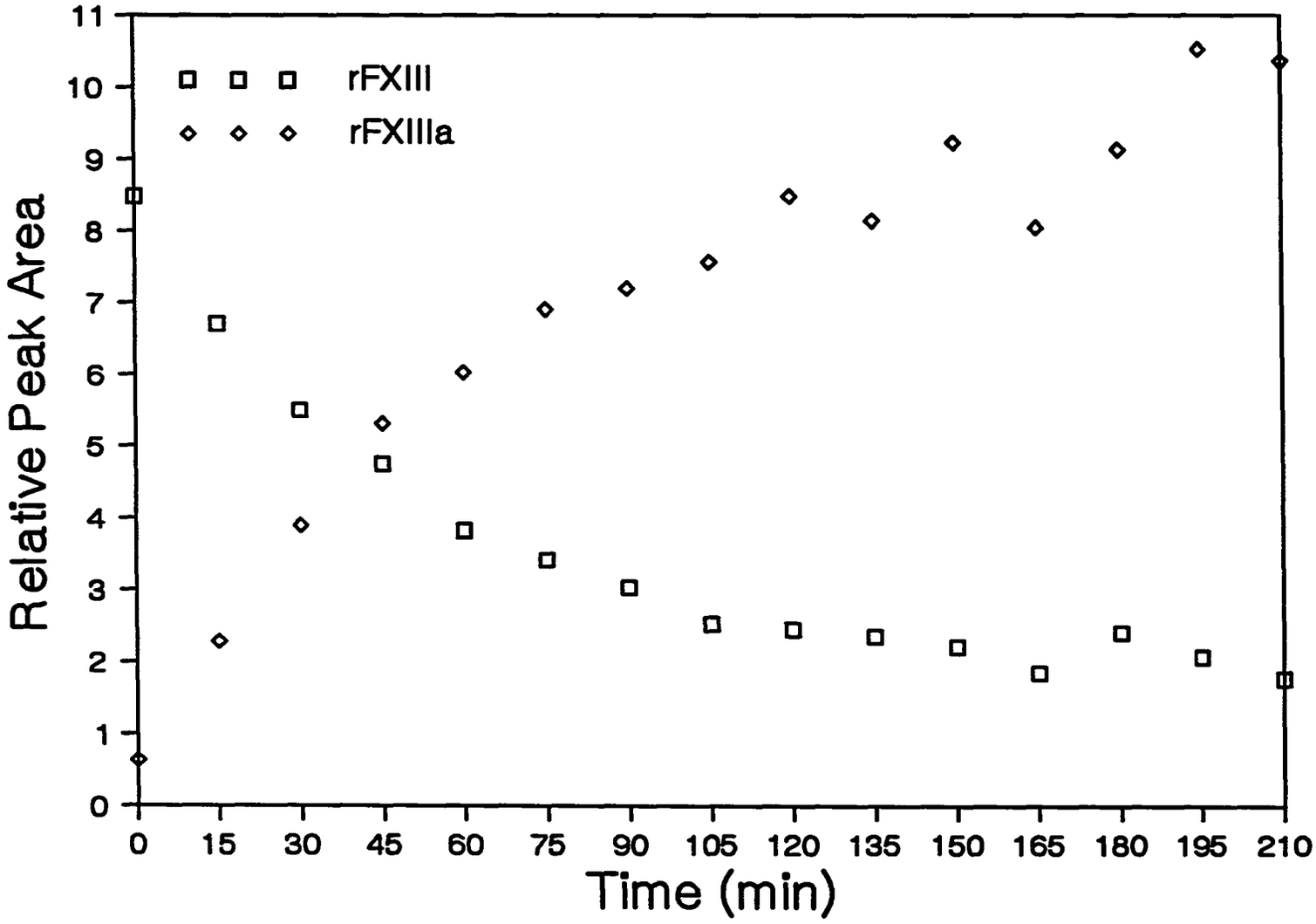
rFXIII
rFXIIIa
Relative Peak Area
Time (min)
0
1
2
3
4
5
6
7
8
9
10
11
0
15
30
45
60
75
90
105
120
135
150
165
180
195
210

experiment and at infinite reaction time. One could measure the increase in the activity of rFXIIIa by monitoring either the increase in rFXIIIa or decrease in rFXIII. This is possible because $(1-A_a/A_{af})$ can be approximated by A_i/A_{io} when A_i is much greater than A_{if}, where A_i, A_{io} and A_{if} represent, respectively the peak areas from rFXIII during the reaction, at the start of the reaction and at infinite reaction time. To extract k_{cat}/K_m, $\ln(1-A_a/A_{af})$ and $\ln(A_i/A_{io})$ are plotted against $c_\alpha t$ (Fig. 10). Not surprisingly, the plot of $\ln(A_i/A_{io})$ versus $c_\alpha t$ deviated from linearity at large $c_\alpha t$ values, as the assumption that A_i is much greater than A_{if} breaks down. Despite the increased scatter due to, as discussed earlier, integration errors, the plot of $\ln(1-A_a/A_{af})$ versus $c_\alpha t$ remains linear even for large $c_\alpha t$ values. This provides support for the contention that the fluorescence quantum yields of a^*a, a^*_2 and their cross-linked species are similar and, indeed, the scatter of the data at large $c_\alpha t$ values stems from integration errors.

To avoid errors arising from non-linearity and scatter, only the early portion of the data in Fig. 10 is subjected to regression analyses. Good coefficients of correlation of 0.95 and 0.98 for, respectively, the $\ln(1-A_a/A_{af})$ and $\ln(A_i/A_{i0})$ versus $c_\alpha t$ plots are found. From the slopes of the plots in Fig. 10, k_{cat}/K_m is found to assume the values of $2.2X10^4$ and $2.6X10^4$ $M^{-1}s^{-1}$, which are in reasonably close agreement in light of the assumptions made. The ability of HPCE/LIF to extract the same kinetic information from multiple observables in a single experiment offers added confidence to the analysis. Since the present experiment was performed at room temperature, the poor agreement with the $1.2X10^5$ $M^{-1}s^{-1}$ found by other methods carried out at 37°C is not unexpected, as k_{cat}/K_m increases rapidly with temperature (33).

Although the present method is not a direct assay for biological activity and

Fig. 10. Plots of $\ln(A_i/A_{io})$ and $\ln(1-A_a/A_{af})$ versus reaction time.

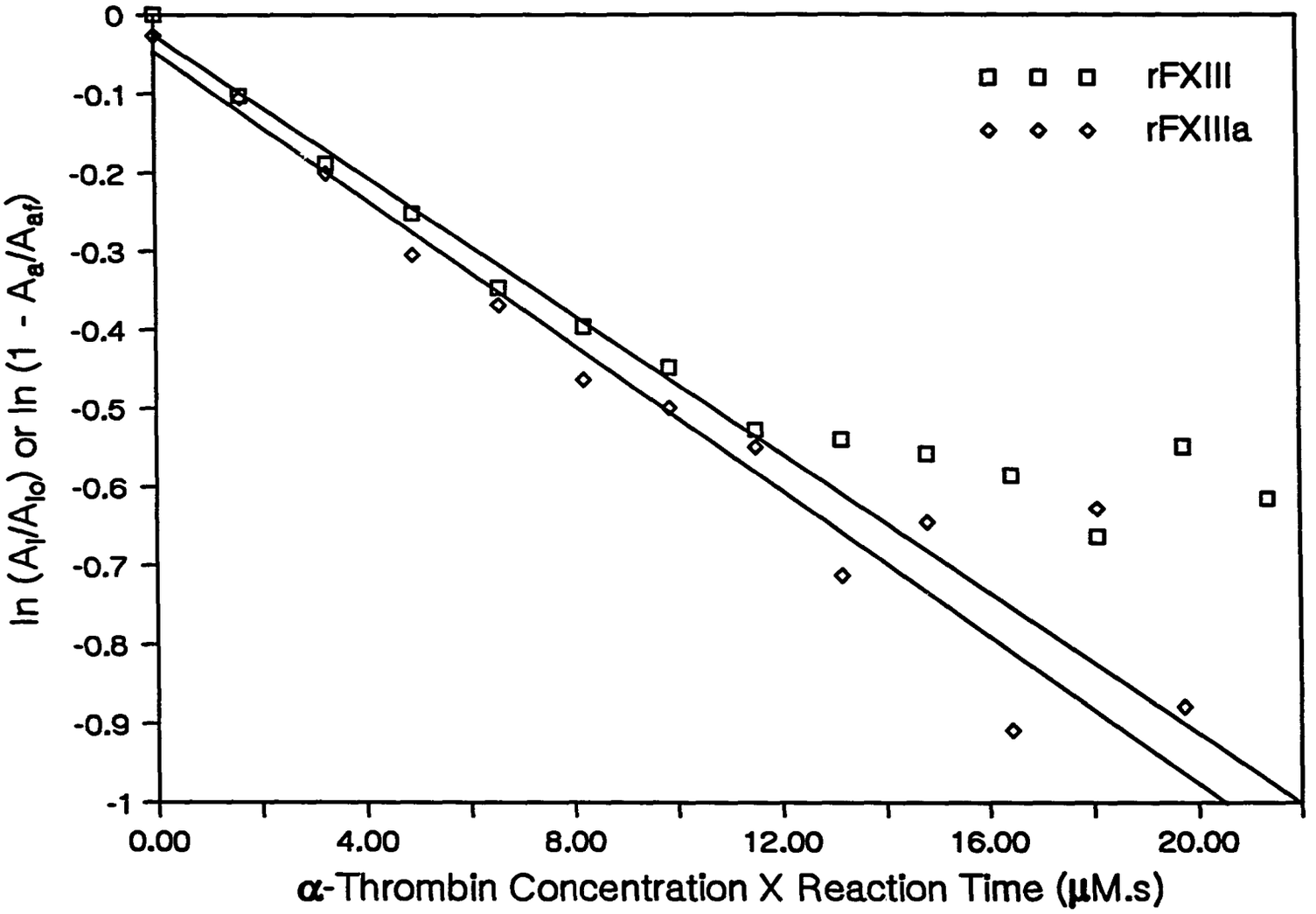
rFXIII
rFXIIIa
0
-0.1
-0.2
-0.3
-0.4
-0.5
-0.6
-0.7
-0.8
-0.9
-1
0.00
4.00
8.00
12.00
16.00
20.00
ln (A_I/A_Io) or ln (1 - A_a/A_af)
α-Thrombin Concentration X Reaction Time (μM.s)

the biochemical reaction chosen may not be the most meaningful one, it does illustrate the immense potential of HPCE/LIF in the development of biochemically based in vitro biomimetic assays. For instance, it is conceivable that HPCE/LIF may be used to obtain kinetic information on the transamidation reaction between fibrin monomers, which mimics the most significant function of rFXIII more closely than merely the activation of rFXIII. Alternatively, if good correlations between HPCE/LIF-based assays and more direct bioassays are found, the replacement of bioassays with HPCE/LIF analyses promises to dramatically reduce the cost of potency assays through the feasibility of automation.

CONCLUSION

The elusive combination of high speed, separation efficiency and detection sensitivity in the analysis of protein mixtures has finally become a reality. HPCE with laser-induced native fluorescence detection proves to be a powerful method capable of solving many important problems encountered in the QC of biopharmaceuticals not tenable previously. HPCE/LIF is able to impose more stringent criteria of purity on biopharmaceuticals and serve as a rapid, automated as well as quantitative means of assaying biopharmaceuticals in dosage formulations. In conjunction with developments in online digestion and separation technologies, HPCE/LIF promises to lower the speed and quantity of biopharmaceuticals required for assuring genetic and structural stability through peptide mapping. Finally, the urgent quest for techniques which can monitor biochemical reactions used in biochemically-based in vitro biomimetic assays in real-time for assessing the potency of biopharmaceuticals is fulfilled by the capability of HPCE/LIF in obtaining kinetic information on drug activity using a multi-parametric approach.

REFERENCES

1. "Points to Consider in the Manufacture and Testing of Monoclonal Antibody Products for Use" (draft), Office of Biologics Research and Review, Food and Drug Administration, Bethesda, MD, 1987.
2. Frenz, J.; Wu, S. L.; Hancock, W. S. J. Chromatogr. 1989, 480, 379.
3. Nielsen, R. G.; Rickard, E. C. J. Chromatogr. 1990, 516, 99.
4. Guzman, N. A.; Ali, H.; Moschera, J.; Iqbal, K.; Malick, A. W. J. Chromatogr. 1991, 559, 307.
5. Hurni, W. M. J. Chromatogr. 1991, 559, 337.
6. Nielsen, R. G.; Sittampalam, G. S.; Rickard, E. C. Anal. Biochem. 1989, 177, 20.
7. Wu, S.-L.; Teshima, G.; Cacia, J.; Hancock, W. S. J. Chromatogr. 1990, 516, 115.
8. Yim, K. W. J. Chromatogr. 1991, 559, 401.
9. Banke, N.; Hansen, K.; Diers, I. J. Chromatogr. 1991, 559, 325.
10. Nickerson, B.; Jorgenson, J. W. J. Chromatogr. 1989, 480, 157.
11. Swaile, D. F.; Sepaniak, M. J. J. Liq. Chromatogr. 1991, 14, 869.
12. Guzman, N. A.; Moschera, J.; Bailey, C. A.; Iqbal, K.; Malick, A. W. J. Chromatogr. 1992, 598, 123.
13. Wallingford, R. A.; Ewing, A. G. Anal. Chem. 1988, 60, 258.
14. Huang, X.; Luckey, J.; Gordon, M.; Zare, R. Anal. Chem. 1989, 61, 766.
15. Caprioli, R.; Moore, W.; Martin, M.; Dague, B.; Wilson, K.; Moring, S. J. Chromatogr. 1989, 480, 247.
16. Pentoney, S.; Zare, R.; Quint, J. Anal. Chem. 1989, 61, 1642.

17. Lee, T. T.; Yeung, E. S. J. Chromatogr. 1992, 595, 319.

18. Lee, T. T.; Yeung, E. S. Anal. Chem. 1992, 64, 1226.

19. Bogdansky, F. M. Pharma. Technol. 1987, 11, 72.

20. Wang, Y.-C. J.; Hanson, M. A. J. Parenter. Sci. Technol. 1988, 42, 53.

21. Tron, F.; Degos, F.; Brechot, C.; Courouce, A.-M.; Gondeau, A.; Marie, F.-N.; Saliou, P.; Laplanche, A.; Benhamon, J.-P.; Girard, M. J. J. Infect. Dis. 1989, 160, 199.

22. Powers, D. C.; Sears, S. D.; Murphy, B. R.; Thumar, B.; Clements, M. L. J. Clin. Microbiol. 1989, 27, 2666.

23. Garnick, R. L.; Solli, N. J.; Papa, P. A. Anal. Chem. 1988, 60, 2546.

24. Atkins, L. M.; Miner, D. J.; Sittampalan, G. S.; Wentling, C. D. J. Assoc. Off. Anal. Chem., 1987, 70, 610.

25. Knisken, P. J.; Hagopian, A.; Burke, P.; Dunn, N.; Montgomery, D. L.; Schultz, L. D.; Schulmen, C. A.; Carty, C. E.; Maigetter, R. Z.; Wampler, D. E.; Lehnman, E. D.; Yamazake, S.; Kubek, D. J.; Emini, E. A.; Miller, W. J.; Hurni, W. M.; Ellis, W. in : Atassi, Z. (Ed.), The Application of Molecular Biology to the Development of Novel Vaccines, Immunobiology of Proteins and Peptides. 5. Vaccine Mechanism, Design and Application (Advances in Experimental Medicine and Biology, Vol. 251), Plenum Press, New York 1989, pp. 83-98.

26. Smith, J. W. G. in : The World Biotech Report 1984 Volume 1, Online Publications, Pinner 1984, pp. 69-76.

27. Hancock, W. S.; Bishop, C. A.; Partridge, R. L.; Hearn, M. T. W. Anal. Biochem., 1978, 89, 203.

28. Cobb, K. A.; Novotny, M. Anal. Chem., 1989, 61, 2226.

29. Cobb, K. A.; Novotny, M. V. Anal. Chem., 1992, 64, 879.

30. Amankwa, L. N.; Kuhr, W. G. Anal. Chem., 1992, 64, in press.

31. Williams, J.; Elleman, T. C.; Kingston, I. B.; Wilkins, A. G.; Kuhn, K. A. Eur. J. Biochem., 1982, 122, 297.

32. Lorand, L.; Losowsky, M. S.; Miloszewski, K. F. M. Prog. Hemostasis Thromb., 1980, 5, 245.

33. Hornyak, T. J.; Bishop, P. D.; Shafer, J. A. Biochemistry, 1989, 28, 7326.

34. Bishop, P. D.; Teller, D. C.; Smith, R. A.; Lasser, G. W.; Gilbert, T.; Seale, K. L. Biochemistry, 1990, 29, 1861.

35. Lorand, L.; Ong, H. H.; Lipinski, B.; Rule, N. G.; Jacobsen, A. Biochem. Biophys. Res. Commun., 1966, 25, 629.

36. Lorand, L.; Campbell, L. K. Anal. Biochem., 1971, 44, 207.

37. Janus, T. J.; Lewis, S. D.; Lorand, L.; Shafer, J. A. Biochemistry, 1983, 22, 6269.

38. Takahashi, N.; Takahashi, Y.; Putnam, F. W. Proc. Natl. Acad. Sci. U.S.A., 1986, 83, 8019.

39. Curtis, C. G.; Lorand, L. Methods Enzymol., 1976, 45, 177.

40. Lorand, L.; Lockridge, O. M.; Campbell, L. K.; Myhrman, R.; Bruner-Lorand, J. Anal. Biochem., 1971, 44, 221.

41. Compton, B. J.; O'Grady, E. A. Anal. Chem., 1991, 63, 2597.

PAPER VI.

MICELLAR ELECTROKINETIC CHROMATOGRAPHIC SEPARATION AND LASER-INDUCED FLUORESCENCE DETECTION OF 2'-DEOXYNUCLEOSIDE 5'-MONOPHOSPHATES OF NORMAL AND MODIFIED BASES

INTRODUCTION

In the past few years, capillary electrophoresis (CE) has emerged as a promising bioanalytical technique (1). In capillary zone electrophoresis (CZE), separation is effected by the distinct electrophoretic mobilities of analytes and, as a consequence, only charged species can be resolved (2). Micellar electrokinetic chromatography (MEKC) is a major subdivision of CE (3). A surfactant at concentrations greater than its critical micellar concentration is added to the buffer solutions. Neutral analytes can be resolved as separation is based upon differences in partitioning behavior between the aqueous and the micellar phases. However, the mechanism of separation for ionic species is a convolution of both electrophoretic migration and partitioning. Hence, MEKC introduces additional selectivity in the separation of charged species with very similar electrophoretic mobilities.

The application of CE to the analysis of nucleosides and nucleotides is well documented (4-15). Detection in CE can utilize modified UV-VIS HPLC detectors, conductance, electrochemical (EC), ^{32}P-radiochemical (RC) and fluorescence (FL) methods along with mass spectral interfacing. The more general detection techniques such as UV-VIS absorbance and conductivity method lack the sensitivity necessary to be broadly applicable to CE. EC detection offers much higher sensitivity but its application is limited by the fact that only electroactive species are amenable to detection. Detection of nucleic acids by RC has been restricted, thus far, to the α-^{32}P labeled triphosphates of A, C and T (11). Detection by mass spectral interfacing involves costly instrumentation and lacks adequate sensitivity. On-column fluorescence detector is not yet commercially available. Kuhr and Yeung (13) reported detection of 5′-monophosphates of normal ribonucleosides by indirect

laser-induced fluorescence detection (LOD 70 attomole, S/N = 3). Due to the lower background and higher signal-to-noise ratio, further improvement in detection sensitivity is expected using laser-induced direct detection of fluorescent labeled nucleotides.

Kelman et al. (16) developed a novel assay for DNA damage by combining enzymatic digestion of DNA with fluorescence postlabeling (16). Briefly, DNA is digested enzymatically to 2′-deoxynucleoside-5′-monophosphates with normal bases (dNmp, N = A,C,G,T) and modified bases. The modified nucleotide is enriched from dNmp by HPLC and labeled with a fluorescent tag. The labeled nucleotides are analyzed by HPLC with fluorescence detection. The labeling procedure involves 5′-phosphoramidation with ethylenediamine followed by in-situ conjugation of the free amino end with dansyl chloride. The efficiency of the labeling procedure is quantitative and has been found to work well with both normal as well as polar, alkylated and bulky aromatic modified nucleotides such as 8-hydroxydGmp (8-OHdGmp), 5-methyldCmp (5-MedCmp) and 8-(N-2-acetylaminofluorene)dGmp (8-AAFdGmp) respectively. 8-OHdGmp is one major modified nucleotide identified when DNA is exposed to ionizing radiation (17). 5-MedCmp is the only naturally occurring modified nucleotide yet found in mammalian DNA. A large body of experimental data suggest the association of DNA methylation with gene activity (18). 8-AAFdGmp is the major adduct of DNA modification by the chemical carcinogen N-acetoxy-N-2-acetylaminofluorene (19). Using conventional HPLC with a conventional fluorescence detector, the sensitivity of the fluorescence postlabeling assay allowed detection of one modified nucleotide per 10^6 normal nucleotides from a 100 μg DNA sample (20). In order to enhance the detection sensitivity, a fluorescent detector with helium-cadium CW laser as an excitation source has been de-

veloped with the cell design of Kuhr and Yeung (21). Analysis of the dansylated nucleotides by microbore HPLC coupled to the laser-induced fluorescence detector is currently under investigation.

In this context, MEKC appears to be the ideal method for the analysis of dansyl-labeled nucleotides and their structurally similar derivatives. In the present work, the extremely high sensitivity of laser-induced fluorescence (LIF) detection is combined with mixed mode MEKC separation to allow the determination of modified nucleotides in the presence of normal nucleotides at the attomole level.

MATERIALS AND METHODS

Chemicals

dNmp and 5-MedCmp were obtained from Sigma Chemical Co. (St. Louis, MO). 8-OHdGmp and 8-AAFdGmp were synthesized as reported earlier (19,20). Dansylation of the monophosphates and the calf-thymus DNA digest were carried out as described previously (16). Sodium dodecyl sulfate (SDS) was purchased from Gallard-Schesinger Industries (Carle Place, NY) and was recrystallized twice from 95% ethanol before use.

Capillary electrophoresis

The CE instrument used has been described previously (21). A 75-cm fused-silica capillary (20 μm i.d.; 150 μm o.d.; PolyMicro Technologies, Phoenix, AZ) was rinsed with a 50/50 (v/v) methanol/water mixture for 30 min followed by a 0.05 M aqueous sodium hydroxide solution for the same period of time. After equilibrating for 24 hr with the buffer solution (0.010 M Na_2HP0_4; 0.007 M $Na_2B_40_7$; 0.045 M SDS; pH 9.0), the capillary was ready for use. All separations were performed at 30 kV and samples were injected hydrodynamically by raising the level of the sample vial 32 cm above the exit end for 6.0 min. (injected volume = 6 nL).

Fluorescence detection

Several important differences exist between the previous and present setups (21). An argon ion laser (Model 2045 Spectra-Physics, Mountain View, CA) operating at 350 nm was used to excite on-column fluorescence. The beam passes through a laser power stabilizer (Cambridge Research and Instrumentation, Cam-

bridge, MA) and then through a band-pass filter (Type UG-1; Schott Glass Technologies, Duryea, PA) to remove plasma emission lines before it was focused on the capillary. 3 Schott long-pass filters (1 CG435 and 2 CG455) were employed to remove scattered light and the detection region was located at 15 cm from the cathodic end of the capillary.

RESULTS AND DISCUSSION

Fig. 1 is an electropherogram showing the separation of a mixture of dansyl dNmp, 8-OHdGmp, 5-MedCmp and 8-AAFdGmp prepared from HPLC-purified samples. Separation of the first 6 components took less than 10 min while the whole separation was completed in approximately 16 min. The peak at 7.6 min resulted from 5-dimethylaminonapthalene sulfonate (deprotonated form of dansyl hydroxide) whereas the broad, short peak at about 15.8 min was probably due to polymers. Both are derivatized forms of impurities that were still present in the HPLC-purified samples. Other than this, baseline separation of all the components was achieved. The unusually long migration time of dansyl 8-AAFdGmp relative to the other components can be understood in terms of the more hydrophobic nature of the former arising from its fluorenyl moiety, which favorably enhances the partitioning of dansyl 8-AAFdGmp into the slow-moving micellar phase. The fact that the pyrimidine derivatives (dansyl dCmp and dTmp) as well as the purine derivatives (dansyl dAmp and dGmp) possessed similar migration times is not surprising in light of the strong resemblances in their structures. The same reasoning applies to the close proximity of the peaks representing dansyl dGmp and its 8-hydroxy-derivative. In fact, dansyl dCmp and dTmp could not be resolved at a wide range of solution acidities based solely upon differences in their electrophoretic mobilities when micelles were not used (data not shown). This illustrates the ability of MEKC in resolving components with very similar electrophoretic mobilities through the introduction of an additional parameter to the separation mechanism namely, selective partitioning between the aqueous and micellar phases. The high efficiency of MEKC can readily be appreciated by comparing the theoretical plate number of

Fig. 1. MEKC-LIF analysis of deprotonated dansyl hydroxide (a), dansy dTmp (b), dansyl dCmp (c), dansyl 5-MedCmp (d), dansyl dAmp (e), dansyl dGmp (f), dansyl 8-OH dGmp (g) and dansyl 8-AAFdGmp (h).

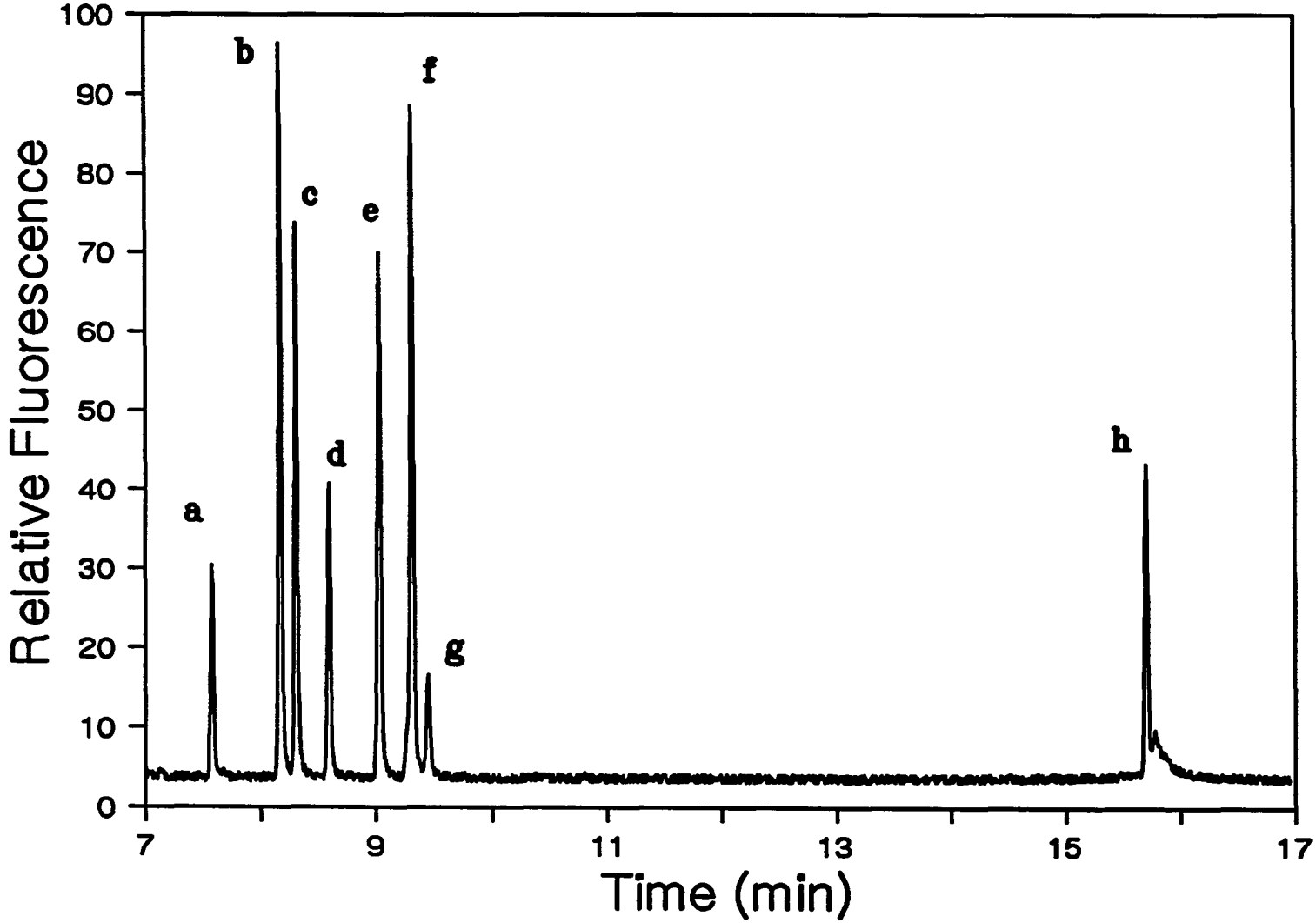
Relative Fluorescence
100
90
80
70
60
50
40
30
20
10
0
a
b
c
d
e
f
g
h
7
9
11
13
15
17
Time (min)

120,000 for dansyl dTmp obtained in the present work with that of 5,000 in an HPLC separation where dansyl dCmp and dGmp were not totally resolved. This is despite the shorter analysis time of 9.5 min with MEKC relative to the 19 min required for the HPLC procedure in the determination of the dansyl dNmp (16).

Depending on the sample preparation steps, it may be desirable to use larger capillaries so that the injection volume can be increased. The same separation was attempted using a 50-μm i.d. capillary, but adequate resolution of the components was not possible at 30 kV. In addition, it was noticed that as the applied potential decreased, a corresponding improvement in the separation was realized. Baseline resolution of all the components was achieved at 10 kV (data not shown) with an analysis time 3 times that with the 20-μm capillary at 30 kV. The fact that higher separation efficiencies at 30 kV were possible with the 20-μm capillary than with the 50-μm one can be explained by the reduced heating of the 20-μm capillary due to its smaller i.d. This is because roughly 6 times more Joule heat is generated in a 50-μm capillary than a 20-μm one, resulting in serious zone broadening due to turbulent mixing in the former. In a theoretical study of MEKC, efficiency for analytes which partition poorly into the micellar phase is predicted to increase with applied potential (22). Indeed, this is the case for the 20-μm separation in the present study, where the same separation carried out at 15 kV showed poorer efficiency (data not shown) than at 30 kV. The discussion above points to the importance of LIF in MEKC because the separation power does not have to be compromised to maintain useful sensitivity and speed of analysis, which would have been the case when wider capillaries, necessary for conventional FL, UV and RC detection schemes, were used.

The remarkably high sensitivity of LIF is demonstrated in Fig. 2 where the peak represents dansyl dTmp. As expected from the more hydrophobic

Fig. 2. Electropherogram showing detection of 6 amol of dansyl dTmp.

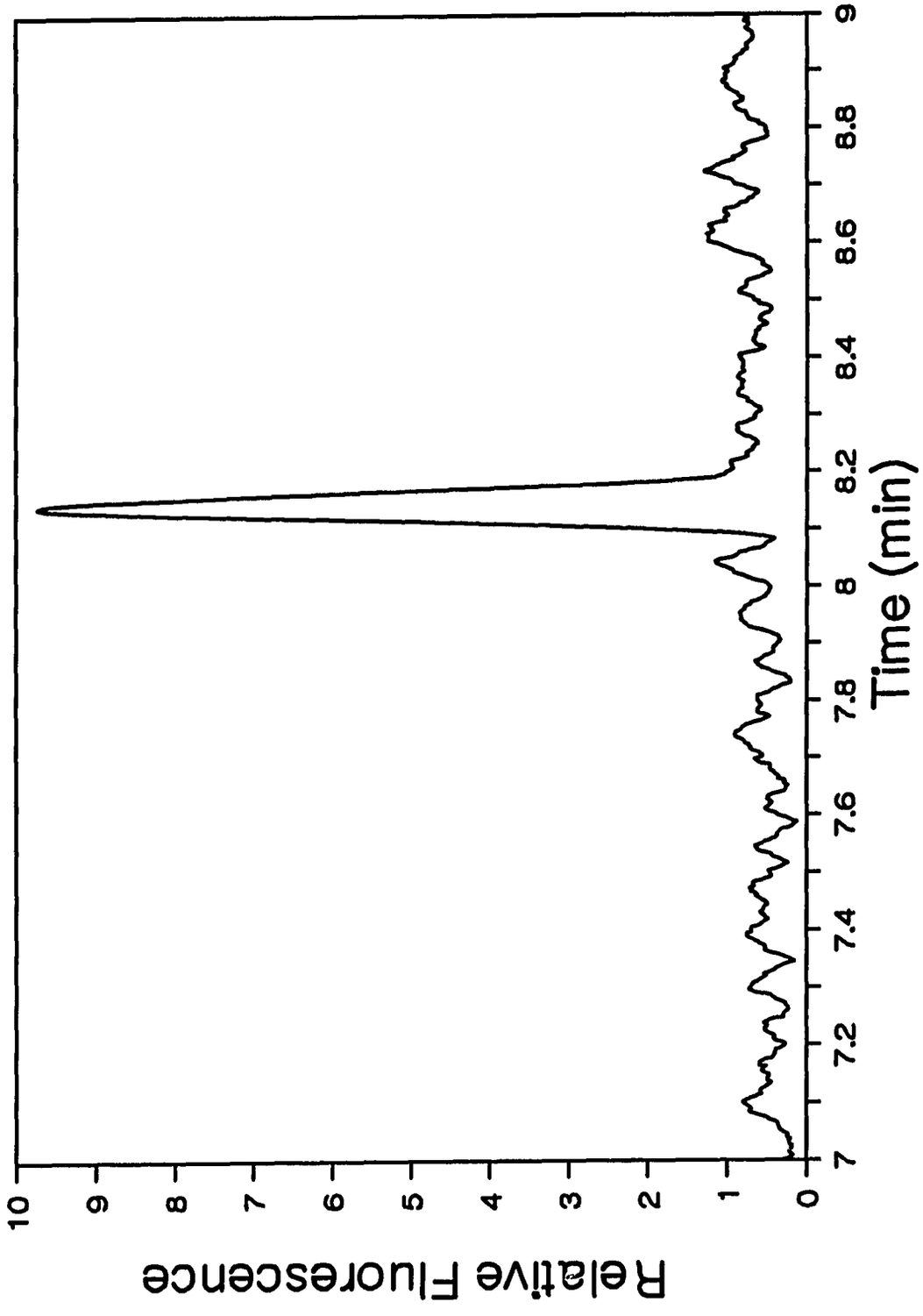
Relative Fluorescence
10
9
8
7
6
5
4
3
2
1
0
7
7.2
7.4
7.6
7.8
8
8.2
8.4
8.6
8.8
9
Time (min)

environment, the fluorescence signal increased in the presence of micelles. However, the background signal also increased (scattering and impurity fluorescence). So, net detectability was not influenced by the micelles. According to the method of Knoll (23), the limit of detection (LOD) for dansyl dTmp here is estimated to be 6 amol or roughly 4 million molecules. From Fig. 1, the variations in sensitivity among the dansyl dNmp are all within 26% of that for dansyl dTmp. It is, therefore, reasonable to expect similar LODs from the remaining components. Table 1 contains a summary of the state-of-the-art LODs with various detection schemes coupled to HPLC or CE in the determination of derivatized or native nucleosides (N), nucleoside-5′-monophosphates (Nmp), nucleoside-5′-diphosphates (Ndp), nucleoside-5′-triphosphates (Ntp), 2′-deoxynucleoside (dN), dNmp, 2′-deoxynucleoside-5′-diphosphates (dNdp) and 2′-deoxynucleoside-5′-triphosphates (dNtp). Several interesting points are noted. First, the mass LODs obtained with CE are typically 5 orders of magnitude lower than those with HPLC when the same type of detection scheme is employed. This is primarily a consequence of the smaller sample size and peak volumes of CE versus conventional HPLC. A comparison of the concentration LODs shows only a difference of one order of magnitude. In the case of the concentration LODs with FL, the 10-time improvement in CE over HPLC is probably due to the employment of LIF and the sharper peaks in the former versus a conventional FL detector in the latter. Secondly, the LODs of FL or RC are often 1000 times lower than that of UV. The explanation for this is that FL and RC measurements are, in theory, shot-noise-limited whereas UV detection is frequently hindered by flicker noise. Thirdly, the mass LOD in the present study is better than those with HPLC-FL by 3×10^4 times, HPLC-UV by 3×10^8 times, CE-UV by 1×10^4 times and matches the 7 amol level obtained for adenosine-5′-triphosphate

Table 1. State-of-the-art Limits of Detection with HPLC and CE

		HPLC	CE
absorption	amount/mol	2×10^{-9} [a]	7×10^{-14} [b]
	concentration/M	2×10^{-4} [a]	3×10^{-5} [b]
electrochemical	amount/mol	2×10^{-13} [c]	-----
	concentration/M	2×10^{-8} [c]	-----
fluorescence	amount/mol	2×10^{-13} [d]	6×10^{-18} [e]
	concentration/M	2×10^{-8} [d]	1×10^{-9} [e]
radiochemical	amount/mol	-----	7×10^{-18} [f]
	concentration/M	-----	1×10^{-10} [f]

[a]From reference 6 for dansyl dNmp
[b]From reference 5 for dAmp, dCmp, dGmp, dUmp
[c]From references 26, 27 for 8-OHdG
[d]From reference 16 for dansyl dNmp
[e]This study
[f]From reference 11 for Atp, Ctp, Ttp

(Atp), cytidine-5′-triphosphate (Ctp) and thymidine-5′triphosphate (Ttp) labeled with α-^{32}P in a CE-RC scheme (11). Fourth, CE-RC can separate and detect ^{32}P-labeled Atp, Ctp and Ttp present at a concentration of 10^{-10} M, an order of magnitude lower than that for CE-LIF which, in turn, is still 20 times better than HPLC-FL, 3 x 10^4 times CE-UV and 2 x 10^5 times HPLC-UV. However, a procedure has not been devised to assay DNA damage in the form of ^{32}P-labeled dNmp, dNdp or dNtp using CE-RC at the present moment, even though separation of dAmp, dGmp, dTmp and dCmp with CE (5) and enzymatic labeling of 8-OHdG with γ-^{32}P tagged Atp (2) have already been accomplished. Furthermore, in our studies using 50-μm capillaries, a concentration LOD of 10^{-10} M was also obtained. This is due to the larger signals and improved stray-light rejection. So, if a longer analysis time is acceptable (see above), FL is competitive with RC detection. Fifth, assuming the modified forms of the nucleotides possess similar sensitivities as the unmodified versions, what was mentioned previously regarding the LODs of the latter is also applicable to the former. Sixth, HPLC-EC offers a mass and concentration LOD for 8-OHdG (24) which are inferior to those of CE-LIF by 3 x 10^4 and 20 times respectively.

It has been claimed that ^{32}P-postlabeling (25) and HPLC-FL (20) each allows the detection of 1 residue of 8-OHdG in 10^6 normal nucleotides from a 100 μg size DNA sample. Using the same argument, CE-LIF is able to detect 1 residue in 10^9 normal nucleotides from a 3 μg size DNA sample. In practice, this kind of sensitivity is difficult, if not impossible, to demonstrate because a procedure capable of selectively removing a large portion of the components excluding the 8-OHdG residue has to be devised, such that the peak of dansyl 8-OHdGmp at its LOD can still be discerned in the presence of peaks due to all the other components in the same

Fig. 3(a). Electropherogram of dansyl dNmp (10^3 excess), dansyl 8-OHdGmp (g) and dansyl 5-MedCmp (d).

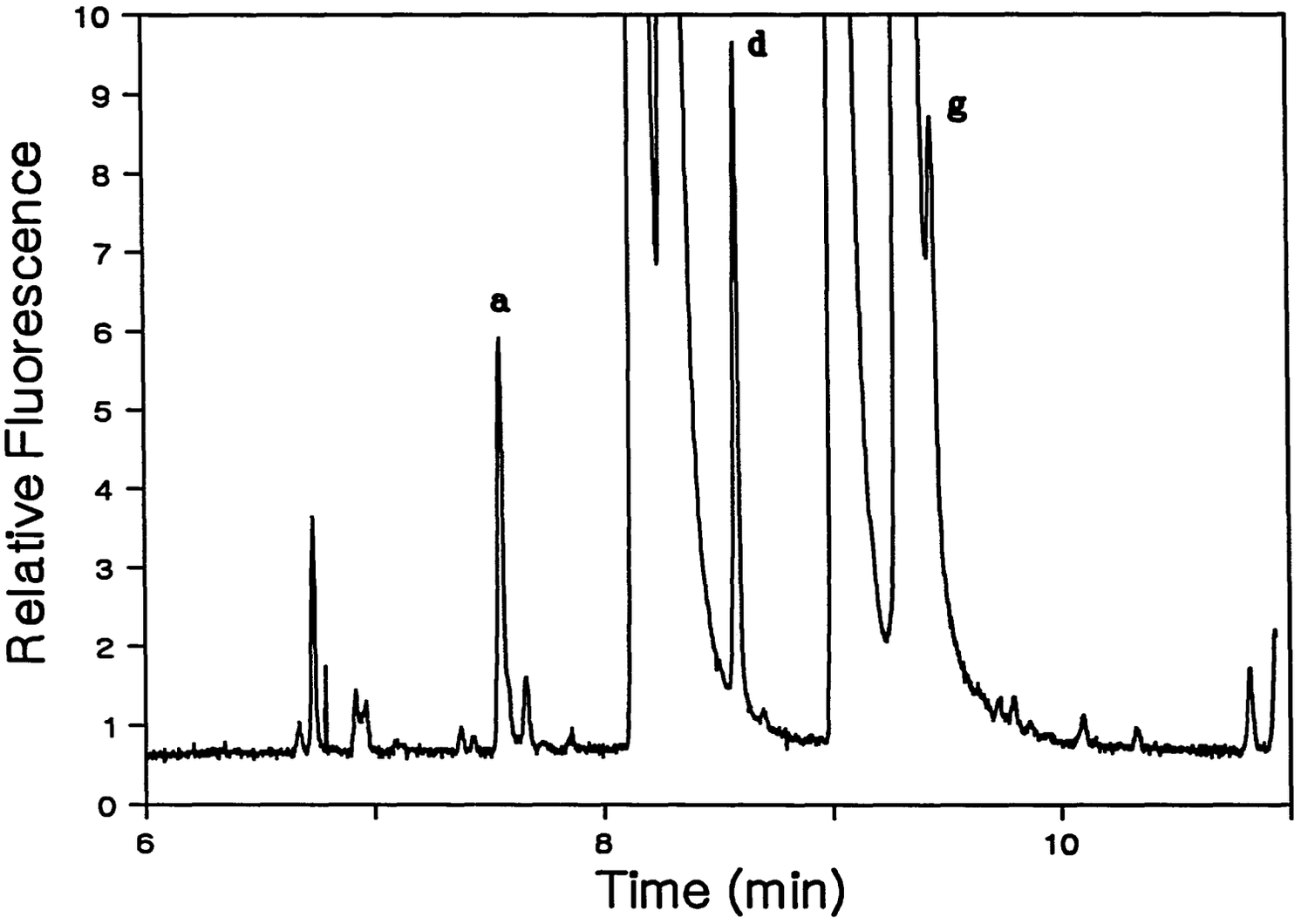
Relative Fluorescence
10
9
8
7
6
5
4
3
2
1
0
a
d
g
6
8
10
Time (min)

Fig. 3(b). Electropherogram of dansyl dNmp (10^4 excess), dansyl 8-OHdGmp (g) and dansyl 5-MedCmp (d).

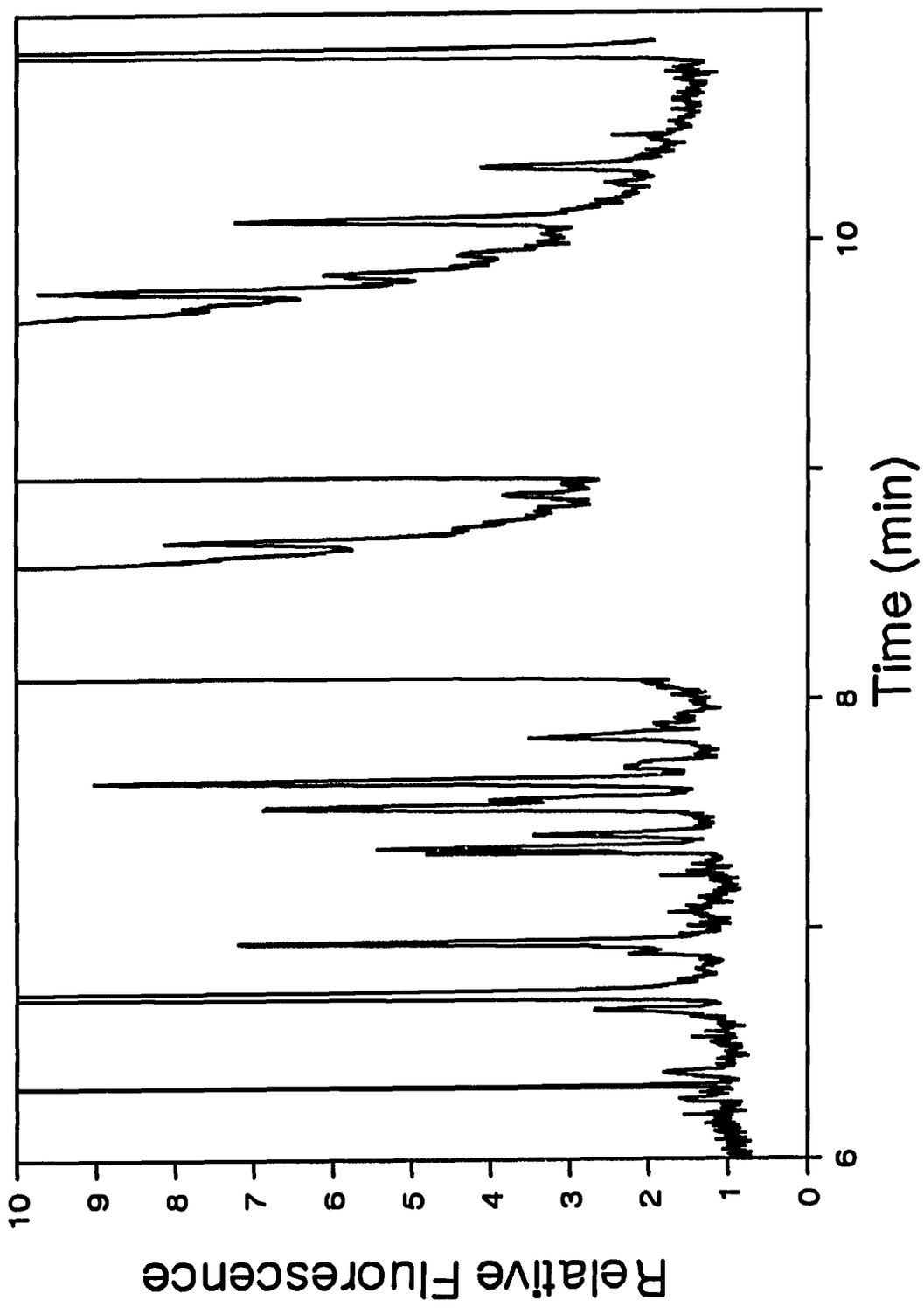
Relative Fluorescence
0
1
2
3
4
5
6
7
8
9
10
6
8
10
Time (min)

electropherogram. Fig. 3a shows the detection of dansyl 8-OHdGmp and 5-MedCmp, each present at a concentration 10^3 times smaller than those of dansyl dNmp. One can clearly distinguish the peaks corresponding to dansyl 8-OHdGmp and 5-MedCmp albeit peaks resulting from impurities in the dansyl dNmp samples can be seen. However, the same cannot be said about Fig. 3b which depicts an electropherogram of dansyl 8-OHdGmp and 5-MedCmp with 10^4 times more dansyl dNmp present. Hence, the practical LOD for both 8-OHdGmp and 5-MedCmp in the presence of an excess of dNmp that can be attained by fluorescence postlabeling (16), as proposed by Sharma et al. (20), with CE-LIF lies between a normal to modified nucleotide ratio of 10^3 and 10^4. Therefore, prior to labeling, the enrichment of the modified nucleotide from the normal nucleotides in the digest is critical to the success of DNA damage studies by CE at its detection limit.

Because of the large quantity of excess reagents relative to analytes, it is crucial that the dansylated impurities elute far from the analytes of interest in the analysis of real samples which have not been purified with HPLC. Otherwise, the analyte baseline would be obscured by peaks from the impurities. With CZE (i.e. in the absence of micelles, data not shown), the major impurity peak not only eluted before those of the analytes, but the impurities also appeared to adhere strongly to the inner wall of the capillary, resulting in severe tailing. This renders the identification and quantitation of the analytes impossible. Fig. 4 shows the electropherogram of a dansylated mixture of dNmp from a digested calf-thymus DNA sample, using the same labeling scheme and analyzed with MEKC-LIF. Prominent in the electropherogram is the large peak due to the ionized form of dansyl hydroxide (a), which has been identified as a major impurity in the derivatization process (5). In contrast to CZE, MEKC was able to slow down the rate of migration of most of the

Fig. 4. MEKC-LIF analysis of dansylated calf-thymus DNA digest.

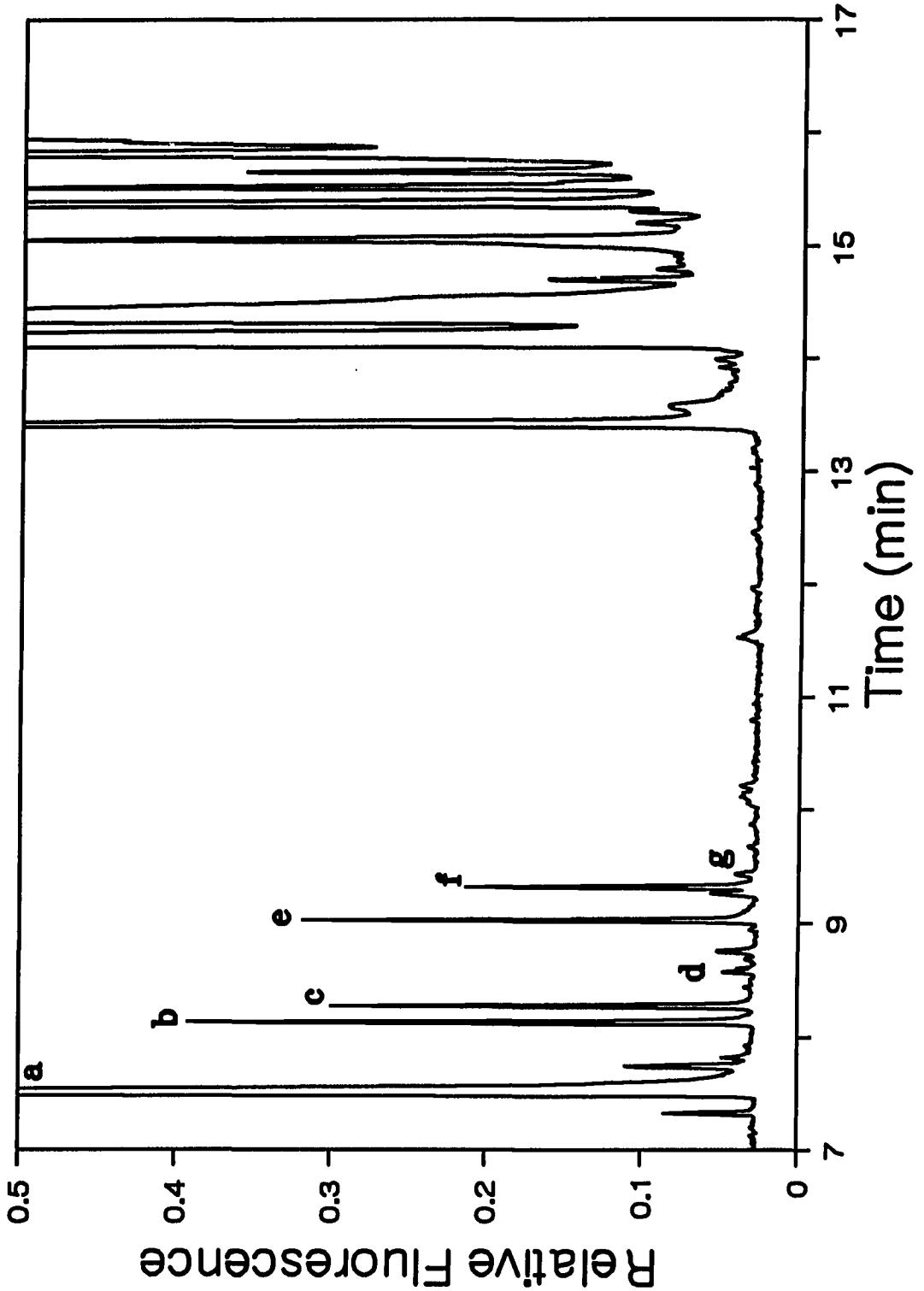
Relative Fluorescence
0.5
0.4
0.3
0.2
0.1
0
7
9
11
13
15
17
Time (min)
a
b
c
d
e
f
g

major impurities (with the exception of the ionized form of dansyl hydroxide) and allowed resolution of all the dansylated analytes. Although tailing of the late-eluting impurity peaks persisted, the extent of tailing was dramatically reduced compared to HPLC. This is probably the result of the stronger partitioning of the impurities into the micellar rather than the aqueous phase. The relative migration times of the impurities in MEKC and CZE suggest that the impurities are more hydrophobic in nature than the dansylated analytes due to the fact that hydrophobic compounds partition well into the slow-moving micelles. This, in turn, lends support to the polymeric character of the late-eluting impurities. Naturally, the size of these impurity peaks can be substantially reduced if one limits the amount of excess reagents during the derivatization step. The long migration time of the major impurities can be circumvented by flushing out the column (hydrodynamically) 17 minutes into each run to speed up the analysis.

REFERENCES

1. Ewing, A. G.; Wallingford, R. A.; Olefirowicz, T. M. Anal. Chem., 1989, 61, 292A.
2. Jorgenson, J. W.; Lukacs, K. D. Science, 1983, 222, 266.
3. Terabe, S.; Otsuka, K.; Ichikawa, K.; Tsuchiya A.; Ando, T. Anal. Chem., 1984, 56, 111.
4. Burton, D.; Sepaniak, M.; Maskarinec, M. Chromatographia, 1986, 21, 583.
5. Row, K. H.; Griest, W. H.; Maskarinec, M. P. J. Chromatogr., 1987, 409, 193.
6. Liu, J.; Banks, J. F. J.; Novotny, M. J. Microcol. Sep., 1989, 1, 136.
7. Cohen, A.; Terabe, S.; Smith J.; Karger, B. Anal. Chem., 1987, 59, 1021.
8. Tsuda, T.; Nakagawa, G.; Sato, M.; Yagi, K. Appl. Biochem., 1983, 5, 330.
9. Dolnik, V.; Liu, J.; Banks, J. F. J.; Novotny, M.; Bocek, P. J. Chromatogr., 1989, 480, 321.
10. Sustacek, V.; Foret, F.; Bocek, P. J. Chromatogr., 1989, 480, 271.
11. Pentoney, S.; Zare, R.; Quint, J. Anal. Chem., 1989, 61, 1642.
12. Pentoney, S.; Zare, R.; Quint, J. J. Chromatogr., 1989, 480, 259.
13. Kuhr, W. G.; Yeung, E. S. Anal. Chem., 1988, 60, 2642.
14. Gross, L.; Yeung, E. S. J. Chromatogr., 1989, 480, 169.
15. Wang, T.; Hartwick, R. A.; Champlin, B. P. J. Chromatogr., 1989, 462, 147.
16. Kelman, D. J.; Lilga, K. T.; Sharma, M. Chem.-Biol. Interact., 1988, 77, 85.
17. Teoule, R. Int. J. Radiat. Biol., 1987, 54, 573.
18. Riggs, A. D.; Jones, P. A. Adv. Cancer Res., 1983, 40, 1.
19. Sharma, M.; Box, H. C. Chem.-Biol. Interact., 1985, 56, 73.

20. Sharma, M.; Box, H. C.; Paul, C. R. Biochem. Biophys. Res. Commun., 1990, 167, 419.

21. Kuhr, W. G.; Yeung, E. S. Anal. Chem., 1988, 60, 1832.

22. Terabe, S.; Otsuka, T.; Ando, T. Anal. Chem., 1989, 61, 251.

23. Knoll, J. E. J. Chromatogr. Sci., 1985, 23, 422.

24. Floyd, R. A.; Watson, J. J.; Wong, P. K.; Altmiller, D. H.; Rickard, R. C. Free Radical Res. Comms., 1986, 1, 163.

25. Povey, A. C.; Wilson, V. L.; Taffe, B. G.; Wood, M. L.; Essigmann, J. M.; Harris, A. E. Proceedings Eighthieth Annual Meeting of the American Association for Cancer Research, May 1989, 30, Abstract 796.

26. Floyd, R. A.; Watson, J. J.; Wong, P. K. J. Biochem. Biophys. Methods, 1984, 10, 221.

27. Floyd, R. A.; Watson, J. J.; Wong, P. K.; Altmiller, D. H.; Rickard, R. C. Free Rad. Res. Comms., 1985, 1, 163.

GENERAL SUMMARY

As scientists begin to unravel the complexities of biological processes through chemical descriptions, the urgent need for a new generation of analytical techniques capable of tackling the often complicated biological matrices becomes obvious. Because of the tremendous potential that capillary electrophoresis holds in the determination of biomolecules, further development of the technique could accelerate the already rapid progress that is being made in the biological sciences. To this end, the demonstration of high detection sensitivity for an important class of biomolecules such as proteins in capillary electrophoresis vastly expands the utility of the technique to a myriad of biological systems. On the other hand, the finding that morphologically homogeneous entities such as human erythrocytes actually possess a wide spectrum of chemical personalities raises interesting but yet unsettling questions regarding the meaning of macroscopic measurements. The presence of the migration indices fills the voids from the absence of order in the transfer of information obtained in capillary electrophoresis. The case of the missing analytes during electrokinetic injection from samples with distinct conductivities is almost exactly solved by the concept of field-amplification. While our understanding of both the ramifications and mechanics of capillary electrophoresis has been enhanced through this work, the need for further development and application of the technique is also apparent.

LITERATURE CITED

1. Kornberg, A. Biochemistry 1987, 26, 6888.
2. Reuss, F. F. Mémoire de la Société Imperiale des Naturalistes de Moscou 1809, 2, 324-347.
3. Picton, H.; Linder, S. E. J. Chem. Soc. 1897, 71, 568-573.
4. Hardy, W. B. J. Physiol. 1899, 24, 288-293.
5. Ellis, R. Z. Physik. Chem. (Leipzig) 1912, 80, 597-603.
6. Tiselius, A. Tran. Faraday Soc. 1937, 33, 524-535.
7. Consden, R.; Gordon, A. H.; Martin, A. J. P. Biochem. J. 1946, 40, 33-40.
8. Kunkel, H. G.; Tiselius, A. J. Gen. Physiol. 1952, 35, 89-99.
9. Bourne, E. J.; Foster, H. B.; Grant, P. M. J. Chem. Soc. IV 1956, 4311-4314.
10. Kunkel, H. G.; Slater, R. J. Proc. Soc. Exptl. Biol. Med. 1952, 80, 42-51.
11. Flodin, P.; Kupke, P. W. Biochim. Biophys. Acta 1956, 21, 368-375.
12. Stein, W. H.; Kunkel, H. G.; Cole, R. D.; Spackman, D. H.; Moore, S. Biochim. Biophys. Acta 1957, 24, 640-650.
13. Raymond, S.; Weintraub, L. Science 1959, 130, 711-713.
14. Ornstein, L. Ann. N.Y. Acad. Sci. 1964, 121, 321.
15. Davis, B. J. Ann. N.Y. Acad. Sci. 1964, 121, 404.
16. Margolis, J.; Kenrick, K. G. Nature (London) 1967, 214, 1334.
17. Hjerten, S. Chromatogr. Rev. 1967, 9, 122.
18. Kolin, A. In Electrophoresis- A Survey of Techniques and Applications, Part A: Techniques; Deyl, Z., Ed.; Elsevier: Amsterdam, 1979; Chapter 2.
19. Virtanen, R. Acta Polytech. Scand. 1974, 123, 1.
20. Mikkers, F.; Everaerts, F.; Verheggen, T. J. Chromatogr. 1979, 169, 1-20.

21. Jorgenson, J. W.; Lukacs, K. D. Anal. Chem. 1981, 53, 1298-1302.

22. Kuhr, W. G. Anal. Chem. 1990, 62, 403R-413R.

23. Kuhr, W. G.; Monnig, C. A. Anal. Chem. 1992, 64, 389R-406R.

24. Jorgenson, J. W.; Lukacs, K. D. Clin. Chem. 1981, 27, 1551-1553.

25. Jorgenson, J. W.; Lukacs, K. D. Science 1983, 222, 266-272.

26. Hjerten, S.; Zhu, M.-D. J. Chromatogr. 1985, 327, 157-164.

27. Cohen, A.; Karger, B. L. J. Chromatogr. 1987, 397, 409-417.

28. Terabe, S.; Otsuka, K.; Ichikawa, K.; Tsuchiya, A.; Ando, T. Anal. Chem. 1984, 56, 111-113.

29. Pretorius, V.; Hopkins, B. J.; Schieke, J. D. J. Chromatogr. 1974, 99, 23-30.

30. Honda, S.; Iwase, S.; Makino, A.; Fujiwara, S. Anal. Biochem. 1989, 176, 72-77.

31. Hogan, B. L.; Yeung E. S. Anal. Chem. 1992, 64, in press.

32. Lee, T. T.; Yeung, E. S. Anal. Chem. 1992, 64, in press.

33. Gozel, P.; Zare, R. N. ASTM Spec. Tech. Publ. 1988, 1009, 41-53.

34. Bushey, M. M.; Jorgenson, J. W. J. Microcol. Sep. 1989, 1, 125-130.

35. Swerdlow, H.; Zhang. J. Z.; Chen, D. Y.; Harke, H. R.; Grey, R.; Wu, S.; Dovichi, N. J.; Fuller, C. Anal. Chem. 1991, 63, 2835-2841.

36. Guthrie, E.; Jorgenson, J.; Dluzneski, P. J. Chromatogr. 1984, 22, 171-176.

37. Sweedler, J. V.; Shear, J. B.; Fishman, H. A.; Zare, R. N.; Scheller, R. H. Anal. Chem. 1991, 63, 496-502.

38. Cheng. Y.-F.; Dovichi, N. J. Science 1989, 242, 562-564.

39. Hernandez, L.; Escalona, J.; Joshi, N.; Guzman, N. J. Chromatogr. 1991, 559, 183-196.

40. Wallingford, R. A.; Ewing, A. G. Anal. Chem. 1987, 59, 1762-1766.

41. Ikonomou, M. G.; Blades, A. T.; Kebarle, P. Anal. Chem. 1989, 63, 1989-98.

ACKNOWLEDGEMENTS

This work was performed at Ames Laboratory which is operated by Iowa State University for the United States Department of Energy under contract number W-7405-Eng-82. The generous gifts of biopharmaceuticals from the following companies are gratefully acknowledged: Merck Sharp & Dohme Research Laboratories, West Point, PA (rHBsAg); Hoffmann-La Roche, Inc., Nutley, NJ (anti-TAC) and ZymoGenetics, Inc., Seattle, WA (rFXIII).

This work would not have been possible without the support from past and present members of Dr. Yeung's group, who provided an excellent environment for scientific research through mutual assistance and stimulation. Although the 3 years of my stay were quite transient (in part a consequence of all the fun that I have had), I realize that the resulting camaraderie and friendship would last a lifetime. The constant support and encouragement from my parents are a major reason why I have gone so far. I especially thank Dr. Derek G. Leaist for first introducing me to the beauty of chemistry through both his insightful lectures and personal guidance. Last but not least, Dr. Yeung's keen sense of importance is only surpassed by his witty intellect. In particular, I very much appreciate the atmosphere of intellectual freedom which he created to allow me to pursue my own interests. His patience and tolerance of my often naive suggestions are especially remarkable.